2018

MONITORING SALT MARSH CONDITION AND CHANGE WITH SATELLITE REMOTE SENSING

Anthony Daniel Campbell
University of Rhode Island, campban@gmail.com

MONITORING SALT MARSH CONDITION AND CHANGE WITH SATELLITE REMOTE SENSING

BY

ANTHONY DANIEL CAMPBELL

A DISSERTATION SUBMITTED IN PARTIAL FULFILLMENT OF THE REQUIREMENTS FOR THE DEGREE OF

DOCTOR OF PHILOSOPHY

IN

BIOLOGICAL AND ENVIRONMENTAL SCIENCES

UNIVERSITY OF RHODE ISLAND

2018

DOCTOR OF PHILOSOPHY DISSERTATION

OF

ANTHONY DANIEL CAMPBELL

APPROVED:

Dissertation Committee:

Major Professor Yeqiao Wang

Peter August

Charles Roman

Nasser H. Zawia
DEAN OF THE GRADUATE SCHOOL

UNIVERSITY OF RHODE ISLAND
2018

ABSTRACT

Salt marshes are a frontline of climate change providing a bulwark against sea level rise, an interface between aquatic and terrestrial habitat, important nursery grounds for many species, a buffer against extreme storm impacts, and vast blue carbon repositories. Since the 1700s salt marshes have been in flux due to anthropogenic actions, such as reclamation for development causing loss and an influx of sediment from land clearing leading to marsh expansion. The Clean Water Act of 1972 provides legal protections for wetlands, limiting wetland reclamation and requiring that impacts be offset. However, salt marshes continue to change rapidly due to anthropogenic stressors including elevated rates of Sea Level Rise (SLR) due to climate change, herbivory driven by overfishing, droughts, and eutrophication. Salt marsh monitoring across large spatial extents requires remote sensing. This dissertation's objectives include: Developing methods for monitoring how mid-Atlantic salt marsh ecosystems are changing and where, determining how restoration and Hurricane Sandy affected Jamaica Bay's salt marshes, and quantifying the effect of the tidal stage at the time of acquisition on very high spatial resolution (<1 m) salt marsh mapping.

This dissertation is composed of three chapters in the format of published and prepared manuscripts for professional journals. In chapter/manuscript 1, a methodology for monitoring salt marsh with very high resolution imagery was developed and applied to the Jamaica Bay Unit of Gateway National Recreation Area. Jamaica Bay's salt marshes were mapped using object-based image analysis (OBIA), random forest classifier, and a diverse set of data including high spatial resolution (<1 m pixel size) satellite imagery. Change analysis was conducted at Gateway National

Recreation Area with satellite imagery collected in 2003, 2008, 2012, and 2013. All classifications achieved >85% overall accuracies. In Jamaica Bay, from 2012 to 2013, restoration efforts resulted in an increase of 10.6 ha of salt marsh. Natural salt marshes within the Bay demonstrated a decreasing trend of loss. Larger salt marshes in 2012 tended to increased vegetation extent in 2013 $F_{(4, 6)} = 13.93$, $p = 0.0357$ and $R^2 = 0.90$).

In chapter/manuscript 2, the effect of the tidal stage on salt marsh mapping was modeled using topobathymetric LiDAR and VDatum. Verification of the tidal effect on very high resolution imagery was explored within Jamaica Bay using bathtub models derived from topobathymetric LiDAR and imagery data collected at a range of tidal stages. The effect of the tidal stage was minimal at 0.6 m above MLW, only 3.5% of *S. alterniflora* was inundated. This varied greatly between salt marsh islands within the Bay.

In chapter/manuscript 3, salt marshes change across seven HUC-8 mid-Atlantic watersheds was mapped from 1999 to 2018 using time series analysis of the Landsat 7 and 8 archives with Google Earth Engine. Back-barrier salt marshes are integral to the barrier systems function and their long-term resilience in the face of SLR and future extreme storms. This analysis included watersheds across Maryland, Delaware, northern North Carolina, Virginia, New York, and New Jersey. Aboveground green biomass across the mid-Atlantic declined by an average of -68 g m^{-2}. The Landsat derived estimates of aboveground green biomass were an indicator of salt marsh vegetation extent within a pixel ($F_{(1165,1)}=1316$, $p < 0.001$) and $R^2=0.53$

Salt marsh environments along the mid-Atlantic coast are in decline and

projected to suffer more losses due to SLR. These changes are evident with both localized mapping and regional assessments. Satellite remote sensing monitoring provides the spatial context necessary for successful salt marsh management. The response of salt marshes to SLR is uncertain, where will migration, persistence, and loss occur? Satellite remote sensing of salt marsh change is necessary for the appropriate management of these ecosystems. The synergistic stressors that are driving loss require both *in situ* monitoring to determine change and remote sensing to expand these analysis beyond a singular location.

ACKNOWLEDGMENTS

I wish to acknowledge my advisor Dr. Y.Q. Wang for his support, guidance, and efforts on my development as a scientist. I would not have started a Ph.D. without your support nor would I have finished it. And to my committee for their guidance, assistance, and insight including Dr. Peter August, Dr. Charles Roman, Dr. Colleen Mouw, and Judith Swift.

I wish to thank the National Park Service and NASA RI Space Grant for funding elements of this research. The Northeast Barrier and Coastal Network including Bill Thompson, Sara Stevens, Dennis Skidds, Robin Baranowski, and all others. Field visit guidance and support from Mark Christiano, Jordan Raphael, and Neil Winn at Jamaica Bay, Fire Island, and Assateague, respectively.

I would also like to acknowledge all the support from members of the Laboratory of Terrestrial Remote Sensing including Bolin Fu, Matt Bernardo, Jenny Petrario, Rebecca Trueman, Shweta Sharma, and Jessica Morgan. I would also like to thank all the members of the Environmental Data Center especially Greg Bonynge, Roland Duhaime, Aimee Mandeville, Chuck LaBash, and Scott Rasmussen.

I wish to thank my family and friends. Special thanks to my parents for listening to me and my father for reading over more drafts than I care to admit. Sarah for your support in the process and for your ability to humor me and to make me laugh. Elliott, Kristina, Smiti, Ella, and Willow, for without their support I would not have started or finished this process. Lastly to Jesse Butler and the friends and family keeping his laughter alive.

PREFACE

This dissertation is written in the manuscript format with three chapters each comprised of a manuscript. Chapter 1, entitled "Salt Marsh Monitoring in Jamaica Bay, New York from 2003 to 2013: A Decade of Change from Restoration to Hurricane Sandy" was published in *Remote Sensing* in January 2017. Chapter 2, entitled "Examining the Influence of Tidal Stage on Salt Marsh Mapping Using High Spatial Resolution Satellite Remote Sensing and Topobathymetric LiDAR" was published in *IEEE Transactions on Geoscience and Remote Sensing* in September 2018. Chapter 3, entitled "Salt Marsh Change Analysis of the mid-Atlantic Coast from 1999 to 2018 using a Google Earth Engine Time Series Approach" has been prepared for *ISPRS Journal of Photogrammetry and Remote Sensing.*

TABLE OF CONTENTS

LIST OF TABLES

TABLE **PAGE**

Chapter 1

Chapter 2

Chapter 3

LIST OF FIGURES

FIGURE **PAGE**

Chapter 1

Chapter 2

Chapter 3

CHAPTER 1

Salt Marsh Monitoring in Jamaica Bay, New York from 2003 to 2013: a Decade of Change from Restoration to Hurricane Sandy

by

Anthony Campbell[1], Yeqiao Wang[1], Mark Christiano[2], Sara Stevens[3]

Published as Campbell, A., Wang, Y., Christiano, M. and Stevens, S., 2017. Salt Marsh Monitoring in Jamaica Bay, New York from 2003 to 2013: A Decade of Change from Restoration to Hurricane Sandy. *Remote Sensing*, *9*(2), p.131.

[1]Department of Natural Resources Science, University of Rhode Island, 1 Greenhouse Rd., Kingston, RI 02881, USA

[2]Kaibab National Forest, Forest Service, United States Department of Agriculture, Williams, AZ 86046, USA

[3] Northeast Coastal and Barrier Network, National Park Service, Kingston, RI 02881, USA

Abstract**:**

This study used Quickbird-2 and Worldview-2, high resolution satellite imagery, in a multi-temporal salt marsh mapping and change analysis of Jamaica Bay, New York. An object-based image analysis methodology was employed. The study seeks to understand both natural and anthropogenic changes caused by Hurricane Sandy and salt marsh restoration, respectively. The objectives of this study were to: (1) document salt marsh change in Jamaica Bay from 2003 to 2013; (2) determine the impact of Hurricane Sandy on salt marshes within Jamaica Bay; (3) evaluate this long term monitoring methodology; and (4) evaluate the use of multiple sensor derived classifications to conduct change analysis. The study determined changes from 2003 to 2008, 2008 to 2012 and 2012 to 2013 to better understand the impact of restoration and natural disturbances. The study found that 21 ha of salt marsh vegetation was lost from 2003 to 2013. From 2012 to 2013, restoration efforts resulted in an increase of 10.6 ha of salt marsh. Hurricane Sandy breached West Pond, a freshwater environment, causing 3.1 ha of freshwater wetland loss. The natural salt marsh showed a decreasing trend in loss. Larger salt marshes in 2012 tended to add vegetation in 2012–2013 ($F_{4,6} = 13.93$, $p = 0.0357$ and $R^2 = 0.90$). The study provides important information for the resource management of Jamaica Bay.

1. Introduction

Jamaica Bay, an estuary within the New York City (NYC) limits, is heavily influenced by urbanization. The salt marshes serve as an interface between the Bay and surrounding urban areas. Currently, over a dozen marsh islands span the Bay. Their landscapes are composed of mudflats, a variety of salt marsh plant species, sediment deposited to rebuild drowning salt marsh, transitional vegetation denoting the shift to upland, and human created upland areas. Salt marshes provide numerous ecological benefits such as high biodiversity, improved water quality, flood reduction, and carbon sequestration [1]. The wetland ecosystems of New York State, including salt marshes, were reduced by 60% from 1780 to 1980 [2]. Nationally, salt marshes have been under particular stress with increasing rates of loss from 2004 to 2009 caused in part by coastal storms [3]. In the past, these trends were exacerbated in the urban-impacted Jamaica Bay.

Jamaica Bay's salt marsh loss is severe. Since 1951, approximately 60% of the Bay's salt marsh has converted into mudflats due to a combination of factors including a reduction in sediment supply, changes in tidal regime, nutrient enrichment and increased hydrogen sulfide concentrations [4]. This estimate does not include areas of wetlands around the estuary lost to land filling and urbanization. From 1989-2003, Jamaica Bay's salt marshes were in rapid decline losing 13.4 ha/year [5]. The nitrogen load of the Bay is one factor that may contribute to this high rate of loss [6].

Remote sensing is uniquely suited for monitoring coastal environments, due to the difficulty of *in situ* access and the high temporal resolution required to understand these dynamic landscapes [7]. Remote sensing monitoring of the salt marsh landscape

can be used to determine vegetation trends for the entire bay and individual islands, facilitating an assessment of restoration impacts. Remote sensing is an important tool for furthering our understanding of how Jamaica Bay's salt marshes are affected by anthropogenic and natural factors [8, 9]. This study used imagery data spanning a decade and two high resolution sensor systems.

In October 2012, Hurricane Sandy impacted the coast of New York and surrounding states with high winds and storm surge. It was a 1 in 500-year storm surge event at the Manhattan Battery [10]. The boroughs of Brooklyn and Queens directly surrounding Jamaica Bay were inundated; the storm caused 2 million New Yorkers to lose power [11]. This study seeks to understand the impact of Hurricane Sandy on salt marsh vegetation within Jamaica Bay. The salt marsh vegetation types of interest are smooth cordgrass (*S. alterniflora),* high marsh (a mixture of *Distichlis spicata*, *Spartina patens,* and *Juncus gerardii*) and the common reed *(Phragmites australis*). Successful management of Jamaica Bay is contingent on continuing to further our understanding of the change experienced by the Bay's salt marshes due to both natural disturbance and human impacts.

The objectives of this study were to: (1) Document salt marsh changes that occurred in Jamaica Bay from 2003-2013, (2) Determine the impact of Hurricane Sandy on salt marshes within Jamaica Bay, (3) Evaluate this long-term monitoring methodology for the determination of change, (4) Evaluate the use of multiple sensor derived classifications to conduct change analysis. The combination of climate change, sea level rise and their impacts on natural disturbances are expected to have detrimental effects on coastal salt marshes [12]; thereby, enhancing the need for

accurate remote sensing monitoring and assessment of coastal wetlands to inform decision-makers.

2. Materials and Methods

2.1 Study Area

Jamaica Bay is an urban estuary residing within the New York City boroughs of Brooklyn and Queens. Kings County, synonymous with Brooklyn, is the most populated county in New York State [13]. Approximately 3,704 ha of the Bay are managed by the National Park Service as Jamaica Bay National Wildlife Refuge, a subunit of Gateway National Recreation Area (Figure 1). The region has a humid continental climate with a mean temperature of approximately 10 °C. Over the last 150 years, anthropogenic impacts to Jamaica Bay have been extensive. The Bay's volume has increased 350% while surface area fell by approximately 4,856 ha [14]. In 2005, Waste Water Treatment Plants serving 1,610,990 people discharged into Jamaica Bay [15]. Beginning in 2003, salt marsh islands including Big Egg, Yellow Bar, Rulers Bar, Black Wall, Elders Point East and West (Figure 1) have undergone salt marsh restoration. After restoration, sites were monitored *in situ* for 5 years [4]. These marsh restoration projects involved the deposition of dredge sediment from channels in the Bay onto the marsh surface then the transplanting and seeding of salt marsh vegetation [16].

2.2 Remote Sensing Data

High spatial resolution Quickbird-2 and Worldview-2 data were employed for salt marsh mapping and change analysis. The spatial resolutions of Worldview-2's multispectral and panchromatic sensors are 1.85 m and 0.42 m, respectively;

Quickbird-2's resolutions are 2.6 m and 0.62 m, respectively. The Worldview-2 sensor collects eight spectral bands including the Coastal Blue, Blue, Green, Yellow, Red, Red Edge, Near Infrared 1 (NIR1), and Near Infrared 2 (NIR2). The Coastal Blue, Yellow, Red Edge, and NIR2 spectral bands of Worldview-2 have been shown to increase the accuracy of wetland vegetation classification [17]. This study used Quickbird-2 imagery data acquired on September 10, 2003 and September 9, 2008, and Worldview-2 data acquired on September 15, 2012 and September 19, 2013. The imagery data were geo-rectified to the 2013 imagery. The data were also atmospherically corrected to top of atmosphere reflectance.

This study uses object-based image analysis (OBIA) which first divides an image into objects, using a segmentation algorithm, and then classifies those objects based on their spectral and spatial attributes [18]. Object-based change detection (OBCD) utilizes image objects to conduct a change analysis between multiple time periods. The change analysis can be conducted with object attributes, classified objects, multi-temporal image objects, or a hybrid of these techniques [19]. This study compared the classified 2003, 2008, 2012 and 2013 objects to understand restoration and Hurricane Sandy's impact on wetlands within Jamaica Bay.

2.3 Segmentation

An important component of OBIA classifications is the determination of segmentation scale, which determines the size and similarity of resulting image objects, and parametrization i.e. the inclusion of texture [20]. Texture is the use of a moving window to quantify measures that represent ideas such as coarseness and roughness [19]. This study arrived at an appropriate segmentation scale with the

comparison of multiple segmentation scales for each time period to maximize intra-segment homogeneity and intersegment heterogeneity [21, 22]. The parametrization of the resulting image objects included spectral values, texture, geospatial attributes, upland data, vegetation indices, and neighborhood and scene difference attributes (Described in Section 2.4). Segmentation scale is the key to accurately mapping a landscape. Scale parameters can be arrived at through "trial-and-error". However, this method risks determining an inappropriate segmentation scale. Over or under segmenting an image can result in lower classification accuracy [23]. In addition, segmentation scale can impact the land cover classes that can be accurately mapped [20]. This study used the mean shift clustering approach to determine segmentation. Mean shift is a non-parametric segmentation algorithm which groups pixels based on their spectral mean in a feature space. The algorithm has improved accuracy when compared to other clustering techniques [24, 25]. Mean shift considers a spectral radius in the feature space as the scale parameter, which results in a hierarchical relationship between segmentation scales [26]. These factors make the algorithm suitable for multiscale segmentation.

There are different methods for assessing the quality of segmentation. This study assessed segmentation scales with an index of intra-segment homogeneity and intersegment heterogeneity [21]. Intersegment heterogeneity was assessed through computation of Global Moran's I that were normalized and then combined with the intra-segment homogeneity, as determined by normalized area controlled variance, to create a single parameter measuring segmentation quality [22]. The mean shift segmentation parameters that were determined were minimum size and spectral radius.

Minimum size refers to the fewest number of pixels that can compose a segment, and spectral radius is the distance in the feature which a pixel must be within to merge into the segment. Each image date was tested with the parameters from 5-50 spectral radii in increments of 1 and minimum size from 5-50 in increments of 5. Appropriate segmentation scale for the Worldview-2 2012 data was determined to be a spectral radius of 15 and a minimum size of 5 pixels. The 25% most over segmented objects were segmented again at a quantitatively determined appropriate scale of spectral radius 20 and minimum size 5 pixels. The same was done for 25% most under segmented objects, for which the appropriate scale was spectral radius 6 and minimum size 5 pixels. The appropriate scale for the Worldview-2 2013 data was determined to be spectral radius 22 and minimum size 20 pixels. The 25% most over segmented objects were segmented again at a quantitatively determined appropriate scale of spectral radius 27 and minimum size 5 pixels. The 25% most under segmented objects were re-segmented at a scale of spectral radius 7 and minimum size 5 pixels. The Quickbird-2 data were segmented at a spectral radius of 8 and a minimum size of 20 pixels. No additional levels of segmentation were done as this scale adequately captured the landscapes and spectral complexity of the Quickbird-2 data.

The classification was conducted with the Random Forest classifier. Random Forest is a non-parametric ensemble learning algorithm that has been demonstrated to achieve appropriate classification accuracy in a variety of landscapes [25, 28, and 29]. The 9 classes used in this study included 6 from a previous study of the Bay [8]. These classes included water, mudflat, sand, high marsh, patchy *S. alterniflora*, and *S. alterniflora* (≥50% vegetation cover). The two *S. alterniflora* classes were based on

percent cover with patchy being between 10%-49% vegetation cover and *S. alterniflora* (≥50% vegetation cover) being above 50%. *Salicornia* species are present within the Bay as a small component of the salt marsh [30], and were not prevalent enough to classify on their own. Additional classes included in this study are wrack, upland vegetation, *Phragmites,* and shadow, however shadow was removed with a decision tree post-classification. The 2003 classification did not include wrack due to the limited separability of the class in those images. These additional classes were included to expand our understanding of the Bay and inform management decisions.

2.4 Object Attributes

Spectral attributes included the mean and standard deviation of all available spectral bands. The spatial variables computed were perimeter, area, and nodes. The panchromatic band was utilized to create Grey-Level Co-Occurrence Matrix (GLCM) textural measurements, including inverse difference moment, entropy, contrast, correlation, and uniformity. GLCM and other texture measures have been shown to improve classification accuracies in both Very High Resolution image classification [28] and object-based wetland classification [32]. Red Edge-based vegetation indices, have been shown to more accurately discern differences between high density vegetation species [33]. In this study, Worldview Vegetation Index (WVVI), Worldview Water Index (WVWI), Red Edge-based NDVI, NDVI, and Soil Adjusted Vegetation Index (SAVI) were calculated after pan-sharpening due to its benefits for detecting small vegetation patches (formulas in Table 1) [34]. Ancillary data included an upland GIS layer created from a geomorphological map of Jamaica Bay [35] and

Digital Elevation Model (DEM) derived from 2014 Topo-bathymetric Light Detection and Ranging [36].

Object neighborhoods, those objects that share a border with an object, and weights were calculated to determine the neighborhood difference of the mean spectral, textural and vegetation index attributes giving additional spatial context to the data [33]. The final Worldview-2 image objects had 79 attributes including 3 spatial attributes, 18 texture attributes, 32 spectrally derived attributes, 7 elevation based, 18 vegetation index, and a binary upland variable (Table A3). The Quickbird-2 image objects had additional attributes including tasseled cap values but no Red Edge based NDVI.

2.5 Accuracy Assessment

The accuracy assessments were conducted for each classification by generating equalized random points. The number of points to generate was calculated with following equation [34].

$$N = \frac{B \prod_i (1 - \prod_i)}{b_i^2}$$

Where B is the Chi-squared distribution with 1 degree of freedom for the target error divided by the number of classes, $\prod_i$ is the percent land cover of the most prevalent class and b is the desired confidence interval of that class. The calculation required over 750 test points to fulfil the accuracy assessment. The final test dataset was composed of 765 test points. The objects were classified by the user based on Worldview-2, Quickbird-2, and Google Earth historic imagery from each time period. Overall accuracy, the Kappa statistic, producer's accuracy, and user's accuracy were

calculated to analyze the confusion matrix results [38, 39]. The study site was visited in 2014 and 2015 to verify the characteristics of the landscape and collect field reference data. The training samples and objects were extracted from Worldview-2 and Quickbird-2 imageries in combination with expert knowledge from the field visits. Land cover points were collected on each of the field visits. The point locations included areas in West Pond, Black Bank, Yellow Bar, JoCo, Elders Point, Canarsie Pol, and East High. The points were navigated to with a Trimble XH and the areas dominant vegetation community was verified.

2.6 Statistical Analysis

The finished classifications were utilized to determine change rates (ha/year) in three time periods, 2003-2008, 2008-2012, and 2012-2013. Jamaica Bay's unique salt marsh structure of individual islands led to their use for statistical analysis. The paired Wilcoxon signed rank test was utilized to test the differences between wrack extent throughout the Bay in 2008, 2012, and 2013 (Table A1). These extents were for each island for each year. The difference between percent change (Δ%/year) of restored and natural salt marsh from 2012 to 2013 was tested with a student's t-test. Before utilizing the t-test, normality was tested with the Shapiro-Wilkes statistic, which indicated normality could not be rejected with p values = 0.37 and 0.80 for restoration and natural, respectively. The natural salt marsh islands for all time periods were used to compare change rates (ha/year) for each of the three time periods. The time periods were tested with Shapiro-Wilkes for normality finding p values of 0.54, 0.29, 0.43, and 0.19 for 2003-2008, 2008-2012, 2012-2013, and 2003-2012 respectively. Linear regressions were used to understand the impact of salt marsh extent, latitude, and

longitude on combined high marsh and both classes of *S. alterniflora* change rates (ha/year). Latitude and longitude were determined from the center point of each salt marsh island.

3. Results

The landscape was mapped accurately throughout the classification results (accuracies of 85.63, 85.20, 90.46, and 92.55 for 2003, 2008, 2012, and 2013, respectively). The overall accuracies were further analyzed by producer's and user's accuracy (Table 2). The 2003 data had an adequate overall accuracy of 85.6 %, with vegetation classes exhibiting the lowest accuracies (Table 2). This led to a focus on comparing vegetated salt marsh and non-vegetated areas as most of the error was between the multiple classes of salt marsh. The three classes of vegetated (*S. alterniflora* classes, high marsh, *Phragmites*), non-vegetated (water, mudflat, sand, wrack) and upland were used for comparisons between periods unless stated otherwise. These three classes had overall accuracies of 96.09, 93.46, 93.46, and 96.73 for 2003, 2008, 2012, and 2013, respectively.

3.1 Wetland Change

The 2003 and 2013 classifications were compared to determine change between all classes (Table 3). From 2003-2013, 54.9 ha of sand, mudflat and water were converted into salt marsh. However during that same period 70.7 ha of high marsh and *S. alterniflora* were converted into sand, mudflat, or water. Salt marsh vegetation gains occurred in restoration sites, however, these were exceeded by losses in areas not subject to intervention (Figure 2). Elders Point East and West were

restored during the study period, an example of restoration driven change in the Bay (Figure 3). West Pond was breached during Hurricane Sandy and areas of freshwater wetland and upland vegetation shifted to mudflat (Figure 4). From 2003 to 2013, 21 ha of salt marsh were lost, including both *S. alterniflora* classes, high marsh, and *Phragmites*. Smaller salt marshes such as Duck Point and Pumpkin Patch nearly disappeared (Figures 1 and 2).

3.2 Restored Islands: 2003-2013

Elders Point East and West were restored in 2006 and 2010 respectively [4]. These islands were not being actively restored during the 2012-2013 period, however they did increase in salt marsh extent (Table A1). From 2012 to 2013, Yellow Bar, Rulers Bar, and Black Wall were the focus of significant restoration. In 2013, Yellow Bar added 8.0 ha of salt marsh vegetation, but had a negligible change in extent from 2003-2013. Yellow Bar's restoration process also added approximately 15 ha of mudflat, however, this does not account for the 32.5 cm higher tide in 2003 as determined from the Sandy Hook tidal gauge [41]. From 2003-2008 restoration of Big Egg and Elders Point East were completed, resulting in increases in salt marsh extent of 4.0 and 9.5 ha, respectively. Big Egg subsequently lost 4.7 ha of salt marsh extent between 2008-2012.

3.3 Impact of Hurricane Sandy

West Pond (Figure 2) is a retention pond created during the construction of the Cross Bay Boulevard and an important resource for migratory birds [42] (Figure 4). Hurricane Sandy breached West Pond, resulting in salt water intrusion into the fresh

water environment [43]. Prior to this breach, West Pond's wetlands were dominated by *Phragmites australis*. The area represents the most drastic change from Hurricane Sandy; alterations to the upland and freshwater wetlands are evident (Figure 4, Table 4).

Between 2003 and 2013, the JoCo site lost salt marsh vegetation going from 131.2 ha to 127.6 ha. However, from 2012 to 2013 vegetation increased (Table A1). This increase in vegetation was accompanied by a reduction in wrack across the Bay compared to both 2008 (W_{15}= 110, $p < 0.003$) and 2012 (W_{15}=113, p=.0011). The area of wrack was reduced after Hurricane Sandy going from 2.2 ha to 0.5 ha. This in part accounts for the 3.6 ha increase of salt marsh vegetation observed in JoCo. The 2008 and 2012 classifications of JoCo had only 0.2 ha of overlapping wrack.

JoCo salt marsh was the most stable during the time period analyzed (Table A1). The restoration salt marshes in 2012-2013 had a larger percentage increase of salt marsh vegetation than natural salt marshes (t_4, p=0.041). The natural salt marshes in 2012-2013 demonstrated a larger positive change than 2003-2008 (t_{10}=2.366, p =0.039), 2008-2012 (t_{10}=2.6893, p= 0.022) and 2003-2012 (t_{10}=2.5434, $p < 0.03$). The 2008-2012 and 2003-2008 change rates were also significantly different (t_{10} =2.8012, $p < 0.02$) (Table A2). However, 2012-2013 was the only period when a mean increase in natural salt marsh vegetation was observed.

We analyzed the natural salt marshes yearly change rates (ha/year) by linear regression for each time period. The only time period where salt marshes towards the eastern side of the Bay tended to gain vegetation was 2012-2013 ($F_{1, 9}$ = 22.21, p<0.002 and R^2 = 0.7116). Larger salt marshes in 2012 tended to gain vegetation in

2012-2013 ($F_{4,6}$ = 13.93, p<0.036 and R^2 = 0.9028). From 2008-2012, larger salt marshes in 2008 tended to lose more vegetation ($F_{4,6}$ = 6.83, p<0.011 and R^2 =0.8199). From 2003-2008, no relationship was found between salt marsh extent and change ($F_{4,6}$=0.75, p = 0.41 and R^2 = 0.33). The switch in the direction of this relationship demonstrates different processes dominating the Bay between 2008-2012 and 2012-2013.

3.4 Accuracy Assessment

Confusion matrices were utilized to determine the performance of each of the classifications. The 2012 and 2013 classifications performed well in all vegetation classes of most interest including *S. alterniflora* and high marsh (Table 2). The lowest performing class was *Phragmites*, which is a difficult to classify land cover with overlap between many of the other classes spectrally and spatially. The 2003 and 2008 classifications had low salt marsh vegetation accuracy due to confusion between the salt marsh vegetation types. The 2003 and 2008 error was mitigated by focusing our analysis on change in vegetation not changes in particular types of vegetation. Overall the Worldview-2 data were better suited for the specificity of this classification.

4. Discussion

Since the 1950s, salt marsh vegetation in Jamaica Bay has been in rapid decline and in the early 2000s, restoration was deemed necessary to maintain the salt marsh. This study and past estimates of salt marsh change were compared to better understand vegetation trends. From 1989-2003 there was an estimated 13.4 ha of yearly loss [5]. From 2003 to 2013 a yearly loss of 2.1 ha was observed. The long-

term rate of salt marsh loss in the Bay slowed due in part to restoration, however, both tidal stage and nutrient inputs may have influenced this result.

The 2003 and 2013 data were collected at a tidal stage of -0.129 m and -0.454 m (North American Vertical Datum) [41]. Between 2003 and 2013 the larger salt marsh islands appeared to gain vegetation in the interior and lose salt marsh on the edges (Figure 2). However, the difference in tidal stage of the data could be responsible for some vegetation increases between the two dates. The tidal stage of the 2012 data was -0.577 NAVD [41]. The small tidal difference in 2012 and 2013 could result in less inundated vegetation in 2012. Tidal stage may have influenced the larger trends from 2003-2013, but was not a factor in the vegetation increase from 2012 to 2013. The impact of the tides on mapping salt marsh in Jamaica Bay should be further explored to account for this uncertainty.

Since the mid-2000s, the Bay has had a 30% reduction in nitrogen load [44]. Nutrient enrichment in salt marsh systems can lead to creek bank collapse and conversion to mudflat [6]. The Waste Water Treatment Plants in Jamaica Bay account for 89% of all nitrogen inputs into the Bay; due to the Bay's currents, the highest nitrogen concentrations were in the south and eastern sides of JoCo [15]. The different responses of salt marshes in the Bay to nutrient enrichment was partly explained by lower elevation marshes having longer periods of inundation increasing decomposition and loss of organic matter [45]. The nitrogen load reduction coincided with the slowing of salt marsh loss, however, the impact is unknown and *in situ* analysis would be necessary to explore this possible connection.

4.1 Restoration

In 2003, the first salt marsh restoration in Jamaica Bay began at Big Egg. The project utilized dredge sediment to increase marsh elevation and then *S. alterniflora* plugs were planted 50 cm apart [17]. In 2006, Elders Point East's elevation was increased with dredge sediment and then vegetated with both plugs and hummock relocation, the removal followed by placement of the entire salt marsh platform on areas of restored elevation [4]. The hummock relocation saves salt marsh that would be covered in dredge sediment, and provides vegetation to the restored area. In 2010, the elevation of Elders Point West was increased with dredge sediment and vegetated with a combination of hummock relocation, planting of high marsh species, seeding of *S. alterniflora*, and a test site with no planting [4]. In early 2012, Yellow Bar was restored with dredge material and vegetated with a mix of hummock relocation and salt marsh seeding [46]. In fall 2012, the elevation of Rulers Bar and Black Wall was increased with dredge sediment. In June 2013, a community effort added vegetation to these islands with plugs [46]. This decade of restoration coincided with our study, and resulted in the evaluation of this methodology for understanding restoration.

Black Wall and Rulers Bar were restored between 2012 and 2013. These marsh islands showed no evidence of revegetation at the time of the 2013 mapping. The salt marsh vegetation of Black Wall and Rulers Bar was reduced from 2.7 to 1.2 ha while sand and mudflat increased from 11.2 to 18.2 ha. The loss of vegetation appeared to be connected with sediment deposition from restoration and lack of hummock relocation. However, the storm event could have exacerbated the loss. Rulers Bar lost nearly all salt marsh vegetation from 2012-2013 (Table A1). In June 2013, plugs had been

planted on Black Wall and Rulers Bar. However, the vegetation was sparse and classified as mudflat.

While restored salt marsh corresponded with a visual change, it may not represent a recovery of all the ecosystem services. Differences between natural and restored salt marshes include lower soil organic matter, insufficient nitrogen availability, stunted plant growth and increased susceptibility to herbivory [47]. Field studies in Jamaica Bay have demonstrated some differences between restored and natural salt marshes, including a high percent of sand and less soil organic matter in the first 10 cm of soil [45]. These differences and the unknown longevity of restored marshes are the reasons long-term monitoring is necessary. Big Egg and Elders Point East both demonstrated losses post restoration from 2008-2012, with a loss of 1.1 ha and 1.0 ha per year, respectively. Post-restoration losses demonstrate the need for further understanding of the underlying processes causing salt marsh loss in Jamaica Bay. The expected lifetime of a restored marsh could be estimated and used to inform management decisions.

Restoration planting occurred on Yellow Bar between the 2012 and 2013 data collections (Table 5). The restoration process added elevation and *S. alterniflora* to the northern area of the site. The restoration resulted in vegetation increasing from 18.2 to 26.3 ha. Elders Point's restoration was already complete in 2012, however, the combined vegetated extent of Elders Point East and West went from 13.0 to 14.5 ha. Restoration sites added vegetation in the post-storm growing season. Restoration sites did not appear to be negatively impacted by Hurricane Sandy. However, post-storm the Yellow Bar restoration required extensive repairs and replanting [46]. The storm

impacted Yellow Bar at an early stage of restoration, which led to a slowing of the process. However considerable vegetation was gained in the post-storm growing season.

4.2 Hurricane Sandy

The response of salt marshes to storm events vary and include net elevation increases leading to vegetation growth [48] and accretion varying with distance to an inlet [49]. The natural and restoration salt marshes responded differently to Hurricane Sandy. The analysis of natural salt marsh separated the restoration and storm impacts. In 2012-2013, larger salt marshes and those further from Rockaway Inlet tended to gain vegetation. This is in agreement with past hurricane impacts which had a wide variation in sediment deposition and salt marsh response including edge erosion [50]. The large salt marshes may have been less impacted by Hurricane Sandy, and captured more of the accompanying sediment pulse.

The response of vegetation in Jamaica Bay to Hurricane Sandy depended on the location and the ecosystem. Saltwater intrusion into freshwater ecosystems is a major source of storm event derived vegetation loss; evident in both coastal wetland environments [51] and forests [52]. The survival and recovery of freshwater wetland vegetation depends on the species [53] and replanting of coastal forests can be limited by the increased soil salinity and herbivory [54]. These long-term impacts emphasize the importance of monitoring the West Pond breach. Post-storm, both freshwater wetland and upland vegetation lost extent declining from 13.3 ha to 10.2 ha and 11.5 ha to 6.0 ha, respectively (Table 4). There was 2.9 ha of change from upland vegetation to freshwater wetland, which can be understood as a loss of vegetation

biomass but not a complete loss of vegetation. Excluding those areas, 5.9 ha of freshwater wetland was lost. The majority of vegetation lost became mudflat. The loss of upland vegetation suggests the approximate extent of salt water intrusion into the upland areas around West Pond. The environmental assessment of the site has resulted in the decision to close the breach and restore the freshwater wetland environment [55]. This approach will create early successional habitat. Continued monitoring of West Pond is necessary to understand both the recovery of the freshwater ecosystem and unforeseen impacts of the management decision.

4.3 Wrack

Wrack is an important component of Jamaica Bay's landscape as persistent wrack deposits, for over 4 months of time, have a negative impact on the growth rate of all the principal marsh species [56]. Storm events including hurricanes are understood as one of the causes of wrack accumulation [50]. Mapping wrack accumulation pre- and post-storm enabled the evaluation of both the deposition and movement of wrack within Jamaica Bay. Post-storm there was less wrack on the salt marsh than in 2008 and 2012. When examining JoCo, it appears areas of wrack moved towards the center of the marsh island (Figure 5). If the same pattern occurred in islands with upland, wrack would have moved under the upland vegetation canopy. Throughout the Bay most wrack became *S. alterniflora*, capturing the removal of wrack and regrowth of impacted salt marsh vegetation in the following growing season. These findings suggest recovery from wrack can be rapid, with storm events as a major driver in the deposition and distribution of the material throughout Jamaica Bay.

4.4 Long-term monitoring;

The two most prevalent mapping protocols for wetland change analysis are the National Wetland Inventory (NWI) conducted by United States Fish and Wildlife Service (FWS) and Coastal Change Analysis Program (C-CAP) conducted by the National Oceanic and Atmospheric Administration (NOAA). These programs are each focused on mapping wetland change across the entire or the majority of the United States. The NWI is an estimate of the trends conducted by mapping a large number of randomly sampled plots which are interpreted based on aerial imagery [57]. The methodology leads to trends in states or regions, however, these conclusions are not necessarily representative of rapidly changing sites such as Jamaica Bay. Between 2004 and 2008, the NWI estimated salt marsh increased in the Atlantic by 133 hectares, a negligible percent increase [3]. Between 2003 and 2008, Jamaica Bay added 6.3 hectares of salt marsh vegetation, a 1.8% increase. The two estimates agree that an increase occurred, however, the NWI estimate lacks the precise location or magnitude of the restoration driven change.

The C-CAP utilizes Landsat, a 30 m spatial resolution sensor, to understand long-term change, however, accuracy reports showed confusion between water, consolidated shore, and emergent marsh [58]. From 2001-2010, C-CAP's estuarine emergent wetland class maintained an extent of 674 ha in Jamaica Bay. During that time frame Big Egg and Elders Point East were restored, which had no discernable change in the extent of estuarine emergent wetland class. Remote sensing with high resolution imagery has been successfully utilized for monitoring restoration [59]. The coarse spatial and temporal resolution of C-CAP makes understanding storm events or

restoration in Jamaica Bay difficult. Localized solutions are necessary for capturing a restoration baseline and then mapping at an appropriate temporal resolution to understand shifts between vegetation communities and long-term restoration trajectories.

Salt marsh losses are increasingly driven by sea level rise and high water events causing migration of *S. alterniflora* into areas previously composed of high marsh [60]. In order to understand these shifts between vegetation communities, a specialized high resolution classification is necessary. When conducting analysis over large areas C-CAP and NWI programs are invaluable. However, a specialized protocol is preferable when presented with single study site and unique management issues.

The regular collection of satellite imagery is necessary for long-term monitoring. This can have a prohibitive cost, when using very high resolution satellite data. This study's five-year data collection interval and additional data collected following the storm event was adequate for understanding both the decadal trends and Hurricane Sandy's impact. Jamaica Bay is representative of the future for increasingly populated coastal communities worldwide, necessitating continued remote sensing monitoring of the impact of urbanization on the Bay's salt marsh. Long-term monitoring requires additional exploration of the impact that multiple sensors have on change analyses. The switch from Quickbird-2 to Worldview-2 could be partly responsible for the change seen from 2008 to 2012. Quantifying this impact is a necessary step as we proceed into the third decade of commercially available very high resolution satellite imagery.

5. Conclusions

This study reiterates the importance of continuing salt marsh monitoring with high spatial resolution satellite data within Jamaica Bay. This long history of monitoring allows an understanding of salt marsh change, restoration, and natural disturbance. Despite 10 years of restoration, salt marshes in Jamaica Bay continue to decline, though the yearly rate of loss slowed from 13.4 ha from 1989-2003 to 2.1 ha from 2003-2013 [5]. While Quickbird-2 data resulted in an adequate classification, a single scene of Worldview-2 was better suited to discern between salt marsh vegetation classes. The analysis of individual marsh islands elucidates the varied responses over the last 10 years such as the stabilization of JoCo and the near complete loss of Pumpkin Patch.

Hurricane Sandy influenced both the salt marsh and freshwater wetlands of Jamaica Bay. The 2013 growing season in the Bay appeared to be impacted by the hurricane. The greatest change in Jamaica Bay attributed to Hurricane Sandy was the breach of West Pond, which caused a die-off of both upland and freshwater wetland vegetation within this important bird habitat. In total 8.6 ha of vegetation was lost around West Pond. Continued monitoring of the site is necessary to understand the long-term recovery of this area. While outside of our study's target salt marsh protocol, the classification and change analysis was robust enough to interpret this landscape's change.

The vegetation loss in Jamaica Bay slowed over the study period. The salt marsh extent increased from 2012 to 2013 which can partly be accounted for by the restoration of Yellow Bar, movement of wrack off the salt marsh, and differences in

phenology between the two dates. Significant vegetation loss occurred in smaller salt marsh islands and the West Pond area.

The dynamic nature and complexity of coastal wetlands makes monitoring with high temporal resolution important and necessary to understand change. This study demonstrates the feasibility of object-based classification and change detection using Worldview-2 data for mapping, monitoring and understanding salt marsh change in Jamaica Bay. The approach could be expanded to other coastal systems, with a focus on areas of restoration or periods of change. The decline of the salt marsh habitats in the Jamaica Bay is of concern from an ecological stand point and for the important role that coastal wetlands have in mitigating storm surge [61]. Future research should explore the impact of tidal stage on vegetation extent within the salt marsh environments of Jamaica Bay.

Table 1. Vegetation Indices, including Worldview-2 Vegetation Index, Worldview-2 Water Index, Red Edge Vegetation Index, Normalized Difference Vegetation Index and Soil Adjusted Vegetation Index.

WVVI	WVWI	NDVI	Red Edge Vegetation Index	SAVI
$\frac{(NIR2 - Red)}{(NIR2 + Red)}$	$\frac{(CB - NIR2)}{(CB + NIR2)}$	$\frac{(NIR - Red)}{(NIR + Red)}$	$\frac{(NIR - Red\ Edge)}{(NIR + Red\ Edge)}$	$\frac{(NIR - RED) * (1 +$ $(NIR + RED + L)$

Table 2. Accuracy assessment analysis (producer's, user's, and overall accuracy).

	Year	Mudflat	Sand	*S. alterniflora* (>50% Vegetation Cover)	Patchy *S. alterniflora*	High Marsh	Water	Wrack	Upland Vegetation	*Phragmites*	Overall Accuracy (%)
Producer's Accuracy (%)	2003	90.12	98.70	70.73	71.43	82.93	97.50	-	92.68	81.01	85.63
	2008	89.53	83.16	76.84	80.23	85.54	96.59	77.46	91.86	85.33	85.23
	2012	89.53	90.70	95.06	88.37	98.77	98.84	80.43	91.46	82.35	90.46
	2013	92.31	92.77	92.05	98.75	91.86	100.0	89.41	94.05	82.35	92.55
User's Accuracy (%)	2003	91.25	95.00	72.50	68.75	85.00	97.50	-	95.00	80.00	85.63
	2008	90.59	92.94	85.88	81.18	83.53	100.0	64.71	92.94	75.29	85.23
	2012	90.59	91.76	90.59	89.41	91.12	100.0	87.06	88.24	82.35	90.46
	2013	98.82	90.59	95.29	92.94	92.94	97.65	89.41	92.94	82.35	92.55

Table 3: Change between 2003 and 2013 (ha). Areas that had no change between the two dates are in grey.

		2013								
	Class	**Water**	**Mudflat**	**Sand**	***S. alterniflora*(50% > Vegetation Cover)**	**Patchy *S. alterniflora***	***Phragmites***	**High Marsh**	**Upland**	**Total 2003 Area (ha)**
2003	Water	485.5	66.3	3.8	12.6	6.7	0.1	0.8	0.0	651.4
	Mudflat	19.4	43.3	3.5	22.4	11.1	0.3	0.7	0.0	102.2
	Sand	0.4	1.0	2.7	0.5	0.2	0.2	0.1	0.1	5.7
	S. alterniflora(50% > vegetation cover)	13.4	16.5	2.5	115.6	10.1	6.1	16.4	1.0	183.4
	Patchy *S. alterniflora*	11.2	19.3	0.8	46.4	8.9	0.4	2.3	0.1	89.9
	Phragmites	0.1	0.2	1.5	2.6	0.8	5.5	1.0	1.1	14.0
	High Marsh	2.3	1.4	0.8	26.6	1.3	3.0	22.8	0.5	59.2
	Upland	0.00	0.2	0.3	0.2	0.2	3.2	0.1	16.5	21.3
	Total 2013 Area (ha)	535.7	148.0	16.1	226.7	36.8	19.0	44.0	19.3	

Table 4. Change of land cover classes between 2012 and 2013 for West Pond area.

		2012					
	Change or No Change Areas (ha)	**Mudflat**	**Sand**	**Wetland**	**Water**	**Upland Veg.**	**Post-Storm Total**
2013	Mudflat	0.3	0.0	4.4	1.0	2.5	8.3
	Sand	0.0	0.4	0.9	0.0	0.4	1.7
	Wetland	0.0	0.0	7.4	0.0	2.8	10.2
	Water	0.1	0.0	0.4	16.9	0.1	17.5
	Upland Veg.	0.0	0.0	0.2	0.0	5.8	6.0
	Pre-storm Total	0.4	0.5	13.3	17.9	11.5	

Table 5. Salt marsh restoration site, year, and extent [16; 46].

Year	Salt Marsh	Area (ha)
2003	Big Egg	1.0
2006–2007	Elders Point East	16.2
2010	Elders Point West	16.2
2012	Yellow Bar	18.2
2013	Black Wall	6.1
2013	Rulers Bar	4.0

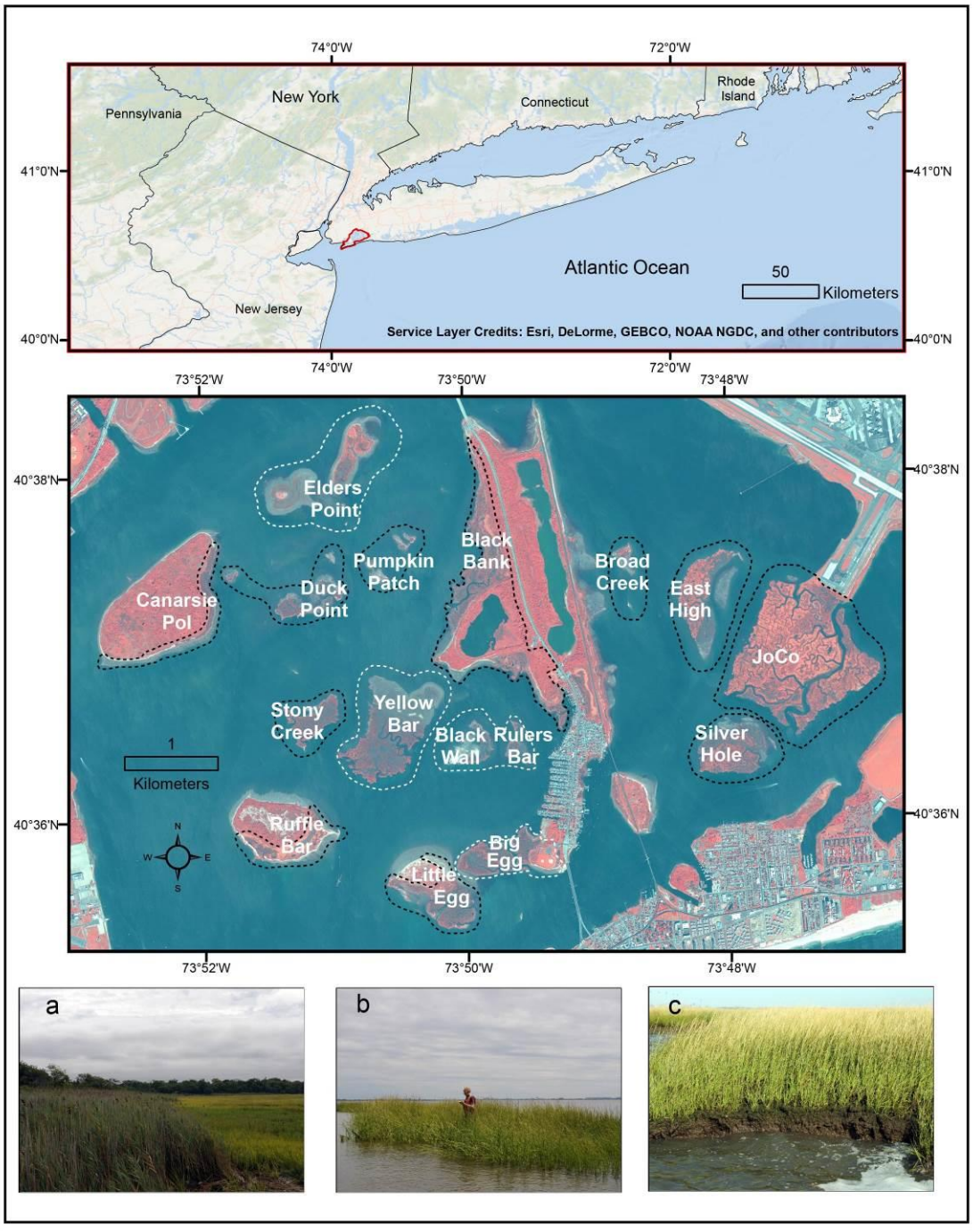

Figure 1. The study area of Jamaica Bay, NYC, includes salt marsh islands as labeled on top of the pseudo color display of 2012 Worldview-2 imagery (NIR-1, G, B in RGB). Field photos illustrate (a) the transition from *Phragmites australis* to salt marsh; (b) Isolated *S. alterniflora* patch; (c) *S. alterniflora* 50-100% cover. Salt marshes that have been restored at some point are indicated by a white border.

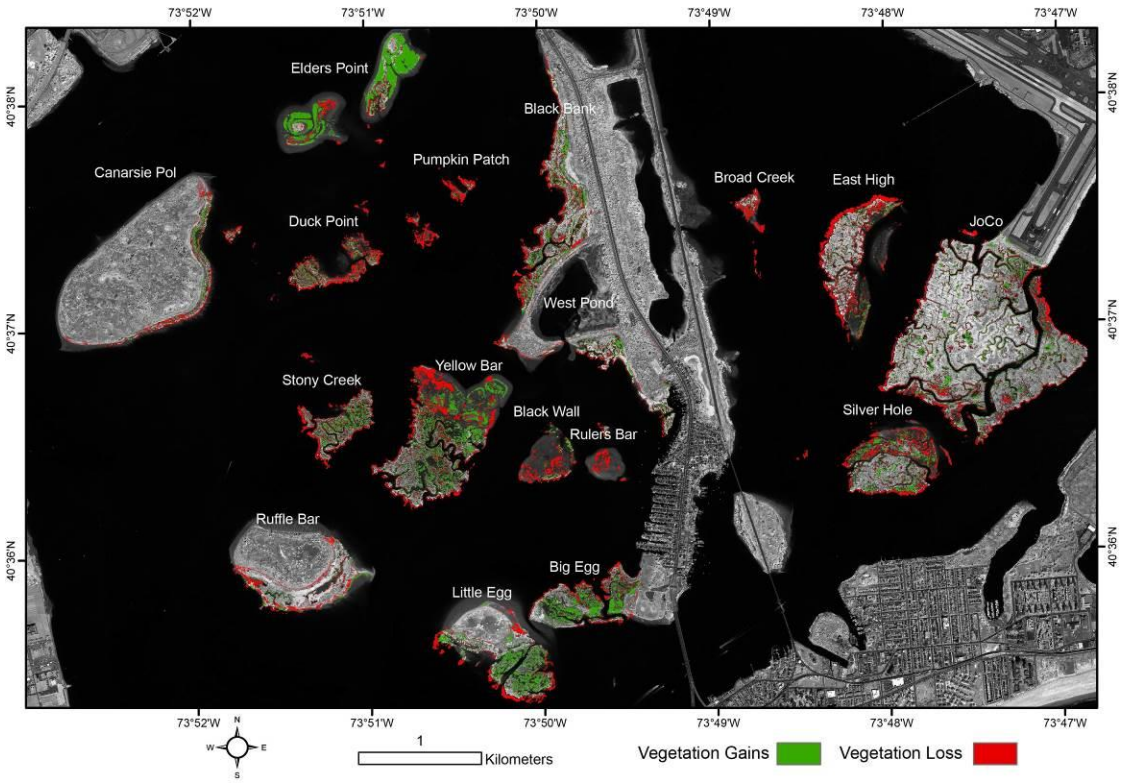

Figure 2: Salt marsh change from 2003 to 2013 displayed on a panchromatic 2013 Worldview-2 imagery.

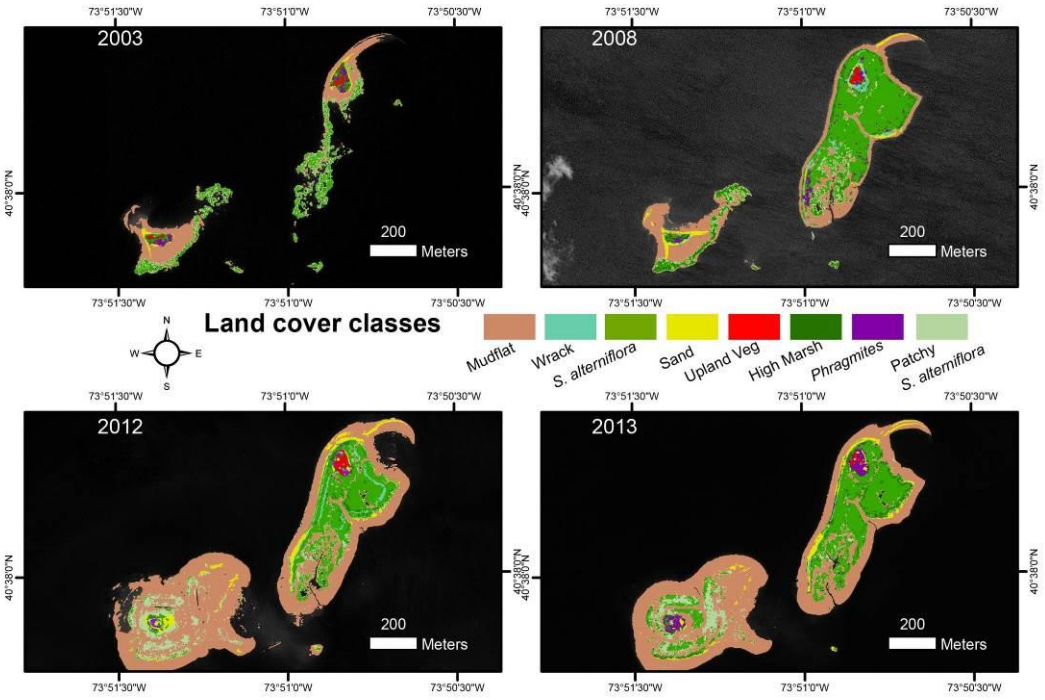

Figure 3: Salt marsh of Elders Point East and West for 2003, 2008, 2012 and 2013.

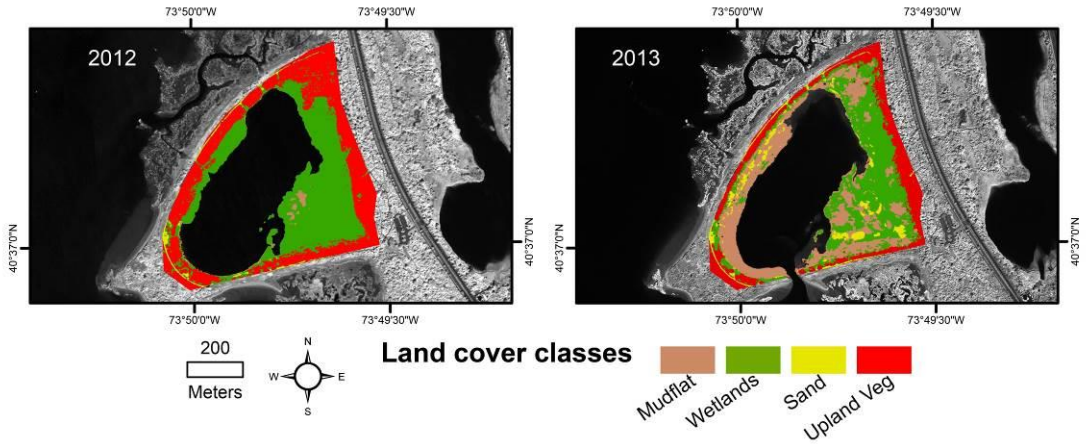

Figure 4: Vegetation change from 2012 to 2013 of the West Pond area.

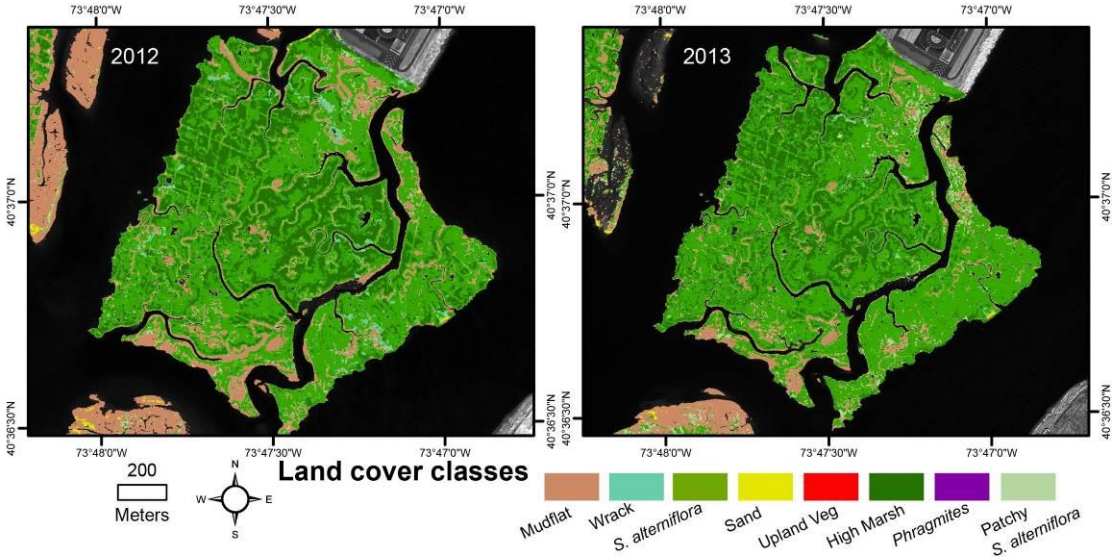

Figure 5: The JoCo salt marsh for 2012 and 2013.

SUPPLEMENTARY MATERIALS
Appendix A

Table A1. Land cover extent of salt marsh islands (ha).

Marsh	Year	Mudflat	Sand	*S. alternifl ora* (50% ≥ Vegetati on Cover)	Patchy *S. alternifl ora*	High Marsh	Water	Wrack	Upland Vegetati on	*Phragm ites*
Pumpk in Patch	2003	0.9	0.0	1.3	1.6	*0.0*	30.3	-	0.0	0.0
	2008	2.1	0.0	0.8	0.7	*0.1*	28.9	0.1	0.0	0.0
	2012	3.3	1.4	0.2	0.3	0.0	27.4	0.1	0.0	0.0
	2013	0.7	0.1	0.2	0.2	0.0	31.4	0.0	0.0	0.0
Canars ie Pol	2003	3.9	0.9	5.4	2.5	1.8	12.6	-	1.2	1.7
	2008	3.9	0.6	5.1	1.6	2.1	12.9	0.7	0.6	2.5
	2012	9.5	1.8	4.2	3.3	0.1	6.2	0.7	0.7	3.4
	2013	7.2	1.8	5.2	1.1	0.3	9.4	0.3	0.3	4.2
Stony Creek	2003	3.9	0.0	5.4	4.8	0.2	41.7	-	0.0	0.0
	2008	4.1	0.0	6.4	2.9	1.2	21.8	0.1	0.0	0.0

	2012	5.4	0.3	6.3	2.3	0.0	22.1	0.0	0.0	0.0
	2013	3.1	0.1	7.5	1.6	0.0	24.2	0.0	0.0	0.0
Little Egg	2003	7.7	0.7	7.1	6.1	0.8	22.6	-	0.0	1.6
	2008	8.2	1.7	9.5	4.0	3.3	18.7	1.8	0.0	0.5
	2012	10.8	4.4	10.3	4.5	0.3	13.8	1.1	0.0	0.2
	2013	6.7	4.8	13.4	2.2	0.6	16.8	0.1	0.0	0.7
Big Egg	2003	8.5	0.1	7.3	5.3	1.4	15.4	-	0.1	0.6
	2008	5.8	0.1	11.9	3.6	2.5	11.7	0.3	0.1	0.6
	2012	12.0	0.3	8.5	4.8	0.2	8.6	0.5	0.0	0.4
	2013	5.9	0.2	12.6	3.2	0.3	12.3	0.1	0.0	0.8
Black Wall + Rulers Bar	2003	2.9	0.0	1.5	2.6	0.0	47.4	-	0.0	0.0
	2008	5.1	0.0	2.1	2.3	1.0	43.9	0.0	0.0	0.0
	2012	8.3	2.9	1.2	1.5	0.0	40.4	0.0	0.0	0.0
	2013	17.1	1.1	0.9	0.3	0.0	34.9	0.0	0.0	0.0
Black Bank	2003	9.5	1.1	27.4	11.5	5.4	27.2	-	19.6	4.8
	2008	8.9	1.7	27.0	6.7	5.0	20.3	3.2	19.7	7.7
	2012	19.3	2.7	25.7	6.8	2.4	15.5	3.0	19.2	5.6

	2013	8.6	2.3	29.4	3.5	3.5	24.7	1.	18.8	8.4
Duck Point	2003	4.6	0.1	3.9	2.6	0.6	40.2	-	0.0	0.0
	2008	2.6	0.1	4.1	4.3	0.1	49.7	0.0	0.0	0.0
	2012	10.4	1.0	3.2	2.1	0.0	35.3	0.2	0.0	0.0
	2013	4.3	0.2	3.8	1.3	0.0	42.6	0.0	0.0	0.0
Broad Creek	2003	1.3	0.0	1.4	0.7	0.6	33.9	-	0.0	0.1
	2008	1.8	0.2	0.8	0.2	0.4	27.4	0.2	0.0	0.0
	2012	2.7	0.4	0.6	0.2	0.1	26.9	0.1	0.0	0.0
	2013	1.3	0.2	0.8	0.2	0.1	28.4	0.0	0.0	0.1
East High	2003	10.5	0.1	14.3	5.8	3.0	49.6	-	0.0	0.0
	2008	15.1	0.1	12.5	3.1	4.0	48.2	0.3	0.0	0.0
	2012	18.7	0.7	11.8	1.6	2.6	47.7	0.2	0.0	0.0
	2013	5.1	0.3	12.7	1.7	2.8	60.6	0.0	0.0	0.0
JoCo	2003	11.1	0.1	72.4	20.1	37.5	83.6	-	0.1	1.3
	2008	11.9	0.1	74.5	11.8	44.6	79.6	3.1	0.0	0.4
	2012	18.5	0.3	82.0	6.5	35.5	80.9	2.2	0.0	0.1

	2013	12.6	0.1	90.7	7.1	29.8	85.1	0.5	0.0	0.0
Elders Point West	2003	2.8	0.2	1.2	0.7	0.2	40.1	-		0.1
	2008	3.9	0.4	1.0	0.5	0.5	38.4	0.1	0.0	0.1
	2012	15.5	0.7	0.5	2.8	0.0	25.3	0.1	0.0	0.1
	2013	14.0	0.3	2.2	2.4	0.2	25.5	0.3	0.0	0.3
Yellow Bar	2003	18.2	0.0	12.9	12.6	0.8	67.9	-	0.0	0.0
	2008	23.1	0.0	17.5	9.0	1.8	56.4	0.1	0.0	0.0
	2012	43.0	0.7	12.5	5.6	0.1	46.0	0.1	0.0	0.0
	2013	33.7	0.1	18.7	7.5	0.1	48.0	0.0	0.0	0.0
Silverhole	2003	11.1	0.0	11.8	8.0	0.9	40.7	-	0.0	0.0
	2008	12.6	0.0	15.2	3.3	1.1	25.5	0.2	0.0	0.1
	2012	16.6	0.4	12.9	3.0	0.2	24.5	0.3	0.0	0.0
	2013	13.3	0.2	14.5	3.4	0.3	26.1	0.0	0.0	0.0
Ruffle Bar	2003	4.1	1.9	7.7	1.8	6.4	12.0	-	0.1	3.0
	2008	3.7	2.5	6.3	0.8	7.7	11.3	2.1	0.0	0.5
	2012	7.7	3.4	6.5	1.5	5.2	7.4	1.0	2.2	0.0

	2013	44.6	3.3	6.1	0.7	5.1	11.1	0.2	3.9	0.0
Elders Point East	2003	2.3	0.2	2.0	1.5	0.2	68.0	0.0	0.1	0.2
	2008	5.4	0.3	11.0	1.0	0.7	54.4	0.7	0.2	0.6
	2012	11.4	1.2	7.5	1.1	0.5	51.1	1.0	0.3	0.1
	2013	9.6	1.0	8.2	0.7	0.9	53.1	0.2	0.1	0.6

Table A2. Salt marsh change rates for 2003-2008, 2008-2012 and 2012-2013 (ha/year).

Marsh	2003–2008	2008–2012	2012–2013
Pumpkin Patch	−0.3	−0.3	−0.1
Canarsie Pol	−0.01	−0.1	−0.2
Stony Creek	0.03	−0.5	0.5
Little Egg	0.3	−0.5	1.5
Big Egg	0.8	−1.2	2.9
Black wall + Rulers Bar	0.2	−0.7	−1.5
Black Bank	−0.5	−1.5	4.3
Duck Point	0.3	−0.8	−0.1
Broad Creek	−0.3	−0.1	0.2
East High	−0.7	−0.9	1.3
JoCo	0.0	−1.7	3.5
Elders Point West	−0.02	0.3	1.6
Elders Point East	1.9	−1.0	1.1
Yellow Bar	0.4	−2.5	8.0
Silverhole	−0.2	−0.9	2.2
Ruffle Bar	−0.7	−0.5	−1.4

Table A3: Object parameters used in OBIA for 2012 and 2013 Worldview-2 imagery classification.

Variable Type	Variable Name	Variable Importance
Elevation	DEM mean	47
Elevation	DEM Standard Deviation (SD)	4
Elevation	DEM min	4
Elevation	DEM max	57
Elevation	DEM range	3
Elevation	DEM sum	17
Geospatial	Node points	0
Geospatial	Perimeter	1
Geospatial	Area	1
Ancillary	Upland binary layer	36
Spectral	Coastal blue mean	24
Spectral	Coastal blue SD	2
Spectral	Blue mean	31
Spectral	Blue SD	1
Spectral	Green mean	28
Spectral	Green SD	0
Spectral	Yellow Mean	26
Spectral	Yellow SD	1
Spectral	Red mean	29
Spectral	Red SD	1
Spectral	Red edge mean	46
Spectral	Red Edge SD	3
Spectral	NIR1 mean	58
Spectral	NIR2 Mean	67
Spectral	Coastal blue mean neighborhood difference	0

Variable Type	Variable Name	Variable Importance
Spectral	Blue mean neighborhood difference	0
Spectral	Green mean neighborhood difference	1
Spectral	Yellow mean neighborhood difference	1
Spectral	Red mean neighborhood difference	1
Spectral	Red edge mean neighborhood difference	0
Spectral	NIR1 mean neighborhood difference	0
Spectral	NIR2 mean neighborhood difference	0
Spectral	Coastal blue mean neighborhood difference	16
Spectral	Blue mean scene difference	20
Spectral	Green mean scene difference	30
Spectral	Yellow mean scene difference	25
Spectral	Red mean scene difference	33
Spectral	Red edge mean scene difference	54
Spectral	NIR1 mean scene difference	51
Spectral	NIR2 mean scene difference	73
Spectral	NIR1 SD	4
Spectral	NIR2 SD	1
Texture	Correlation mean	0
Texture	Entropy mean	0

Variable Type	Variable Name	Variable Importance
Texture	Inverse Difference Moment(IDM) mean	0
Texture	Uniformity mean	0
Texture	Contrast mean	0
Texture	Correlation mean neighborhood difference	0
Texture	Entropy mean neighborhood difference	0
Texture	IDM mean neighborhood difference	0
Texture	Uniformity mean neighborhood difference	0
Texture	Contrast mean scene difference	0
Texture	Correlation mean scene difference	0
Texture	Entropy mean scene difference	0
Texture	IDM mean scene difference	0
Texture	Uniformity mean scene difference	0
Texture	Contrast SD	0
Texture	Entropy SD	0
Texture	IDM SD	0
Texture	Uniformity SD	0
Vegetation Index	REVI mean	26
Vegetation Index	WVVI mean	74
Vegetation Index	WVWI mean	93
Vegetation Index	REVI mean neighborhood difference	0.9
Vegetation Index	WVVI mean neighborhood difference	1

Variable Type	Variable Name	Variable Importance
Vegetation Index	WVWI mean neighborhood difference	1
Vegetation Index	REVI mean scene difference	12
Vegetation Index	WVVI mean scene difference	66
Vegetation Index	WVWI mean scene difference	100
Vegetation Index	REVI SD	0
Vegetation Index	WVVI SD	0
Vegetation Index	WVWI SD	0
Vegetation Index	SAVI range	0
Vegetation Index	SAVI mean	39
Vegetation Index	SAVI SD	0
Vegetation Index	NDVI range	0
Vegetation Index	NDVI mean	50
Vegetation Index	NDVI SD	0

Acknowledgments

This study was funded by the Northeast Coastal and Barrier Network of the National Park Service. We appreciate the support by administrators and professionals from the Gateway National Recreation Area of the National Park Service, in particular Tami Pearl, Mary-Jo Marino, Patti Rafferty, Doug Adamo, Mark Ringenary for their expertise, insights and guidance. Thom Curdts provided thoughtful editorial comments. We appreciate the insightful and constructive comments and suggestions by the anonymous reviewers that helped improve the quality of the manuscript.

References

1. Zedler, J.B.; Kercher, S. Wetland Resources: Status, Trends, Ecosystem Services, and Restorability. Annu. Rev. Environ. Resour. **2005**, 30, 39–74. [CrossRef]
2. Dahl, T.E. Wetlands Losses in the United States, 1780's to 1980's; Report to the Congress; U.S. Department of the Interior, Fish and Wildlife Service: Washington, DC, USA, 1990.
3. Dahl, T.E.; Stedman, S. Status and Trends of Wetlands in the Conterminous United States 2004 to 2009; U.S. Department of the Interior, U.S. Fish and Wildlife Service, Fisheries and Habitat Conservation: Washington, DC, USA, 2011.
4. Rafferty, P.; Castagna, J.; Adamo, D. Building Partnerships to Restore an Urban Marsh Ecosystem at Gateway National Recreation Area; Park Science: Integrating Reseearch and Resource Management in the National Parks; National Park Service: Washington, DC, USA, 2010.
5. National Park Service. An Update on the Disappearing Salt Marshes of Jamaica Bay, New York; Prepared by Gateway National Recreation Area; National Park Service: Washington, DC, USA, 2007.
6. Deegan, L.A.; Johnson, D.S.;Warren, R.S.; Peterson, B.J.; Fleeger, J.W.; Fagherazzi, S.;Wollheim,W.M. Coastal Eutrophication as a Driver of Salt Marsh Loss. Nature **2012**, 490, 388–392.
7. Wang, Y.; Tobey, J.; Bonynge, G.; Nugranad, J.; Makota, V.; Ngusaru, A.; Traber, M. Involving Geospatial Information in the Analysis of Land-Cover Change along the Tanzania Coast. Coast. Manag. **2005**, 33, 87–99.

8. Wang, Y.; Christiano, M.; Traber, M.;Wang, J. Mapping salt marshes in Jamaica Bay and terrestrial vegetation in Fire Island National seashore using QuickBird satellite data. In Remote Sensing of Coastal Environments; CRC Press: Boca Raton, FL, USA, 2010; pp. 191–208.
9. Wang, Y.; Traber, M.; Milstead, B.; Stevens, S. Terrestrial and Submerged Aquatic Vegetation Mapping in Fire Island National Seashore using High Spatial Resolution Remote Sensing Data. Mar. Geod. **2007**, 30, 77–95.
10. Aerts, J.C.; Lin, N.; Botzen, W.; Emanuel, K.; de Moel, H. Low-Probability Flood Risk Modeling for New York City. Risk Anal. **2013**, 33, 772–788.
11. Rosenzweig, C.; Solecki, W. Hurricane Sandy and Adaptation Pathways in New York: Lessons from a First-Responder City. Glob. Environ. Chang. **2014**, 28, 395–408.
12. Michener,W.K.; Blood, E.R.; Bildstein, K.L.; Brinson, M.M.; Gardner, L.R. Climate Change, Hurricanes and Tropical Storms, and Rising Sea Level in Coastal Wetlands. Ecol. Appl. **1997**, 7, 770–801.
13. United States Census Bureau—American FactFinder. DP02: Selected Social Characteristics in the United States. American Community Survey 2014. Available online: https://factfinder.census.gov/faces/tableservices/jsf/pages/productview.xhtml?pid=ACS_15_5YR_S0101&prodType=table (accessed on 30 October 2016).
14. New York City Department of Environmental Protection. Jamaica Bay Watershed Protection Plan. In Planning for Jamaica Bay's Future: Final Recommendations on the Jamaica Bay Watershed Protection; Jamaica Bay Watershed Protection Plan Advisory Committee: New York, NY, USA, 2007; pp. 1–75.

15. Benotti, M.J.; Abbene, M.; Terracciano, S.A. Nitrogen Loading in Jamaica Bay, Long Island, New York: Predevelopment to 2005; U.S. Geological Survey Scientific Investigations Report 2007-5051; U.S. Geological Survey, New YorkWater Science Center: Troy, NY, USA, 2007; pp. 1–17.
16. Frame, G.W.; Mellander, K.M.; Adamo, D.A. Big egg marsh experimental restoration in Jamaica Bay, New York. In People, Places, and Parks: Proceedings of the 2005 George Wright Society Conference on Parks, Protected Areas, and Cultural Sites; Harmon, D., Ed.; The George Wright Society: Hancock, MI, USA, 2006; pp. 2–9.
17. Lane, C.R.; Liu, H.; Autrey, B.C.; Anenkhonov, O.A.; Chepinoga, V.V.; Wu, Q. Improved Wetland Classification using Eight-Band High Resolution Satellite Imagery and a Hybrid Approach. Remote Sens. **2014**, 6, 12187–12216.
18. Hay, G.J.; Castilla, G. Geographic Object-Based Image Analysis (GEOBIA): A new name for a new discipline. In Object-Based Image Analysis; Springer: Berlin/Heidelberg, Germany, 2008; pp. 75–89.
19. Chen, G.; Hay, G.J.; Carvalho, L.M.; Wulder, M.A. Object-Based Change Detection. Int. J. Remote Sens. **2012**, 33, 4434–4457.
20. Powers, R.P.; Hay, G.J.; Chen, G. How Wetland Type and Area Differ through Scale: A GEOBIA Case Study in Alberta's Boreal Plains. Remote Sens. Environ. **2012**, 117, 135–145.
21. Espindola, G.; Câmara, G.; Reis, I.; Bins, L.; Monteiro, A. Parameter Selection for region-growing Image Segmentation Algorithms using Spatial Autocorrelation. Int. J. Remote Sens. **2006**, 27, 3035–3040.

22. Johnson, B.; Xie, Z. Unsupervised Image Segmentation Evaluation and Refinement using a Multi-Scale Approach. ISPRS J. Photogramm. Remote Sens. **2011**, 66, 473–483.

23. Liu, D.; Xia, F. Assessing Object-Based Classification: Advantages and Limitations. Remote Sens. Lett. **2010**, 1, 187–194.

24. Bo, S.; Ding, L.; Li, H.; Di, F.; Zhu, C. Mean shift-based Clustering Analysis of Multispectral Remote Sensing Imagery. Int. J. Remote Sens. **2009**, 30, 817–827.

25. Yang, G.; Pu, R.; Zhang, J.; Zhao, C.; Feng, H.; Wang, J. Remote Sensing of Seasonal Variability of Fractional Vegetation Cover and Its Object-Based Spatial Pattern Analysis Over Mountain Areas. ISPRS J. Photogramm.Remote Sens. **2013**, 77, 79–93.

26. Ming, D.; Li, J.; Wang, J.; Zhang, M. Scale Parameter Selection by Spatial Statistics for GeOBIA: Using Mean-Shift Based Multi-Scale Segmentation as an Example. ISPRS J. Photogramm. Remote Sens. **2015**, 106, 28–41.

27. Rodriguez-Galiano, V.F.; Ghimire, B.; Rogan, J.; Chica-Olmo, M.; Rigol-Sanchez, J.P. An Assessment of the Effectiveness of a Random Forest Classifier for Land-Cover Classification. ISPRS J. Photogramm. Remote Sens. **2012**, 67, 93–104.

28. Corcoran, J.M.; Knight, J.F.; Gallant, A.L. Influence of Multi-Source and Multi-Temporal Remotely Sensed and Ancillary Data on the Accuracy of Random Forest Classification of Wetlands in Northern Minnesota. Remote Sens. **2013**, 5, 3212–3238.

29. Van Beijma, S.; Comber, A.; Lamb, A. Random Forest Classification of Salt Marsh Vegetation Habitats using Quad-Polarimetric Airborne SAR, Elevation and Optical RS Data. Remote Sens. Environ. **2014**, 149, 118–129.

30. Hartig, E.K.; Kolker, A.; Gornitz, V. Investigations into recent salt marsh losses in Jamaica Bay, New York. In Integrated Reconnaissance of the Physical and Biogeochemical Characteristics of Jamaica Bay: Initial Activity Phase; Gateway National Recreation Area and the Columbia Earth Institute: New York, NY, USA, 2002; pp. 21–40.
31. Akar, Ö.; Güngör, O. Integrating Multiple Texture Methods and NDVI to the Random Forest Classification Algorithm to Detect Tea and Hazelnut Plantation Areas in Northeast Turkey. Int. J. Remote Sens. **2015**, 36,442–464.
32. Kim, M.; Warner, T.A.; Madden, M.; Atkinson, D.S. Multi-Scale GEOBIA with very High Spatial Resolution Digital Aerial Imagery: Scale, Texture and Image Objects. Int. J. Remote Sens. **2011**, 32, 2825–2850.
33. Mutanga, O.; Adam, E.; Cho, M.A. High Density Biomass Estimation for Wetland Vegetation using WorldView-2 Imagery and Random Forest Regression Algorithm. Int. J. Appl. Earth Obs. Geoinf. **2012**, 18, 399–406.
34. Johnson, B. Effects of Pansharpening on Vegetation Indices. ISPRS Int. J. Geo-Inf. **2014**, 3, 507–522.
35. Psuty, N.; McLoughlin, S.; Schmelz,W.; Spahn, A. Unpublished Digital Geomorphological-GIS Map of the Jamaica Bay Unit, Gateway National Recreation Area. IRMA 2014. Available online: https://irma.nps.gov/DataStore/Reference/Profile/2233887 (accessed on 30 October 2016).
36. National Oceanic and Atmospheric Administration. NOAA Post Hurricane Sandy Topobathymetric LiDAR Mapping for Shoreline Mapping. 2014. Available online:

https://data.noaa.gov/dataset/2014-noaa-posthurricane-sandy-topobathymetric-lidar-mapping-for-shoreline-mapping (accessed on 30 October 2016).

37. Duro, D.C.; Franklin, S.E.; Dubé, M.G. A Comparison of Pixel-Based and Object-Based Image Analysis with Selected Machine Learning Algorithms for the Classification of Agricultural Landscapes using SPOT-5 HRG Imagery. Remote Sens. Environ. **2012**, 118, 259–272.

38. Lantz, N.J.;Wang, J. Object-Based Classification ofWorldview-2 Imagery for Mapping Invasive Common Reed, Phragmites Australis. Can. J. Remote Sens. **2013**, 39, 328–340.

39. Congalton, R.G. A Review of Assessing the Accuracy of Classifications of Remotely Sensed Data. Remote Sens. Environ. **1991**, 37, 35–46. [CrossRef]

40. Congalton, R.G.; Green, K. Assessing the Accuracy of Remotely Sensed Data: Principles and Practices; CRC Press: Boca Raton, FL, USA, 2008.

41. Center for Operational Oceanographic Products and Services (CO-OPS). Sandy Hook Tidal Station. 2015. Available online: https://tidesandcurrents.noaa.gov/waterlevels.html?id=8531680 (accessed on 30 October 2016).

42. Brand, C.J.;Windingstad, R.M.; Siegfried, L.M.; Duncan, R.M.; Cook, R.M. Avian Morbidity and Mortality from Botulism, Aspergillosis, and Salmonellosis at Jamaica Bay Wildlife Refuge, New York, USA. Colonial Waterbirds **1988**, 11, 284–292.

43. National Park Service. Jamaica Bay Wildlife Refuge West Pond Trail Breach Repair Environmental Assessment; National Park Service: Washington, DC, USA, 2015; Volume 1, pp. 1–304.

44. New York City Department of Environmental Protection. Jamaica Bay Watershed Protection Plan 2014 Update; New York City Department of Environmental Protection: New York, NY, USA, 2014; pp. 1–57.

45. Wigand, C.; Roman, C.T.; Davey, E.; Stolt, M.; Johnson, R.; Hanson, A.; Watson, E.B.; Moran, S.B.; Cahoon, D.R.; Lynch, J.C. Below the Disappearing Marshes of an Urban Estuary: Historic Nitrogen Trends and Soil Structure. Ecol. Appl. **2014**, 24, 633–649.

46. U.S. Army Corps of Engineers New York District. Vision of a World Class Harbor Estuary; Harbor Inspection: Huntington, NY, USA, 2015; pp. 1–70.

47. Zedler, J.B.; Callaway, J.C. TrackingWetland Restoration: Do Mitigation Sites Follow Desired Trajectories? Restor. Ecol. **1999**, 7, 69–73.

48. McKee, K.L.; Cherry, J.A. Hurricane Katrina Sediment Slowed Elevation Loss in Subsiding Brackish Marshes of the Mississippi River Delta. Wetlands **2009**, 29, 2–15.

49. Roman, C.T.; Peck, J.A.; Allen, J.; King, J.W.; Appleby, P.G. Accretion of a New England (USA) Salt Marsh in Response to Inlet Migration, Storms, and Sea-Level Rise. Estuar. Coast. Shelf Sci. **1997**, 45, 717–727.

50. Guntenspergen, G.R.; Cahoon, D.R.; Grace, J.; Steyer, G.D.; Fournet, S.; Townson, M.A.; Foote, A.L. Disturbance and Recovery of the Louisiana Coastal Marsh Landscape from the Impacts of Hurricane Andrew. J. Coast. Res. **1995**, 21, 324–339.

51. Day, J.W.; Britsch, L.D.; Hawes, S.R.; Shaffer, G.; Reed, D.J.; Cahoon, D. Pattern and Process of Land Loss in the Mississippi Delta: A Spatial and Temporal Analysis ofWetland Habitat Change. Estuaries **2000**, 23, 425–438.

52. Hook, D.D.; Buford, M.A.;Williams, T.M. Impact of Hurricane Hugo on the South Carolina Coastal Plain Forest. J. Coast. Res. **1991**, 291–300.

53. Flynn, K.; McKee, K.; Mendelssohn, I. Recovery of Freshwater Marsh Vegetation after a Saltwater Intrusion Event. Oecologia **1995**, 103, 63–72.

54. Stanturf, J.A.; Goodrick, S.L.; Outcalt, K.W. Disturbance and Coastal Forests: A Strategic Approach to Forest Management in Hurricane Impact Zones. For. Ecol. Manag. **2007**, 250, 119–135.

55. National Park Service. Finding of No Significant Impact Jamaica Bay Wildlife Refuge West Pond Trail Breach Repair; National Park Service: Washington, DC, USA, 2016; pp. 1–56.

56. Byer, M.; Frame, G.; Panagakos, W.; Waaijer, M.; Aranbayev, Z.; Michaels, Y.; Stalter, R.; Schreibman, M. Effects of Wrack Accumulation on Spartina Alterniflora, Jamaica Bay Wildlife Refuge, New York City. WIT Trans. Ecol. Environ. **2004**, 68, 1–8.

57. Stedman, S.; Dahl, T.E. Status and Trends of Wetlands in the Coastal Watersheds of the Eastern United States 1998 to 2004; United States Fish and Wildlife Service: Washington, DC, USA, 2008; pp. 1–32.

58. National Oceanic and Atmosphere Administration. Northeast 2010 Coastal Change Analysis Program Accuracy Assessment; National Oceanic and Atmosphere Administration: Silver Spring, MD, USA, 2014; pp. 1–11.

59. Shuman, C.S.; Ambrose, R.F. A Comparison of Remote Sensing and Ground-Based Methods for Monitoring Wetland Restoration Success. Restor. Ecol. **2003**, 11, 325–333.

60. Raposa, K.B.;Weber, R.L.; Ekberg, M.C.; Ferguson,W. Vegetation Dynamics in Rhode Island Salt Marshes during a Period of Accelerating Sea Level Rise and Extreme Sea Level Events. Estuar. Coasts **2016**, 1–11.

61. Costanza, R.; Perez-Maqueo, O.; Martinez, M.; Sutton, P.; Anderson, S.J.; Mulder, K. The Value of Coastal Wetlands for Hurricane Protection. Ambio **2008**, 37, 241–248.

CHAPTER 2

Examining the Influence of Tidal Stage on Salt Marsh Mapping Using High Spatial Resolution Satellite Remote Sensing and Topobathymetric LiDAR

By

Anthony Campbell, Yeqiao Wang*

Published as Campbell, A. Wang, Y. 2018. Examining the Influence of Tidal Stage on Salt Marsh Mapping using High Spatial Resolution Satellite Remote Sensing and Topobathymetric LiDAR. 56 (9). *IEEE Transactions on Geoscience and Remote Sensing.*

Department of Natural Resources Science
University of Rhode Island
Kingston, RI 02881

*Corresponding author, Yeqiao Wang, yqwang@uri.edu, 1 Greenhouse Road, Kingston RI, 02881.

Abstract

Salt marsh vegetation extent and zonation are often controlled by bottom up factors determined in part by the frequency and duration of tidal inundation. Tidal inundation during remote-sensing mapping of salt marsh resources can alter the resulting image classification. The degree of this impact on mapping with very high resolution (VHR) imagery has yet to be determined. This paper utilizes topobathymetric light detection and ranging (LiDAR) data and bathtub models of a tidal stage at 5 cm intervals from mean low water (MLW) to mean high water (MHW) and determines the impact of tidal variation in salt marsh mapping within Jamaica Bay, NY, USA. Tidal inundation models were compared with the Worldview-2 and Quickbird-2 imageries acquired at a range of tidal stages. The modeled inundation of normalized difference vegetation index and smooth cordgrass (*S. alterniflora*) maps was compared from MLW to MHW. This paper finds that at 0.6 m above MLW, only 3.5% of *S. alterniflora* is inundated. This paper demonstrates a modeling approach integrating VHR satellite remote-sensing data and topobathymetric LiDAR data to address tidal variation in salt marsh mapping. The incremental modeling of the tidal stage is important for understanding areas most at risk from sea level rise and informs management decisions in accordance with this.

I. INTRODUCTION

Salt marshes are an important coastal ecosystem providing habitat, denitrification, carbon sequestration, and coastal resilience by reducing the impacts of wave energy and storm surge and by their process of adaption to sea level rise (SLR) [1], [2]. Salt marsh losses in Jamaica Bay, an estuary within New York City, are driven primarily by nutrient enrichment, an increased tidal range, a lack of sediment, and increased sulfide concentrations [3]. Jamaica Bay has a long history of salt marsh mapping and monitoring using remote sensing. Salt marshes mapped from aerial photographs acquired in the 1950s demonstrated significant losses [4]. Since 2003, very high-spatial-resolution satellites have been used to monitor and determine the change in the bay [5], [6]. An object-oriented classification using the Worldview-2 satellite imagery has been used to map the salt marsh extent and the change caused by a storm event and restoration activities in the bay [6].

The accurate determination of the salt marsh extent and the change by remote sensing is impacted by the tidal stage at the time of image acquisition. When mapping a vegetation change in tidal environments, differences in the tidal stage can lead to an erroneous identification of change [7]. The influence of the tidal stage on salt marsh vegetation mapping is a topic that has been addressed infrequently in the literature. Salt marsh vegetation zonation and extent are dependent on many factors driven by tidal inundation. For example, the lower bound of the growth range of smooth cordgrass, *S. alterniflora*, is limited by physical stress from abiotic factors [8]. A tidal stage above mean low water (MLW) can reduce the extent of vegetation mapped; an imagery acquired above mean highest high water corresponded with a 40% reduction

in the mapped vegetation extent [9]. That study led to the recommendation that when mapping salt marsh, an imagery should be acquired within 0–0.6 to a maximum of 0.9 m above MLW. These guidelines have been applied to the Coastal Change Analysis Program protocol and other salt marsh mapping projects [10], [11]. The spatial resolution of remote-sensing data can influence many aspects of image classification and the coastal change analysis [12]. A variety of high-spatial-resolution imageries, including Worldview-2, Quickbird-2, orthoimagery, and historic imageries, have been utilized for mapping salt marshes [13]. Therefore, understanding the impact of the tidal stage on a very high resolution (VHR) imagery in coastal mapping is necessary. In this study, impact is defined as an increase in misclassification of salt marsh vegetation due to tidal inundation muting spectral differences. The study quantifies this as those areas with normalized difference vegetation index (NDVI) < 0 in the imagery and inundated areas in the models.

There have been several approaches to quantifying and accounting for tidal uncertainty in remote-sensing classifications. *In situ* measurements and the Quickbird-2 satellite-obtained spectra have been found to be similar despite a variety of tidal stages [14]. For a medium-resolution imagery, a digital elevation model (DEM) in combination with a satellite imagery has been used to quantify and limit the impact of the tidal stage on vegetation mapping [15]. In this paper, we explored a novel approach to understand the impact of the tidal stage on the vegetation extent using VHR satellite remote-sensing data and topobathymetric light detection and ranging (LiDAR).

LiDAR is often incorporated into salt marsh classifications with the creation of LiDAR-derived vegetation indices [16] or LiDAR-derived elevation to augment spectral classifications [17]. The limited penetration of LiDAR into the salt marsh canopy can result in a bias toward higher elevations [18]. However, areas of dense canopy are minimally impacted by tidal inundation unless completely submerged. This makes the bias toward including the salt marsh vegetation height in ground elevations within salt marshes a minor concern for this paper.

Bathtub models are a method to determine inundation. A DEM is used to determine whether a pixel is inundated or not at a certain tidal stage or flood elevation. Additional nuance can be added by adjacency rules, i.e., a number of adjacent pixels must be inundated before a pixel is considered inundated [18]. Bathtub models have been used to determine SLR [19] and storm surge impacts [20] for coastal landscapes. Inundation has been shown to increase with the spatial resolution of the DEM [19]. Local tides can influence these predictions, and tidal variation can be included in bathtub models by converting elevation data to a tidal datum with software, such as VDatum [21]. Bathtub models are commonly used to assess SLR and have yet to be utilized to understand tidal impacts on VHR salt marsh mapping.

This paper seeks to understand the relationship between the elevation and the salt marsh vegetation extent within Jamaica Bay by modeling the tidal stage impact on NDVI and classified *S. alterniflora* from MLW to mean high water (MHW). This paper addresses the following questions: 1) if VHR satellite imagery reduced the error introduced by tidal stage when mapping salt marsh and 2) how the impact of tidal stage varies between Jamaica Bay's salt marsh islands?

II. METHODS

A. Study Area

Jamaica Bay is an estuary within the boundaries of the New York City boroughs of Brooklyn and Queens. The majority of the bay's undeveloped areas have been managed by the National Park Service since 1972. The bay's tidal range has increased, and high water across the Bay is increased by 40–52 cm, due to the expansion of Breezy Point, a barrier spit to the south, dredging for navigation, and other anthropogenic alterations [22]. From 2007 to 2012, there was a 3-cm mean increase in the tidal range within the bay [23]. Alterations to the bay have resulted in an increase in volume coinciding with a decrease in surface area [24]. The bay's salt marsh islands are a combination of restored and natural salt marshes. Restoration in the bay began in 2003 with thin-layer deposition, a process of depositing sediment from channel deepening, onto the marsh surface followed by revegetation [25].

B. Satellite Imagery

This paper used Worldview-2 imagery data collected on September 12, 2012 at 4:25 P.M. and September 9, 2013 at 4:26 P.M. (UTC) (Table I). The Worldview-2 sensor is composed of eight multispectral bands, including Coastal Blue, Blue, Green, Yellow, Red, Red Edge, near-infrared (NIR)-1, and NIR-2. Worldview-2 data had a multispectral spatial resolution of 2 m and a panchromatic resolution of 0.5 m. The study also used the Quickbird-2 imagery which is composed of four spectral bands, including Blue, Green, Red, and NIR. Quickbird-2 has a multispectral spatial resolution of 2.16 m and a panchromatic spatial resolution of 0.65 m. The tides at the time of imagery acquisition were verified with the tidal station at Sandy Hook, NJ, USA, with MLW of −0.799 m North American Vertical Datum 1988 (NAVD 88) [26]

(Table I). United States Geological Survey (USGS) tidal stations 01311875 and 01311850 located at Gil Hodges Memorial Bridge and Inwood Marina, respectively, were used to understand the tidal variation across Jamaica Bay [27], [28] (Fig. 1). The 2013 Worldview-2 imagery was coregistered to the LiDAR generated DEM. All other satellite imageries used in the analysis were coregistered to the 2013 Worldview-2 imagery (Table I).

C. Object-Oriented Classification

An object-oriented classification approach was used, which begins with segmentation, i.e., dividing an image into spectrally similar patches. Objects were then classified giving a greater geospatial context and addressing many limitations of pixel-based methods [29]. Jamaica Bay's salt marsh islands were segmented using mean shift segmentation at multiple scales; the random forest classifier and a diverse set of parameters, including neighborhood differences, gray level co-occurrence matrix texture, and vegetation indices, were used in the classification [5]. The classification scheme included nine classes, *Spartina alterniflora*, Patchy *S. alterniflora*, *Phragmites*, upland, mudflat, water, high marsh, wrack, and sand. The Patchy *S. alterniflora* classes were those objects with 10%–49% cover, and *S. alterniflora* were those segments with ≥50% vegetation cover. A multiscale segmentation approach was implemented using local Moran's I and variance to determine which objects were under- and oversegmented and resegment those objects at a more appropriate scale [30]. The classification excluded DEMs to remain independent of the bathtub models which used the topobathymetric LiDAR. The classification results from September 19, 2013 Worldview-2 data were used as a baseline for analysis due to a tidal stage near MLW, and temporal proximity to the topobathymetric LiDAR collection date.

D. Topobathymetric LiDAR Data

Topobathymetric LiDAR systems collect both terrestrial and nearshore elevation simultaneously. The topobathymetric data were collected from January 8, 2014 to May 22, 2014 and achieved submerged accuracy and terrestrial vertical accuracy of 0.062 and 0.214 m, respectively [31]. The LiDAR point cloud data were binned and averaged into a DEM with 0.5-m spatial resolution to match the spatial resolution of the pan sharpened Worldview-2 data.

E. Tidal Analysis

Elders Point East, a salt marsh island in the northern portion of the study area (Fig. 1), was analyzed due to the overlap of imagery collected at variable tidal stages across 2012–2013. The site underwent salt marsh restoration in 2006, adding elevation and salt marsh vegetation [3]. The southern point of the island was used as a subset to analyze the tidal impacts on a restoration salt marsh within Jamaica Bay. Visual tidal differences between the dates are evident, with higher tides resulting in less visible vegetation (Fig. 2). The Worldview-2 image acquired on September 19, 2013 represented a non-inundated scene with the tidal stage within 0–0.6 m of MLW (Table I).

NDVI was used as a proxy for the vegetation extent. A threshold of NDVI > 0 was applied to each of the images, all areas with NDVI > 0 were determined to be potentially vegetated. Imageries from 2012 and 2013 were included in the analysis as the area experienced a little change. The largest land cover change from 2012 to 2013 for Elders Point East was the reduction in areas classified as wrack [6]. This should have minimal impact due to the inclusion of wrack in the NDVI threshold.

Stony Creek, a salt marsh island in the western side of the bay (Fig. 1), was selected to compare the NDVI of objects derived from Worldview-2 imagery data as vegetated at two extents of tidal inundation. Two dates of the Quickbird-2 and Worldview-2 imageries were used to explore the impact of the tidal stage on areas classified as *S. alterniflora* in 2013. This NDVI was differenced with two dates of the Quickbird-2 imagery acquired at 70.1 cm above MLW on September 28, 2013 and 124.4 cm above MLW on September 7, 2012. The differenced NDVIs were compared across three elevation ranges: 1) objects inundated in both the images (34.5–70.1 cm); 2) objects inundated only on September 28, 2013 (70.1–124.4 cm); and 3) non-inundated objects (>124.4 cm).

F. Bathtub Modeling of S. alterniflora

The bathtub models of the tidal stage went from MLW to MHW at 5-cm intervals to correspond with the growth range of *S. alterniflora*. The growth range of *Spartina alterniflora* varies in the region with a lower bound above MLW and an upper bound around MHW [32]. VDatum was used to convert the LiDAR data from NAVD 88 to MLW. VDatum has been evaluated for use at the study site finding *in situ* and modeled elevations differed by a mean of 6.4 cm [32]. However, the conversion did introduced areas of no data to several marsh islands due to the VDatum's conversion extent. The study used only salt marsh islands which were completely converted into the MLW tidal datum (Fig. 1). Salt marsh islands with more high-marsh and upland areas, such as JoCo and Black Bank, were not fully converted and therefore excluded. The tidal surfaces were utilized to simulate the impact of a tidal stage on the classified vegetation and the NDVI of the 2013 Worldview-2 imagery.

G. Statistical Analysis

The RMSE of the tidal inundation bathtub modeling was calculated using comparisons of imagery collected at a range of tidal stages. The RMSE quantifies the level of uncertainty in this approach to modeling tidal stage impact on vegetation mapping.

Linear regression was used to test the modeled tidal inundation's impact on the percentages of *S. alterniflora* and NDVI. The interaction between tidal stage elevation and islands was tested to determine if the slopes of the islands were homogenous. An analysis of covariance (ANCOVA) further explored the relationships between islands with Tukey's Honest Significant Difference. A t-test was also conducted comparing the modeled response of classified *S. alterniflora* and NDVI > 0.

The imagery analysis of Stoney Creek salt marsh used a one-way analysis of variance (ANOVA) to understand differences in the means between the three elevations classes of vegetation: 1) inundated in both the images (34.5–70.1 cm); 2) inundated on September 28, 2013 (70.1–124.4 cm); and 3) not inundated (>124.4 cm).

A Tukey's Honest Significant Difference was then computed to determine which of these stages were significantly different for the September 28, 2013 and September 7, 2012 Quickbird-2 images.

III. RESULTS

A. Image Classifications for Salt Marsh Mapping

The 2013 salt marsh classification included all tidally influenced areas of the salt marsh islands (Fig. 3). The 2013 classification with and without a DEM was trained with the same data. The out of box overall accuracy, a subset of samples withheld during each iteration of the classifier, was compared finding overall accuracies of 94.4% and 92.5% with and without a DEM, respectively. The

classification with a DEM achieved a 92.81% overall accuracy with an independent accuracy assessment (Table II) [5].

B. Tidal Stage

The impact of the tidal stage on the NDVI for the Elders Point East site was determined for five dates of imagery across a tidal range of 162 cm. In the subset, areas with an NDVI > 0 were reduced by 82% (Table III). It is important to note that while the September 19, 2013 data included approximately 10 ha with NDVI > 0, only 4.415 ha was classified as vegetation for the imagery at the greatest inundation (Table III). At a tidal stage of 124.4 cm above MLW, there was a ~6-ha reduction of areas above the NDVI threshold. However, mudflat accounted for much of this reduction, and only 20.3% of areas classified as low marsh vegetation were inundated. The 70.1-cm above MLW image demonstrates a very little loss of either NDVI or vegetation. The imagery collected at 196.4 cm above MLW data had the greatest difference between actual and modeled tidal impact on NDVI. The imagery collected at 83.4 cm had a large difference too due to being outside the growing season. The RMSE was 0.9003 with all data included or 0.2364 without the October 18, 2012 and December 30, 2012, as those data were outside this study's target tidal range (MLW–MHW) and growing season, respectively

C. Bathtub Modeling

Bathtub modeling of the tidal stage at 5-cm intervals was applied to an NDVI > 0 layer and a *S. alterniflora* classified layer for a subset of salt marsh islands. Bay wide inundation of the salt marsh vegetation was minimal before 0.6 m above MLW (Fig. 4). However, the salt marsh islands, including Black Wall, Rulers Bar, and Pumpkin Patch, had ~20% of the *S. alterniflora* inundated at 0.6 m above MLW; these

salt marshes had significantly different inundation regimes than other salt marshes (see Fig. 4 and Table IV). A multiple linear regression of bathtub modeled percentage of inundation found that the tidal stage and the island had a significant impact on percent vegetation across the salt marsh [$F_{(11, 318)} = 79.3$, $p < 0.001$, and $R^2 = 0.72$] (Table IV). A multiple linear regression of the percentage of inundated NDVI areas found that the tidal stage and islands had a significant impact on the percentage of vegetation [$F_{(11,318)} = 201.5$, $p < 0.001$, and $R^2 = 0.87$] (Table IV). The tidal impact on the NDVI of restoration salt marshes was less than natural salt marshes [$F_{(1, 328)} = 15.53$, $p < 0.001$, and $R^2 = 0.042$], given R^2 that is a very little of the variability was explained due to restoration. However, linear regression of *S. alterniflora* saw no significant difference between the restoration and natural salt marsh response [$F_{(1, 328)} = 0.1085$, $p = 0.742$, and $R^2 = 0.0$]. The tidal inundation was variable across the bay's salt marsh islands with many having significantly different modeled responses to the tidal stage (Fig. 4). The comparison of the NDVI with *S. alterniflora* models found that the NDVI was more impacted by the tidal stage than the *S. alterniflora* layer ($t_{650} = 2.47$ and $p < 0.01$).

The NDVI of areas classified as *S. alterniflora* was compared between two tidal stages at Stony Creek. The results showed that the NDVI of the *S. alterniflora* objects was significantly different for the September 28, 2013 imagery (70.1 cm above MLW) [$F_{(2, 15280)} = 343.6$ and $p < 0.001$]; vegetated areas from 34.5–70.1 cm and those >70.1 cm were significantly different. However, areas between 70.1 and 124.4 cm and those above 124.4 cm MLW were not different. When comparing the Worldivew-2 and Quickbird-2 data on September 7, 2012, all tidal levels were

significantly different [$F_{(2, 15265)} = 159.4$ and $p < 0.001$]. Including the objects with elevation between 70.1 and 124.4 cm and those above 124.4 MLW. Inundated areas were not reduced to zero NDVI and they were impacted by the tidal stage.

S. alterniflora height increases with the depth of tidal inundation due to increased nutrients and reduced edaphic stress [34]. The relationship between *S. alterniflora* and tidal inundations gives the possibility that these bathtub models are applicable between study sites. The relationship between the tidal range and the lower bound of *S. alterniflora* has been quantified as

$$zmin = 0.7167 * (TidalRange) - 0.0483 [35].$$

At the tidal station located at Sandy Hook, NJ, USA, the range from MLW to MHW is 1.433 m, which results in a lower boundary of *S. alterniflora* growth at 45.4 cm above MLW or 97.87 cm below MHW. This range matches the bay wide modeled inundation of S. alterniflora. VDatums MHW and MLW grids were used to determine local estimates of growth range for each salt marsh island finding only a 3.5-cm maximum difference between the eastern and western side of the bay. At or below the lower growth range of *S. alterniflora* is an ideal tidal stage for image acquisition to ensure no impacts from tidal inundation at this site.

IV DISCUSSION

The model was able to capture the impact of inundation, with an RMSE of 0.2364 for the Elders Point East tidal site for the VHR imagery acquired between MLW and MHW in the growing season. The inundation of vegetation varied by island throughout Jamaica Bay, suggesting site characteristics, such as restoration status, available data, tidal regime, and vegetation type should be considered when

determining an appropriate tidal stage. The models and image analysis demonstrated that the tidal stage impacts restoration salt marshes less.

In Jamaica Bay, algae deposited on beaches and mudflats is common due to eutrophic conditions and could add to misclassifications when mapping salt marsh. Algal blooms are common within the bay during the late spring and summer months [36]. Algal blooms result in algal deposition on mudflats which can be misclassified as vegetation due, in part, to the strong NIR value of the algae [7]. Algal mats on mudflats and beaches within Jamaica Bay create uncertainty in change between land cover classes and are difficult to include in the analysis due to their transience. The analysis of Elders Point East suggested that at 70.1 cm above MLW, the tidal stage had a reduction (1/2 hectares) in areas above the NDVI threshold, and a little *S. alterniflora* was impacted. However, due to the restoration activity on the island, this model was not representative of other salt marsh islands in the bay (Table IV). Higher tidal stages can reduce mudflats with seaweed deposition, however bay wide there was no single appropriate tidal stage for this application.

Coregistration is another source of error. The fine resolution imagery requires careful registration or risks overestimating tidal inundation. The georegistration achieved an appropriate level of agreement between the imagery and the DEM. The registration error would not impact the comparisons between salt marsh islands. Registration errors would be systematic throughout the 2013 scene. The temporal proximity of the LiDAR and VHR imagery acquisitions is another source of error. From 2007 to 2009 and from 2009 to 2010, Elders Point East had significant elevation change, including increases and decreases of >30.48 cm [37]. The 1–2 years between

image and LiDAR acquisitions is another potential source of error. These sources of error and LiDAR accuracy are a component of the RMSE of the imagery analysis.

The conversion to MLW datum was necessary for the bathtub models to capture the variation in the tidal regime in the bay. However, tidal variation alone does not account for modeled variation between the responses of salt marsh islands to inundation. The model overestimated inundation. This could be mitigated with the inclusion of a digital surface model to provide an indicator of the complete submersion of vegetation and the use of a minimum bin method for DEM creation. The analysis at Stoney Creek found differences between the NDVI of inundated and non-inundated *S. alterniflora*. Inundated areas can still be mapped as vegetation, though it is likely that spectra will be altered leading to more variability in the spectral signature for the *S. alterniflora* vegetation class.

The impact of the tidal stage on the VHR mapping of *S. alterniflora* was similar to past estimates with a medium resolution imagery [8]. The image analysis method is preferred for determining local tidal impacts. However, the acquisition of several VHR images is often prohibitively expensive, making the modeling approach reasonable for understanding local tidal characteristics. The tidal impact on *S. alterniflora* was varied by a salt marsh island. These differences were due to Jamaica Bay's tidal variability, vegetation characteristics, and restoration actions. *S. alterniflora* marshes have an area of taller high biomass vegetation along the marsh edge [38]. The finer spatial resolution would pick up some of these differences between edge and interior salt marsh. In addition, ground elevation was used in this analysis not accounting for differences in the vegetation height. These taller edge areas

were less impacted by canopy inundation than shorter interior *S. alterniflora*. The use of the VHR imagery did not, on its own, limit the impact of the tidal stage on the mapped vegetative extent. Salt marsh mapping requires accurate measure of fine-scale changes in land cover; therefore, even minor tidal impacts are of concern and should be quantified.

Previous classifications and the change analysis of the study site (2003–2013) used imagery acquired at a range of tidal stages [6]. The tidal stage of the 2003 imagery was 78.1 cm and outside the recommended 60 cm of MLW (Table I). The 2008 and 2012 data were 57.0 and 22.2 cm, respectively. The bay wide bathtub models corresponding with image acquisitions, rounded up to the nearest 5-cm increment, found an estimated 9.5%, 3.5%, and 0.008% of *S. alterniflora* was inundated in 2003, 2008, and 2012, respectively. This analysis suggests that *S. alterniflora* was underestimated in 2003. However, *S. alterniflora* in the 2003 classification was 73.31-ha extent which was similar to the 2008 classification which found 73.84 ha [6]. This coincided with the restoration of Elders Point East which added significant areas of *S. alterniflora*. Variable tidal stages during acquisition are one reason to encourage a temporally extensive change analysis, when determining salt marsh change. In addition, a post classification change analysis is preferable in salt marsh environments to limit differences in spectra for a single species due to inundation.

Determining the salt marsh extent and tidal regimes are important aspects of understanding the risk that SLR poses to a salt marsh ecosystem. The rate of global mean SLR from 1993 to 2010 has doubled when compared with the 1901–1990 observed rates and is likely to continue to increase due to global warming [39].

Regional SLR in the mid-Atlantic is projected to be between 30 and 50 cm greater than global SLR by 2100 [40]. SLR is a major concern for Jamaica Bay. A 30-cm SLR scenario is projected to cause extensive salt marsh loss in the western portion of the bay [41] and could be further exacerbated by eutrophication [42], [43]. This tidal inundation analysis can be utilized to understand the areas of potential salt marsh loss within Jamaica Bay.

V. CONCLUSION

This paper demonstrates the importance of assessing the tidal stage and characteristics when mapping salt marsh extent and change. The impact on imagery is unique to the local tidal regime. The analysis demonstrated that restored salt marsh vegetation was less impacted at higher tidal stages than expected, and the bathtub model performed worse at higher tidal stages due to below canopy inundation. The bathtub models identified areas of uncertainty when an imagery was acquired at a particular tidal stage. The study illustrates one application for the topobathymetric LiDAR in coastal mapping. The tidal response across the salt marsh islands of Jamaica Bay varied greatly due to the tidal range, elevation, restoration, and vegetation extent. The high variability of responses makes it clear that to accurately understand degrading salt marsh islands within Jamaica Bay, a tidal stage below 45.4 cm (relative to MLW) is preferred. However, there is no guarantee of consistent low-tidal stage imagery. Therefore, it is important to understand the potential error due to the tidal stage. When considering the impact of a tidal stage from 60 to 90 cm above MLW for the entirety of the bay, there was only a small amount of *S. alterniflora* inundated. However, when considering a 60–90-cm tidal stage on a particular salt marsh islands,

such as Duck Point, nearly all vegetation was inundated. The analysis demonstrates several lessons for mapping salt marsh vegetation.

1) Tidal stage is even more a concern for VHR coastal mapping due to the desire for fine-scale measurements.

2) Tidal stage variation throughout a study site can be modeled improving the estimates of uncertainty.

3) When mapping *S. alterniflora*, the lower growth range of the species can be used to ensure limited impact and allow for an understanding of tidal impacts in microtidal areas.

TABLE I. TIDAL STAGE AT TIME OF WORLDVIEW-2 (WV-2) AND QUICKBIRD-2 (QB-2) IMAGE ACQUISITION FOR THE DATA UTILIZED

DATE	TIME (UTC)	SENS-OR	MLW SANDY HOOK **ERROR! REFERENCE SOURCE NOT FOUND.** (CM)	MLLW SANDY HOOK **ERROR! REFERENCE SOURCE NOT FOUND.** (CM)	MLLW INWOOD**ERROR! REFERENCE SOURCE NOT FOUND.** (CM)	MLLW ROCK-AWAY INLET**ERROR! REFERENCE SOURCE NOT FOUND.** (CM)	RMSE***
9/10/2003	15:34	QB-2	78.1*	84.0	NA	NA	-
9/15/2008	16:00	QB-2	57.0	62.9	54.0	27.7	-
09/15/2012	16:25	WV-2	22.2	28.1	6.7	0.1	0.135
09/19/2013	16:26	WV-2	34.5	40.4	20.4	6.4	0.223
09/07/2012	15:07	QB-2	124.4**	130.3	157.0	152.0	0.1485
10/18/2012	15:14	QB-2	196.4**	202.3	204.5	182.3	1.120
12/30/2012	16:16	QB-2	83.4*	89.3	75.0	51.8	0.123
09/19/2013	15:01	QB-2	92.7**	98.6	77.4	58.8	-
09/28/2013	15:02	QB-2	70.1*	76	95.7	97.2	0.128

*** EXCEEDING THE RECOMMENDED 0.0-0.6 M ABOVE MLW**
**** EXCEEDING THE 0.9 M ABOVE MLW**

TABLE II

TABLE II: ACCURACY ASSESSMENT CONDUCTED WITH STRATIFIED RANDOM SELECTION OF 765 POINTS. PRODUCERS, USERS AND OVERALL ACCURACY WERE CALCULATED FOR THE 2013 CLASSIFICATION **ERROR! REFERENCE SOURCE NOT FOUND.**. LAND COVER CLASSES ARE ABBREVIATED AS MUD=MUDFLAT, SAND, WK=WRACK, SA=*S. ALTERNIFLORA*, PSA= PATCHY *S. ALTERNIFLORA*, HM= HIGH MARSH, PHG= *PHRAGMITES*, WTR= WATER, UP= UPLAND, UA = USERS ACCURACY, PA = PRODUCERS ACCURACY, OA=OVERALL ACCURACY

CLASS	**MUD**	**SAND**	**WK**	**SA**	**PSA**	**HM**	**PHG**	**WTR**	**UP**	**UA**
MUD	**84**	**1**	**0**	**0**	**0**	**0**	**0**	**0**	**0**	**98.8**
SAND	**3**	**77**	**3**	**0**	**1**	**0**	**1**	**0**	**0**	**90.5**
WK	**0**	**5**	**76**	**0**	**0**	**0**	**4**	**0**	**0**	**89.4**
SA	**0**	**0**	**0**	**81**	**0**	**3**	**1**	**0**	**0**	**95.2**
PSA	**2**	**0**	**0**	**2**	**79**	**0**	**2**	**0**	**0**	**92.9**
HM	**0**	**0**	**0**	**5**	**0**	**79**	**1**	**0**	**0**	**92.9**
PHG	**0**	**0**	**6**	**0**	**0**	**4**	**70**	**0**	**5**	**82.3**
WTR	**0**	**0**	**0**	**0**	**0**	**0**	**0**	**85**	**0**	**100.0**
UP	**0**	**0**	**0**	**0**	**0**	**0**	**6**	**0**	**79**	**92.9**
PA	**94.3**	**92.7**	**89.4**	**92.0**	**98.7**	**91.8**	**82.3**	**100.0**	**94.0**	**OA: 92.8**

TABLE III: MODELED AND CLASSIFIED IMPACT OF TIDAL STAGE ON NDVI FOR ELDERS POINT EAST.

DATE	TIME (UTC)	ABOVE MLW (CM)*	NDVI > 0 (HA)	MODELED INUNDATION IMPACT (HA)	MODELED VEGETATION INUNDATION (%)
9/19/2013	4:26 PM	34.5	10.385	10.3762	0
09/28/2013	3:02 PM	70.1	9.9089	9.5283	0.0014
12/30/2012	4:16 PM	83.4	7.2796	8.1561	--
09/07/2012	3:07 PM	124.4	4.2511	4.1002	0.2032
10/18/2012	3:14 PM	196.4	1.7977	0.0323	--

*MLW AS DETERMINED BY THE NOAA TIDAL GAGE AT SANDY HOOK, NJ

TABLE IV. ANCOVAS RESULTS COMPARING INUNDATION BETWEEN ISLANDS FOR *S. ALTERNIFLORA* AND NDVI.

ISLAND NAME	ISLAND NAME	VEGETATION (*P* VALUE)	NDVI > 0 (*P* VALUE)	RESTORATION SALT MARSH
BLACK WALL (BW)	BIG EGG	< 0.01	1.00	YES
BROAD CREEK (BC)	BIG EGG	0.08	1.00	NO
CANARSIE POL (CP)	BIG EGG	1.00	0.39	NO
DUCK POINT	BIG EGG	<0.05	<0.01	NO
EAST HIGH	BIG EGG	0.21	0.94	NO
ELDER POINT EAST (EPE)	BIG EGG	<0.05	<0.05	YES
ELDER POINT WEST (EPW)	BIG EGG	<0.01	<0.05	YES
PUMPKIN PATCH (PP)	BIG EGG	<0.01	<0.01	NO
RULERS BAR	BIG EGG	< 0.01	0.23	YES
STONY CREEK	BIG EGG	1.00	1.00	NO
BROAD CREEK	BW	<0.01	0.99	NO
CP	BW	<0.01	1.00	NO
DUCK POINT	BW	070	<0.01	NO
EAST HIGH	BW	<0.01	1.00	NO
EPE	BW	<0.01	0.57	YES
EPW	BW	<0.01	0.57	YES
PP	BW	1.00	<0.01	NO
RULERS BAR	BW	0.99	0.94	YES
STONY CREEK	BW	<0.01	0.98	NO
CP	BC	0.27	0.66	NO
DUCK POINT	BC	<0.01	<0.01	NO
EAST HIGH	BC	1.0	0.99	NO
EPE	BC	1.0	0.10	YES
EPW	BC	0.91	0.10	YES
PP	BC	<0.01	<0.01	NO
RULERS BAR	BC	<0.01	0.45	YES
STONY CREEK	BC	<0.05	1.00	NO
DUCK POINT	CANARSIE POL (CP)	<0.01	<0.01	NO
EAST HIGH	CP	0.54	0.99	NO
EPE	CP	0.12	0.99	YES
EPW	CP	<0.01	0.99	YES
PP	CP	<0.01	<0.01	NO
RULERS BAR	CP	<0.01	1.00	YES
STONY CREEK	CANARSIE POL	0.99	0.42	NO
EAST HIGH	DUCK POINT	<0.01	<0.01	NO
EPE	DUCK POINT	<0.01	<0.01	YES
EPW	DUCK POINT	<0.01	<0.01	YES
PP	DUCK POINT	0.86	<0.01	NO
RULERS BAR	DUCK POINT	0.28	<0.01	YES
STONY CREEK	DUCK POINT	<0.05	<0.01	NO
EPE	EAST HIGH	1.00	0.67	YES
EPW	EAST HIGH	0.70	0.67	YES
PP	EAST HIGH	<0.01	<0.01	NO
RULERS BAR	EAST HIGH	<0.01	1.00	YES
STONY CREEK	EAST HIGH	0.12	0.95	NO
EPW	EPE	0.98	1.00	YES
PP	EPE	<0.01	<0.01	NO
RULERS BAR	EPE	<0.01	0.99	YES
STONY CREEK	EPE	<0.05	<0.05	NO
PUMPKIN PATCH	EPE	<0.01	<0.01	NO
RULERS BAR	EPW	<0.01	0.99	YES
STONY CREEK	EPW	<0.01	<0.05	NO
RULERS BAR	PP	1.00	<0.01	YES
STONY CREEK	PP	<0.01	<0.01	NO
STONY CREEK	RULERS BAR	<0.01	0.25	NO

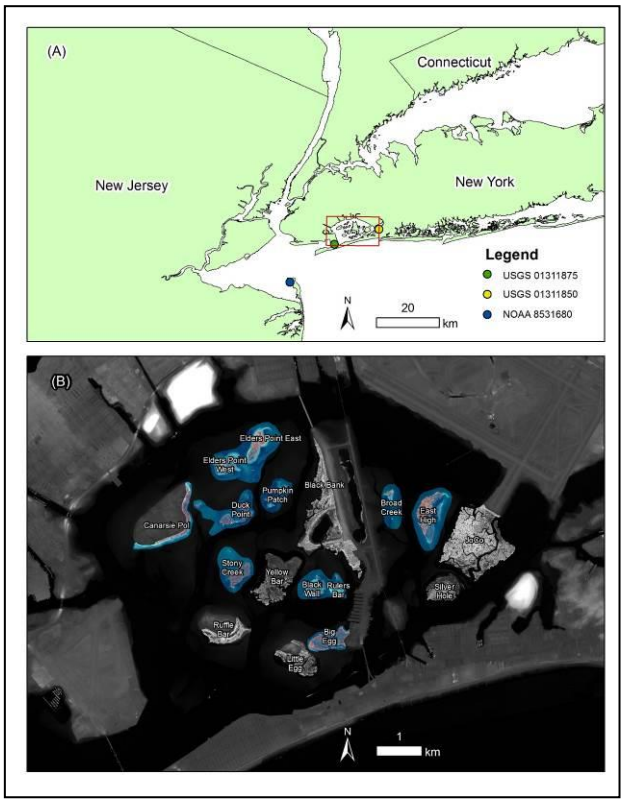

Fig. 1. (A) The locations of tidal stations used in this study including USGS tidal station 01311875 on Gil Hodges Memorial Bridge, USGS tidal station 01311850 at Inwood Marina, and NOAA tidal station 8531680 on Sandy Hook, NJ. (B) The map displays a subset of salt marsh islands denoted by pseudo color that were analyzed in this study. The background display is a topobathymetric DEM of Jamaica Bay, New York.

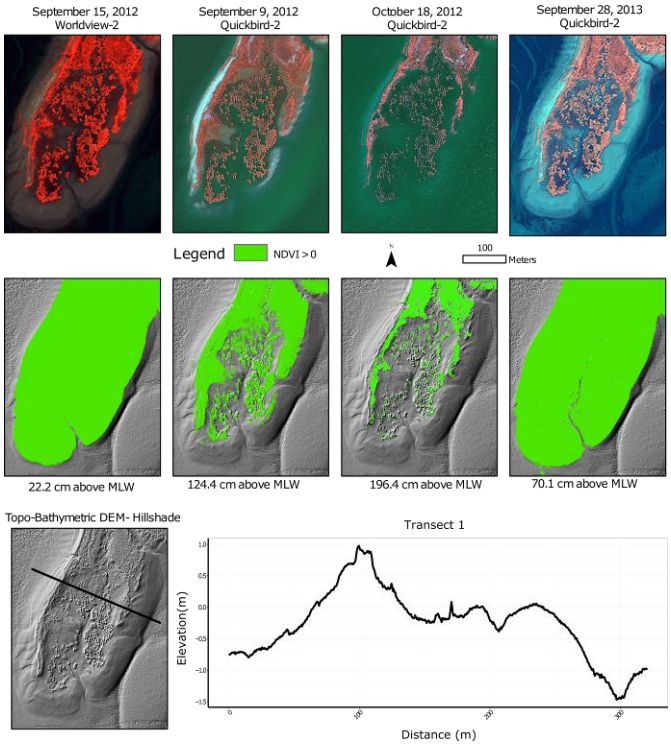

Fig. 2. Visualization of tidal stage impact on salt marsh vegetation, Worldview-2 data acquired in September 16, 2012 and Quickbird-2 data acquired in September 9, 2012, October 18, 2012, and September 28, 2013. The maps show vegetation inundation in relation to tidal stage at the time of image acquisition. Background panchromatic display is a hillshade from Topo-bathymetric LiDAR. The elevation profile across the salt marsh island demonstrates the salt marsh island's elevation gradient.

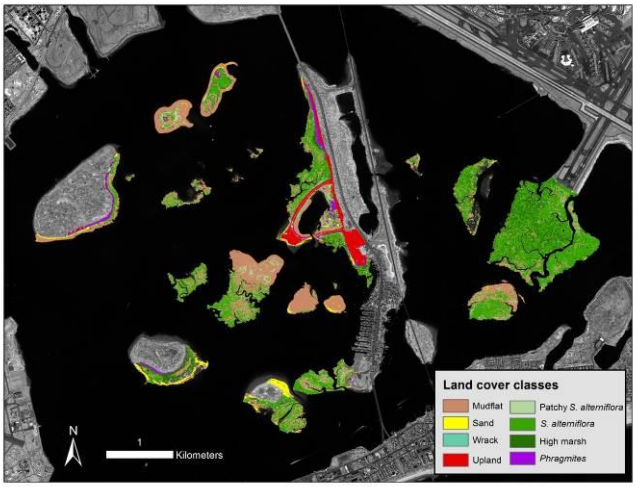

Fig. 3. The results of the object-oriented classification of salt marsh vegetation in Jamaica Bay using Worldview-2 imagery acquired September 19, 2013.

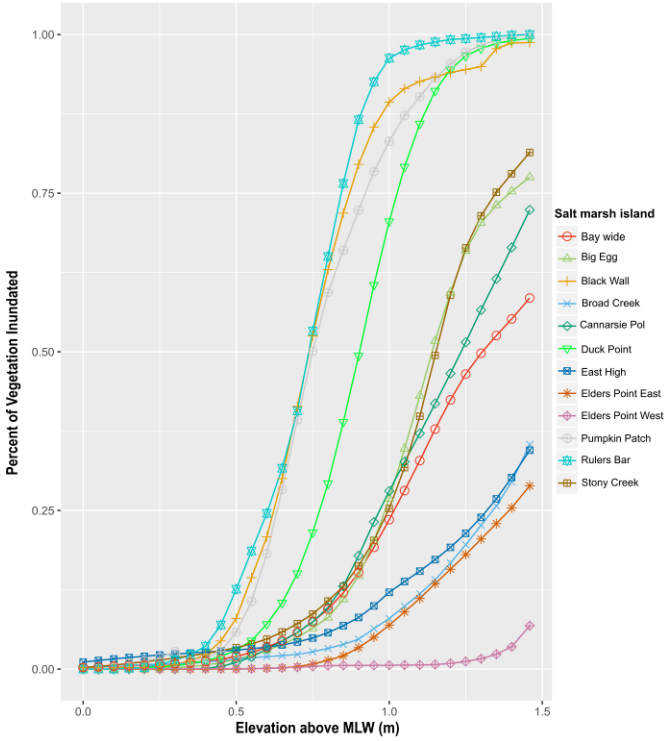

Fig. 4. The figure illustrates the modeled % of salt marsh vegetation inundated at tidal stages in relation to MLW for each salt marsh island and the entirety of Jamaica Bay. The vegetation inundation was determined using the object-oriented classification of S. alterniflora and bathtub models at 5 cm intervals. Island inundation regimes varied widely across the bay.

ACKNOWLEDGMENT

The authors would like to thank National Park Service for the support and in particular T. Pearl, M.-J. Marino, P. Rafferty, D. Adamo, M. Ringenary, S. Stevens, and M. Christiano for their expertise, insights, and guidance. They would also like to thank the anonymous reviewers for the comments and suggestions that helped to improve the quality of this paper

REFERENCES

[1] J. B. Zedler and S. Kercher, “Wetland resources: Status, trends, ecosystem services, and restorability,” Annu. Rev. Environ. Resour., vol. 30, pp. 39–74, Nov. 2005.

[2] S. Temmerman, P. Meire, T. J. Bouma, P. M. J. Herman, T. Ysebaert, and H. J. De Vriend, “Ecosystem-based coastal defence in the face of global change,” Nature, vol. 504, no. 7478, pp. 79–83, 2013.

[3] P. Rafferty, J. Castagna, and D. Adamo, “Building partnerships to restore an urban marsh ecosystem at gateway national recreation area,” Park Sci., vol. 27, no. 3, pp. 34–41, 2010.

[4] An Update on the Disappearing Salt Marshes of Jamaica Bay, New York, Gateway Nat. Recreation Area, Nat. Park Service, U.S. Dept. Interior Jamaica Bay Watershed Protection Plan Advisory Committee, New York, NY, USA, 2007.

[5] Y. Wang, M. Christiano, and M. Traber, “Mapping salt marshes in Jamaica Bay and terrestrial vegetation in Fire Island national seashore using QuickBird satellite data,” in Remote Sensing of Coastal Environments. Boca Raton, FL, USA: CRC Press, 2010, pp. 191–208.

[6] A. Campbell, Y. Wang, M. Christiano, and S. Stevens, “Salt marsh monitoring in Jamaica Bay, New York from 2003 to 2013: A decade of change from restoration to hurricane sandy,” Remote Sens., vol. 9, no. 2, p. 131, 2017.

[7] K. A. Tuxen, L. M. Schile, M. Kelly, and S. W. Siegel, “Vegetation colonization in a restoring tidal marsh: A remote sensing approach,” Restoration Ecol., vol. 16, no. 2, pp. 313–323, 2008.

[8] J. M. Levine, J. S. Brewer, and M. D. Bertness, “Nutrients, competition and plant zonation in a New England salt marsh,” J. Ecol., vol. 86, no. 2, pp. 285–292, 1998.

[9] J. R. Jensen, D. J. Cowen, J. D. Althausen, S. Narumalani, and O. Weatherbee, “An evaluation of the CoastWatch change detection protocol in South Carolina,” Photogramm. Eng. Remote Sens., vol. 59, no. 6, pp. 1039–1046, 1993.

[10] J. E. Dobson et al., “NOAA coastal change analysis program (C-CAP): Guidance for regional implementation,” Nat. Marine Fisheries Service, Seattle, WA, USA, NOAA Tech. Rep. NMFS 123, 1995.

[11] V. V. Klemas, “Remote sensing of landscape-level coastal environmental indicators,” Environ. Manage., vol. 27, no. 1, pp. 47–57, 2001.

[12] E. W. Ramsey, III, and S. C. Laine, “Comparison of Landsat thematic mapper and high resolution photography to identify change in complex coastal wetlands,” J. Coast. Res., vol. 13, no. 2, pp. 281–292, 1997.

[13] W. Rodriguez, I. C. Feller, and K. C. Cavanaugh, “Spatio-temporal changes of a mangrove–saltmarsh ecotone in the northeastern coast of Florida, USA,” Global Ecol. Conservation, vol. 7, pp. 245–261, Jul. 2016.

[14] M. S. Gilmore et al., “Integrating multi-temporal spectral and structural information to map wetland vegetation in a lower Connecticut River tidal marsh,” Remote Sens. Environ., vol. 112, no. 11, pp. 4048–4060, 2008.

[15] J. R. Jensen, D. J. Cowen, J. D. Althausen, S. Narumalani, and O. Weatherbee, “The detection and prediction of sea level changes on coastal wetlands using satellite imagery and a geographic information system,” Geocarto Int., vol. 8, no. 4, pp. 87–98, 1993.

[16] A. Collin, B. Long, and P. Archambault, “Merging land-marine realms: Spatial patterns of seamless coastal habitats using a multispectral LiDAR,” Remote Sens. Environ., vol. 123, pp. 390–399, Aug. 2012.

[17] G. Chust, M. Grande, I. Galparsoro, A. Uriarte, and Á. Borja, “Capabilities of the bathymetric hawk eye LiDAR for coastal habitat mapping: A case study within a Basque estuary,” Estuarine, Coastal Shelf Sci., vol. 89, no. 3, pp. 200–213, 2010.

[18] C. Hladik, J. Schalles, and M. Alber, “Salt marsh elevation and habitat mapping using hyperspectral and LIDAR data,” Remote Sens. Environ., vol. 139, pp. 318–330, Dec. 2013.

[19] B. Poulter and P. N. Halpin, “Raster modelling of coastal flooding from sea-level rise,” Int. J. Geograph. Inf. Sci., vol. 22, no. 2, pp. 167–182, 2008.

[20] A. Murdukhayeva, P. August, M. Bradley, C. LaBash, and N. Shaw, “Assessment of inundation risk from sea level rise and storm surge in northeastern coastal national parks,” J. Coast. Res., vol. 29, no. 6A, pp. 1–16, 2013.

[21] A. Schmid, B. C. Hadley, and N. Wijekoon, “Vertical accuracy and use of topographic LIDAR data in coastal marshes,” J. Coast. Res., vol. 27, no. 6A, pp. 116–132, 2011, doi: 10.2112/JCOASTRES-D-10-00188.1.

[22] R. L. Swanson and R. E. Wilson, “Increased tidal ranges coinciding with Jamaica Bay development contribute to marsh flooding,” J. Coast. Res., vol. 24, no. 6, pp. 1565–1569, 2008.

[23] F. Shafiei, “Topography, hydrology and Spartina alterniflora growth range for restored salt marsh Elders Point East, Jamaica Bay, New York,” Dept. Biol., Nat. Park Service Lund Univ., Lund, Sweden, Tech. Rep., 2012.

[24] The Jamaica Bay Watershed Protection Plan, New York City Dept. Environ. Protection, New York, NY, USA, 2007.

[25] G. W. Frame, M. K. Mellander, and D. A. Adamo, “Big Egg Marsh experimental restoration in Jamaica Bay, New York,” in Proc. George Wright Soc. Conf. Parks, Protected Areas, Cultural Sites People, Places, Parks, 2006, pp. 2–9.

[26] Center for Operational Oceanographic Products and Services. (2017). Sandy Hook Tidal Station. Accessed: May 17, 2015. [Online]. Available: https://tidesandcurrents.noaa.gov/stationhome.html?id=8531680

[27] United States Geological Survey. (2017). USGS Current Conditions for New York: Jamaica Bay at Inwood, NY. [Online]. Available: https://waterdata.usgs.gov/nwis/uv/?site_no=01311850

[28] United States Geological Survey. (2017). USGS Current Conditions for New York: Rockaway Inlet Near Floyd Bennett Field, NY. [Online]. Available: https://waterdata.usgs.gov/nwis/uv/?site_no=01311875

[29] T. Blaschke, “Object based image analysis for remote sensing,” ISPRS J. Photogramm. Remote Sens., vol. 65, no. 1, pp. 2–16, Jan. 2010.

[30] B. Johnson and Z. Xie, “Unsupervised image segmentation evaluation and refinement using a multi-scale approach,” ISPRS J. Photogramm. Remote Sens., vol. 66, no. 4, pp. 473–483, Jul. 2011.

[31] NOAA Post Hurricane Sandy Topobathymetric LiDAR Mapping for Shoreline Mapping, Nat. Ocean. Atmos. Admin., Nat. Ocean Service, Nat. Geodetic Survey, Remote Sens. Division, Silver Spring, MD, USA, 2014.

[32] K. L. Mckee and W. H. Patrick, Jr., “The relationship of smooth cordgrass (Spartina alterniflora) to tidal datums: A review,” Estuaries Coasts, vol. 11, no. 3, pp. 143–151, 1988.

[33] D. Ullman, A. Babson, and M. Bradley, “Evaluating VDatum in coastal national parks: Fire Island National Seashore, Gateway National Recreation Area, and Assateague Island National Seashore,” Nat. Park Service, Fort Collins, CO, USA, Tech. Rep. 2016/1148, Mar. 2016.

[34] B. L. Howes, J. W. H. Dacey, and D. D. Goehringer, “Factors controlling the growth form of Spartina alterniflora: Feedbacks between aboveground production, sediment oxidation, nitrogen and salinity,” J. Ecol., vol. 74, no. 3, pp. 881–898, 1986. [35] M. L. Kirwan and G. R. Guntenspergen, “Influence of tidal range on the stability of coastal marshland,” J. Geophys. Res., Earth Surf., vol. 115, no. F2, p. F02009, 2010.

[36] R. B. Wallace and C. J. Gobler, “Factors controlling blooms of microalgae and macroalgae (Ulva rigida) in a eutrophic, urban estuary: Jamaica Bay, NY, USA,” Estuaries Coasts, vol. 38, no. 2, pp. 519–533, 2015.

[37] D. S. Davis, P. M. Weppler, P. Rafferty, D. G. Clarke, and D. Yozzo, “Elders point East Marsh Island restoration monitoring data analysis,” USACE, Washington, DC, USA, Tech. Rep. ERDC/EL CR-17-1, 2017, pp. 1–97.

[38] J. R. Jensen, C. Coombs, D. Porter, B. Jones, S. Schill, and D. White, “Extraction of smooth cordgrass (Spartina alterniflora) biomass and leaf area index parameters from high resolution imagery,” Geocarto Int., vol. 13, no. 4, pp. 25–34, 1998.

[39] J. A. Church et al., “Sea level change,” in Climate Change: The Physical Science Basis. Contribution of Working Group I to the Fifth Assessment Report of the Intergovernmental Panel on Climate Change, T. F. Stocker et al., Eds. Cambridge, U.K.: Cambridge Univ. Press, 2013.

[40] W. V. Sweet et al., “Global and regional sea level rise scenarios for the United States,” NOAA, Silver Spring, MD, USA, Tech. Rep. NOS CO-OPS 083, 2017.

[41] Detailed Method for Mapping Sea Level Rise Marsh Migration, NOAA Office Coastal Management, Charleston, SC, USA, 2017, pp. 1–8. https://coast.noaa.gov/slr/

[42] L. A. Deegan et al., “Coastal eutrophication as a driver of salt marsh loss,” Nature, vol. 490, pp. 388–392, Oct. 2012.

[43] C. Wigand et al., “Below the disappearing marshes of an urban estuary: Historic nitrogen trends and soil structure,” Ecol. Appl., vol. 24, no. 4, pp. 633–649, 2014.

CHAPTER 3

Salt Marsh Change Analysis of the mid-Atlantic Coast from 1999 to 2018 Using a Google Earth Engine Time Series Approach

Anthony Campbell, Yeqiao Wang*

Will be submitted for publication in *ISPRS Journal of Photogrammetry and Remote Sensing.*

Department of Natural Resources Science
University of Rhode Island
Kingston, RI 02881

*Corresponding author, Yeqiao Wang, yqwang@uri.edu, 1 Greenhouse Road, Kingston RI, 02881.

Abstract:

Salt marshes are a frontline of climate change providing a bulwark against sea level rise (SLR), an interface between aquatic and terrestrial habitat, important nursery grounds for many species, a buffer against extreme storm impacts, and vast blue carbon repositories. However, salt marshes are at risk of loss from a variety of stressors such as SLR, nutrient enrichment, sediment deficits, and herbivory. Determining the dynamics of salt marsh change with remote sensing requires high temporal resolution due to the spectral variability caused by disturbance, tides, and seasonality. Time series analysis of salt marshes can broaden our understanding of these changing environments. In this study, Google Earth Engine (GEE) enabled time series of the Landsat archive to be used to determine salt marsh change from 1999 to 2018 along the mid-Atlantic coast of the United States. These time series were filtered by cloud cover and the Tidal Marsh Inundation Index (TMII). The Landsat derived TMII correctly identified 10 out of 14 inundated and 148 out of 150 of the non-inundated test pixel areas. The study analyzed aboveground green biomass in seven mid-Atlantic Hydrological Unit Code 8 watersheds. This study revealed that the Chincoteague watershed had the highest average loss, and the Eastern Lower Delmarva watershed had the largest reduction in salt marsh aboveground green biomass from 1999-2018. A comparison of Worldview-2 derived interior mudflats and aboveground green biomass estimates found a positive relationship between biomass estimates and the area of mudflat within the Landsat test pixel area ($F_{(1165,1)}=1316$, $p < 0.001$) and $R^2=0.53$. This study developed a method for regional analysis of salt marsh change and identified at risk watersheds and salt marshes providing insight into resilience and management of these ecosystems.

1. Introduction

Development of methods for monitoring the response of salt marsh to drivers of loss is necessary to improve our ability to understand both the resilience and change of these ecosystems. Drivers of salt marsh loss are diverse from replacement by mangroves due to increasing temperature (Saintilan *et al*. 2014; Armitage *et al*. 2015), eutrophication (Deegan *et al*. 2012), herbivory impacts (Holdredge *et al*. 2009; Silliman & Zieman 2001), and sea level rise (SLR) (Watson *et al*. 2017). Less than half of salt marshes are predicted to keep pace with SLR under the Intergovernmental Panel on Climate Change's (IPCC) representative concentration pathway 2.6 (Crosby *et al*. 2016). The mid-Atlantic coast is one region where salt marshes are unlikely to keep pace with SLR due in part to high projected rates of SLR (Boon 2012) and relative SLR due to glacial isostatic adjustment and anthropogenic processes (Sweet *et al*. 2017). Time series analysis of mid-Atlantic salt marshes can improve our understanding of current trends and develop the capacity for monitoring future change.

A variety of remote sensing data have been applied to evaluate salt marsh change including very high resolution (VHR) satellite imagery, Landsat, Synthetic Aperture Radar (SAR), and aerial imagery (Campbell *et al*. 2017; Kearney *et al*. 2002; Fu *et al*. 2017; Watson *et al*. 2017). Salt marsh time series analysis has been conducted using Moderate Resolution Imaging Spectroradiometer (MODIS) data for prograding coasts (Zhao *et al*. 2009), wetland classification using SPOT-5 data (Davranche *et al*. 2010), Landsat yearly Normalized Difference Vegetation Index combined with tasseled cap values to determine change (Kayastha *et al*. 2012), aboveground biomass time series of *S. alterniflora* (O'Donnell & Schalles 2016), and Google Earth Engine

(GEE) to understand freshwater wetland change (Hird *et al*. 2017). Recent, time series studies have employed all available Landsat images to quantify ecological processes, and land-use and land-cover change (Vogelmann *et al*. 2016; Fu & Weng 2016; Pasquarella *et al*. 2016). The utilization of GEE to process and derive time series has the potential to elucidate the changes these ecosystems are experiencing regionally.

Estimates of salt marsh change have shown a slowing of loss across the Atlantic coast of the USA from 2004 to 2009 with a 0.4 % reduction of estuarine emergent vegetation (Dahl & Stedman 2013). Estimates from specific sites have demonstrated extensive losses of salt marsh including Rhode Island, Jamaica Bay, and Chesapeake Bay, however these studies evaluated long-term change (Watson *et al*. 2017; Campbell *et al*. 2017; Schepers *et al*. 2017). Salt marshes composed predominantly of *S. alterniflora* or *S. patens* in the mid-Atlantic coast are peat dominated (Elsey-Quirk *et al*. 2011). Salt marshes which rely on organic matter to build elevation, as opposed to those accreting mostly through sedimentation, such as those along the southeast U.S. coast (Morris *et al*. 2002), may adapt more slowly to SLR (Mudd *et al*. 2004).

In the mid-Atlantic, SLR is exceeding accretion rates at many locations (Crosby *et al*. 2016). Salt marshes with microtidal ranges and low sediment budget are at greater risk from SLR (Roman 2017). The elevated risk to these salt marshes makes them the equivalent of canaries in the coal mine; ideal systems for studying and monitoring the effect of SLR on salt marsh resilience. Loss of back-barrier salt marshes also has implications for the entire barrier island system. Barrier islands are predicted to follow a runaway transgression model in which SLR drives salt marsh

drowning causing an increase in the back bay tidal prism and less sediment reaching the barrier beach, which results in additional erosion and migration of the barrier island (FitzGerald *et al*. 2008). However, the opposite relationships has been observed in the mid-Atlantic barrier islands where localized drivers of barrier island migration have been suggested (Deaton *et al*. 2017). Landsat's global and temporally-rich archive is the ideal data source for monitoring the persistence of salt marshes across the mid-Atlantic with the potential to expand these methods.

Remote sensing of salt marsh is prone to time series outliers due to tidal inundation, extreme water events, and atmospheric anomalies. However, with the use of spectral indices tidal inundation events can be filtered (O'Connell *et al*. 2017). The tidal stage at the time of image acquisition can directly impact the extent of salt marsh vegetation in Landsat imagery (Jensen *et al*. 1993) and in VHR imagery due to low marsh being submerged at high tide (Campbell & Wang 2018). Time series outliers can alter the attributes and the results of an analysis (Basu & Meckesheimer 2007). Therefore, the effect of tidal outliers is a concern in salt marsh environments. The tidal marsh inundation index (TMII) has been successfully used to identify inundated pixels and improve time series results for MODIS (O'Connell *et al.* 2017). Additionally, time series analysis with season and trend decomposition has been found to be robust to noise when detecting change (> 0.1 NDVI) (Verbesselt *et al*. 2010). In this study, the effect of tidal inundation on the time series has been mitigated by the use of filtering and seasonal and trend decomposition.

This study explores the capacity of time series analysis to help understand salt marsh dynamics in association with locations of stability, gradual loss, loss driven by

disturbance, or a combination of loss and recovery and the sources of change such as tidal loss, interior drowning, edge erosion, barrier island migration processes, and shifts in vegetation composition. The objectives of this study include: (1) to test the TMII for use with Landsat time series; (2) to model the aboveground biomass of mid-Atlantic salt marshes and show how it changed from 1999 to 2018 and (3) to evaluate the salt marsh aboveground biomass estimates with high spatial resolution imagery and *in situ* aboveground biomass estimates.

2. Methods

2.1 Study site

The mid-Atlantic coastal region has a variety of estuaries and bays including drowned river valleys such as the Chesapeake and Delaware Bays and barrier island lagoon systems such as Great South Bay and Barnegat Bay. Watersheds were used as the spatial extents for this study because salt marshes are affected by their watershed's sediment supply (Weston 2014) and nutrient loads (Deegan *et al*. 2012). The study selected USGS Hydrological Unit Code 8, i.e. HUC-8, watersheds covering areas including southern New York, New Jersey, Delaware, Maryland, Virginia, and Northern North Carolina (Figure 1). The majority of these watersheds are dominated by back-barrier lagoon systems with extensive salt marshes. The exception was the Tangier watershed within the Chesapeake Bay which is a drowned river valley. The Tangier watershed is an area of extensive land loss due to SLR, low sediment load, and groundwater withdrawal (Kearney & Stevenson 1991). The dominate salt marsh species in these watersheds are *S. alterniflora* in the low marsh and *Juncus gerardii*, *S. patens*, *Distichlis spicata*, and *J. roemerianus* in the high marsh. Extensive changes in the mid-Atlantic are projected from climate change including shifts in salt marsh plant composition and extent, displacement of species (Najjar *et al*. 2000), increases in decomposition rates leading to a reduction of organic accretion in the low marsh (Crosby *et al*. 2017), and possible reductions in belowground biomass due to earlier senescence of *S. alterniflora* (Crosby *et al*. 2015).

2.2 Data

Landsat 7 and Landsat 8 Tier-1 imagery accessible with GEE were used for the

time series analysis. Multispectral Landsat 7 Enhanced Thematic Mapper + (ETM+) has a 30 m spatial resolution for bands 1-5 and 7. The panchromatic band 8 has a 15 m spatial resolution. Landsat 8 Operational Land imager (OLI) and Thermal Infrared Sensor (TIRS) are instruments onboard the Landsat 8 satellite. OLI has a 30 m spatial resolution for bands 1-7 and 9. The OLI panchromatic band 8 has the same spatial resolution as the ETM+ panchromatic band.

The selected ETM+ imageries were acquired 7/01/1999 to 4/01/2017. The OLI imageries were acquired 3/20/2013 – 7/28/2018. The HUC-8 watersheds are covered by Landsat scenes of WRS-2 Path/Row 14/34, 14/33, 13/32, 13/31, 14/32, and 14/35. The selection and filtering resulted in ≈144 scenes for most pixels in the study area (Figure 2). GEE was used to convert Landsat 7 surface reflectance to Landsat 8 surface reflectance following the methods in Roy *et al*. (2016). The converted values were then used to calculate vegetation indices utilized in the tidal filtering and random forest regression estimating aboveground green biomass (Byrd *et al*. 2018). Raw time series of the spectral indices were computed for each pixel within the defined extent of salt marsh and exported from GEE. The spectral indices were converted to aboveground green biomass following the methods put forth in Byrd *et al*. (2018), which achieved a RMSE of 310 g m^{-2} and $R^2 = 0.59$, for calculating aboveground biomass with Landsat data. All Landsat 7 and 8 scenes were filtered by cloud cover <50%, pixel quality, and a TMII value of >0.2. Landsat 5 data were not utilized due to a lack of conversion into Landsat 8 surface reflectance and lack of verification of the aboveground green biomass model (Roy *et al*. 2016; Byrd *et al*. 2018).

National Wetland Inventory (NWI) data were used to select estuarine emergent

vegetation pixels and VHR satellite imagery to verify the relationship of aboveground green biomass estimates and vegetation extent. The spatial resolution excluded areas which fell directly within creeks, ditches, and mapped pools, resulting in the removal of some partial salt marsh pixels from the analysis.

The Worldview-2 imagery was collected on October 11 and October 16, 2016 for the Chincoteague watershed. This imagery included the entirety of Assateague Island. Multispectral Worldview-2 imagery possesses 2.4 m spatial resolution and a panchromatic band of 0.46 m. The spectral coverage includes 8 bands ranging from coastal blue, blue, green, yellow, red, red edge, to near infrared.

2.3 Time Series Analysis

NDVI is frequently used in time series analysis including monitoring forest disturbance with Landsat (DeVries *et al*. 2016), determining wetland variability in a river delta (Zoffoli *et al*. 2008), mapping agricultural abandonment across decades (Estel *et al*. 2015), and mapping change in salt marsh environments (Klemas 2011). NDVI is an indicator of many aspects of aboveground biomass (Anderson *et al*. 1993). Recent methods for estimating aboveground green biomass in freshwater and salt marsh environments have relied on vegetation indices (Byrd *et al.* 2014; Byrd *et al*. 2018). This method allows for the estimation of aboveground green biomass for the majority of plants common in the estuarine emergent wetland category of Cowardin *et al*. (1979).

The R package Prophet was used for time series analysis (Taylor & Letham 2018). The seasonal-trend decomposition method uses locally weighted regression smoother (LOESS) to isolate the seasonality, trend, and noise (Cleveland et al. 1990).

The approach has been used for many remote sensing time series studies (Verbesselt *et al*. 2010; Fu & Weng 2016; Zhu *et al*. 2016) The prophet package was used due to its robustness to irregular time series, ability to calculate many time series, and identify trends and seasonality.

2.4 TMII

Many spectral indices such as the Enhanced Vegetation Index share formulas between Landsat and MODIS. TMII was developed for MODIS data. This study assessed the index for use with Landsat data. $NDWI_{green, swir}$ and $NDWI_{nir, swir}$ were calculated for each salt marsh pixel. The $NDWI_{nir, swir}$ was averaged for each month across each pixel's time series for a single sensor. This replaced the rolling average of the MODIS TMII which included 44 adjacent time periods (O'Connell *et al*. 2017). Replicating such a rolling average would not be reasonable for our coarse temporal resolution. The adapted formulas and the original MODIS formulation are shown below.

1) MODIS TMII

$$\text{TMII} = (1 - (1/\text{e}\text{\^{}}(0.3 + 16.6 * \text{NDWI}_{4,6} - 25.2 * \text{rolling mean}\left(\text{NDWI}_{2,5}\right)))$$

(O'Connell *et al*, 2017).

2) Landsat 7 TMII

$$\text{TMII} = (1 - (1/\text{e}\text{\^{}}(0.3 + 16.6 * \text{NDWI}_{4,5} - 25.2 * \text{monthly mean}\left(\text{NDWI}_{2,5}\right)))$$

3) Landsat 8 TMII

$$\text{TMII} = (1 - (1/\text{e}\text{\^{}}(0.3 + 16.6 * \text{NDWI}_{3,6} - 25.2 * \text{monthly mean}\left(\text{NDWI}_{5,6}\right)))$$

The resulting index was evaluated at the Sapelo Island phenocam across Landsat 7 and Landsat 8 images from WRS-2 Path/Row 16/38 and 17/38 and a date range from 8/09/2013 to 5/03/2018. The evaluation followed the approach of O'Connell *et al*. (2017).

2.5 Statistical Analysis

In this study, the time series were analyzed for breakpoints with the Breaks for Additive Season and Trend (BFAST) algorithm. The algorithm as implemented in the BFASTspatial package for R was used (Dutrieux & DeVries 2014; R Core Team 2013). The algorithm has been used to successfully detect trends in remote sensing imagery (Verbesselt *et al*. 2010). The algorithm requires a defined stable period to which subsequent dates are compared to determine if the new data fits the expected time series model. The stable period was defined as 1999-2012. The performance of this algorithm was evaluated using the Southern Long Island and the Eastern Lower Delmarva watersheds. These disturbances represent deviations from the expected time series, and could correspond with disturbance events of >30 m scale including Hurricane Sandy, tidal loss, and barrier migration. For Southern Long Island, the average biomass in the summer of 2012 (July, August, September) was compared to the final average biomass in 2018 with Spearman's rank correlation for both disturbed and non-disturbed pixels.

The effect of tidal range on salt marsh change was explored with the use of data from NOAA tidal stations. The tidal ranges of each tidal station within our study

area were interpolated into a raster map of tidal ranges as they coincided with HUC-12 watersheds within the study area. All Landsat centroids that were in the interior of the salt marsh (>30 m from an edge) were analyzed. The effect of tidal range on average change across HUC-12 watersheds and the four dominate salt marsh classes (estuarine emergent regularly flooded, estuarine emergent irregularly flooded, estuarine emergent ditched regularly flooded, and estuarine emergent ditched irregularly flooded) were compared with linear regression. The average change in aboveground green biomass for each HUC-12 watershed was compared to the average tidal range within that watershed. The Albemarle watershed, NC was excluded due to the larger distances between tidal stations.

An analysis of all Landsat pixels of the estuarine emergent regularly flooded, estuarine emergent irregularly flooded, estuarine emergent ditched regularly flooded, and estuarine emergent ditched irregularly flooded classes was conducted for each watershed. Kruskal-Wallis and post-hoc Dunn's test with Bonferroni adjustment compared the trend in aboveground green biomass from 1999 to 2018 for each watershed across these four dominate classes.

Worldview-2 image classification of interior salt marsh mudflats was used to assess the relationship of aboveground biomass estimates and vegetation extent within the test pixel. The Wordlview-2 classification was an object-based image analysis utilizing the approach of Campbell *et al.* (2017; Wang & Campbell, 2018). This analysis was conducted for a portion of the salt marsh on the Maryland side of Assateague Island within the Chincoteague watershed. This analysis was conducted for mudflats on Assateague Island which corresponded with WRS-2 Path/Row 14/33.

End of season i*n situ* biomass estimates from 1999-2014 for the Eastern Lower Delmarva were accessed from Christian & Blum (2014). These estimates included 17 sites at Mill Creek, Bellvue, Steelman's landing, Gator Track, Cushman's landing, Oyster Marsh, Indian Town, Box Tree, Brownsville, Hog Island north, Hog Island south, Kegotank, Green Creek, Wallops Island, Woodland Farm, and Assateague (Christian & Blum, 2014). The sites were sampled along transects at four locations, creek side, low marsh, high marsh, and upland transition (Christian & Blum, 2014). These locations and replicates were averaged to get an estimate of each sites aboveground biomass in a single year which were compared to the average aboveground green biomass estimates for July, August, and September in the corresponding years. RMSE was calculated considering each year and each site, and a site-wide RMSE including all years.

3. Results

3.1 Biomass modeling and change

The ability of the time series trend component to reveal salt marsh change was evident in the identification of both losses and gains across the watersheds. Across the studied watersheds 52% of salt marsh experienced a decline in aboveground green biomass with an average reduction of -17 g m^{-2} (Table 1). In the Chincoteague watershed, declines were most common and interior loss along the back-barrier of Assateague Island National Seashore was apparent (Figure 3). Increases in aboveground green biomass were most prominent in the prograding areas to the south of Assateague Island (Figure 3c) and on the overwash fans on northern Assateague Island (Figure 3b). In general, Chincoteague, Eastern Lower Delmarva, and Southern Long Island all had moderate declines in biomass (Table 1). Tangiers, Mullica-Toms,

Albemarle, and Great Egg Harbor had slight increase. The Chincoteague, Eastern Lower Delmarva, and Southern Long Island watersheds demonstrated considerable net loss of aboveground green biomass (Figure 4). The Chincoteague watershed had the largest average loss which was -61 g m^{-2}. The Tangier watershed had the largest average gain which was 15 g m^{-2}.

3.2 TMII

The TMII was assessed by evaluating the inundation of each Landsat image date and time of collection at the phenocam and by plotting the decomposed time series before and after filtering (Figure 5). The filtered time series removed all pixels with a TMII >0.2. This level of TMII was suggested previously and performed well in the analysis with the phenocam. The filtered time series removed extreme outliers reduced the observed trend and improved the seasonal graph. The phenocam analysis had a limited number of inundated scenes to work with using images from both WRS-2 Path/Row 16/38 and 17/38. For Landsat 7 and 8, the phenocam image evaluation verified that 10 of the 14 images with TMII >0.2 were inundated. The performance improved slightly when just considering the Landsat 8 imagery, which found 7 out of 9 inundated images were correctly identified. The index had few false negatives for inundation with 148 out of 150 non-inundated images being accurately identified. The filter was applied due to its ability to remove outliers and improve both the seasonal and trend component of the time series decomposition (Figure 5).

3.3 Salt marsh trend

The rates of change varied greatly across watersheds with the Chincoteague watershed having the largest average change and the Tangiers watershed having the

largest average increase. The Eastern Lower Delmarva watershed had the largest total loss (Figure 4). The trend maps reveal clustering of loss around landscape features such as ditches, inlets, and rivers even in stable watersheds (Figure 6). Moran's I for each of the watershed confirmed clustering of salt marsh change (Table 2).

Kruskal-Wallis test was used to test the difference between dominant salt marsh types with each analysis finding significant differences (Table 3). Dunn's *post hoc* test determined that Chincoteague watersheds had no statistically significant difference between regularly and irregularly flooded salt marsh (Table 3). Chincoteague and Albemarle were the only watersheds were ditched regularly flooded lost vegetation at a lesser rate than regularly flooded salt marshes. Eastern Lower Delmarva and Tangiers were the only watersheds were regularly flooded salt marsh lost more biomass than irregularly flooded salt marsh. Mullica-Toms, Great Egg Harbor, and Tangier watersheds were the only watersheds to demonstrate a small increase in aboveground green biomass. These watersheds were mosaics composed of a combination of increases and decreases in aboveground biomass (Figure 6; Figure 7; Figure 8).

3.4 Tidal range

No significant effect of tidal range was found for the entirety of the average aboveground green biomass change by HUC-12 watersheds ($F_{(1,573)}=0.52$, $p = 0.52$) and $R^2=0$. However, when comparing those sites with irregular tidal inundation, mosquito ditches, and a tidal range < 0.8 m; then sites with small tidal ranges saw significantly more loss ($F_{(1,34)}=6.2$, $p < 0.05$) and $R^2 = 0.16$). When comparing those sites with regular tidal inundation, mosquito ditches, and a tidal range < 0.8 m; then

small tidal ranges also saw significantly more loss ($F_{(1,14)}=7.1$, $p < 0.05$) and $R^2 = 0.33$). Neither inundation regime without mosquito ditches had a significant relationship to tidal range.

3.5 Disturbance

The Southern Long Island and Eastern Lower Delmarva watersheds were analyzed with the BFAST algorithm to detect disturbances. The watersheds were selected as they had high average rate of. In the Eastern Lower Delmarva, 46% of pixels were disturbed and the average disturbance was a loss of -59. In the Southern Long Island watershed, 28% of pixels were disturbed and the average disturbance was a loss of 46. The resulting maps demonstrated that disturbances captured some of the long-term change, however, many of the detected disturbances in the time series did not represent a permanent change (Figure 9). Spearman's rank correlation showed that in non-disturbed pixels average summer aboveground green biomass in 2012 was correlated with the summer 2018 average biomass ($r\tau=0.74$, $p < 0.001$). Disturbance pixels had a smaller correlation with 2018 average biomass ($r\tau=0.54$, $p < 0.001$). In the long-term change maps areas and types of change are identifiable for example interior loss (Figure 10).

3.6 Verification

The relationship of Landsat derived estimates of aboveground green biomass and salt marsh extent were verified with Worldview-2 image classification of salt marsh on Assateague Island National Seashore (Wang & Campbell, 2018). The Worldview-2 classification was used to compare non-vegetated extent within a pixel to the estimates of aboveground green biomass. This comparison found a positive

relationship between biomass estimates and the area of mudflat within a pixel ($F_{(1165,1)}$=1316, $p < 0.001$) and R^2=0.53. The verification with VHR imagery suggests that the Landsat aboveground green biomass is related to vegetation extent.

The *in situ* analysis resulted in a site-wide RMSE of 144±7 with the confidence interval resulting in a conversion factor from wet biomass to dry of between 0.55 and 0.6. The *in situ* yearly RMSE for the Eastern Lower Delmarva watershed 1999 to 2014 was found to be 298 ±15. This compares favorably with the RMSE calculated internally for this type of modeling (Byrd *et al*. 2018). The areas of uncertainty include the exact location of the sampling sites and differences between dates of the end of season sampling and July, August, and September satellite estimates.

4. Discussion

Aboveground biomass declined throughout three of study watersheds. These watershed-wide declines were driven by clusters of significant loss, even stable watersheds had areas of significant loss (Figure 3; Figure 6-8; Figure 10). The analysis of tidal range makes it clear that ditched salt marshes with < 0.8 m tidal range were more prone to loss of aboveground green biomass than the relatively more stable areas (> 0.8 m). This result is supported by previous modeling which found for the same suspend sediment concentrations macrotidal marshes (>4m tidal range) can adapt to much higher rates of SLR than microtidal (<2 m tidal range) salt marsh (Kirwan *et al*. 2010). The filling of mosquito ditches has been identified as a possible contributing factor to salt marsh dieback and loss of *Spartina patens* in Rhode Island (Raposa *et al*. 2017). The fragility of microtidal marshes is likely due to the relationship between tidal range and the growth range of *Spartina alterniflora* (McKee and Patrick 1988;

Cahoon *et al*. 2018). Ditched salt marshes comprised approximately 1/3 of all salt marsh pixels analyzed. These salt marshes are undergoing hydrological changes that are altering vegetation extent and quantity of plant biomass.

The analysis with high-resolution satellite imagery suggests that these Landsat estimates are partly explained by salt marsh extent within a pixel. However, vegetation extent does not explain all variation in the aboveground green biomass. The estimates are also influenced by the amount of water, vegetation composition, and geometric rectification of the two datasets. The composition of plants, salt marsh edge, and high marsh to low marsh are all possible sources of variability. These differences and other site characteristics result in variability of the biomass estimates. Aboveground green biomass estimates were determined to be an indicator of salt marsh change, especially in the interior salt marsh. Additional *in situ* verification would be necessary to determine the relationship of these changes to shifts in the vegetation community.

The *in situ* aboveground biomass samples from the Eastern Lower Delmarva verify a similar accuracy to internal out-of-box accuracy assessments. The model achieved a RMSE of 298 ±15 g m^{-2} compared to previous out-of-box estimates of 310 ±42 g m^{-2} (Byrd *et al*. 2018). However, models have been observed to perform better at the site scale (Byrd *et al.* 2014). The site wide RMSE, compared site averages for all available years, was 144±7. This observed improvement could be due to a reduction in the variability of *in situ* biomass, which was collected at a much finer resolution (0.0625 m^2). The site wide RMSE are likely a more appropriate assessment of the time series' performance.

The higher spatial resolution of NWI resulted in the inclusion of edge pixels

which are only partially composed of salt marsh. However, in most watersheds, these did not impact the trends as they changed little. The widespread loss of aboveground green biomass that was observed included several processes: 1) interior loss and fragmentation, 2) salt marsh loss due to inlet widening and change, 3) conversion of high marsh to low marsh, 4) edge erosion, and 5) overwash. Comparing edge (within 20 m of the salt marsh polygon edge) and interior marshes found that in all watersheds besides Chincoteague edge had a higher average rate of loss. In Chincoteague watershed edge areas lost on average 56 g m^{-2} compared to interior areas which lost on average 63 g m^{-2}. Interior loss appears to be the most frequent type of loss in Chincoteague. Chincoteague interior losses were likely connected to the microtidal range and site conditions such as mosquito ditches (Figure 3c). The higher rates of loss of regularly flooded compared to irregularly or regularly flooded ditched salt marsh for Chincoteague, suggests a relationship between these losses with SLR (Table 3).

Tidal loss corresponded with high magnitude disturbances, but were much less common (Figure 11). Small declines (<100 g m^{-2}) across the salt marsh were of little concern as they fall well within the uncertainty of this data. These areas are likely stable, however, if a dramatic increase in SLR or other stressors occur this could change, and all locations need monitoring. Due to the medium spatial resolution, used in this study, the cause of these minor changes is difficult to determine. Small declines in aboveground green biomass could be the result of a variety of changes within a pixel including vegetation type, plant composition, and percent cover or some combination of these factors. For example, increased inundation can cause replacement of high marsh plants with *S. alterniflora* and this is likely to reduce

aboveground biomass (Sneddon *et al*. 2015). Declines in irregularly flooded areas are possibly related to the replacement of high marsh with *S. alterniflora* which has been observed on Long Island (Cameron Engineering and Associates 2015) and Rhode Island (Raposa *et al*. 2017). In the mid-Atlantic, estimates of aboveground biomass for *S. patens, J. roemerianus,* and *S. alterniflora* were 1399 g m^{-2}, 853 g m^{-2}, and 257 g m^{-2}, respectively (Elsey-Quirk *et al*. 2011). The shift from *S. patens* or *J. roemerianus* to *S. alterniflora* would be accompanied by a large loss of above, and presumably, belowground biomass.

Edge erosion is a common salt marsh process with variable rates depending on basin characteristics (Mariotti & Fagherazzi, 2013). These erosional processes are likely to be less than the width of a Landsat pixel and therefore were frequently a subpixel change. However, extensive edge erosion was evident in the time series data (Figure 11c-d). Overwash was a loss process evident in all of the barrier island lagoon systems, however, both recovery (Figure 3c) and loss from overwash (Figure 10b; Figure 8) were evident. These types of change are easily detected due to their location along the barrier island interior and the magnitude of the loss.

4.1 Tidal filtering

The use of all available data is vital for understanding seasonal and long-term vegetation trends (Vogelmann *et al*. 2016). Keeping all quality data is especially important with Landsat time series given the limited temporal phases due to clouds, tides, 16-day revisit, and Landsat 7's shutter synchronization anomalies. The TMII filter is unique to the vegetation cover of a particular pixel. Therefore, it did not over filter those areas with frequent inundation. Adapting the index to Landsat posed

several challenges, including different bandwidths and lower temporal resolution. These issues were addressed with the conversion of rolling to monthly averages and substitution of bands with appropriate equivalents. The index could be further improved by considering a subset of a date's month for years directly preceding and following it. The filtering improved time series trend estimates (Figure 5). The rarity of false positives limited any reduction of quality data while removing many suspect images. In this study, the amount of data was essential to ensure enough images were available to filter by tides, cloud cover, and data quality. Tidal filtering is necessary to improve time series modeling of salt marsh and in turn our understanding of long-term salt marsh change.

4.2 Salt marsh change

Persistence versus die-off of salt marshes has been attributed to a variety of drivers such as sediment supply (Anisfeld *et al*. 2017), edaphic characteristics of the salt marsh (Crawford & Stone 2015), elevation (Watson *et al*. 2017), nutrient enrichment (Deegan *et al*. 2012), and basin characteristics (Mariotti & Fagherazzi 2013). Honeycombing of the interior salt marsh was evident particularly in ditched salt marshes and across the Chincoteague watersheds (Figure 3 d-e.). This relationship was most likely due to the combination of altered hydrology from mosquito ditches and small tidal ranges being more at risk due to SLR. There is no expected impact of mosquito ditches as a sediment sink on salt marshes response to SLR (Corman *et al*. 2012). The clustering of change in the salt marsh environments was evident visually and from the results of the Moran's I analysis (Table 1).

The Eastern Lower Delmarva watershed, had a significant average rate of loss (Figure 3) and a low average biomass, 529 g m^{-2} over July, August, and September of

2017 (Figure 11b). Salt marsh losses in the region are driven by barrier island migration at rates of 1-6 m yr^{-1} (Deaton *et al*. 2017), including shifts in the barrier island extent (Figure 11c). Edge erosion driven by sediment supply and salt marsh basin width have been proposed as significant contributors of salt marsh loss within the Eastern Lower Delmarva watershed (Mariotti & Fagherazzi, 2013). This represents a different change regime than the other barrier island watersheds in this study. Migration of the seaward salt marsh boundary, minor shifts in the interior back bay salt marsh, and significant edge erosion due to inlet shifts were evident from the aboveground biomass change maps (Figure 11). The BFAST algorithm determined disturbances (>100 g m^{-2}) corresponded with changes evident in the NAIP image record (Figure 11d). These moderate, but temporally discrete, changes represent a significant reduction in percent aboveground green biomass for many of the back bay areas. In the Eastern Lower Delmarva, 17% of all areas analyzed experienced a disturbance of this magnitude. Previous studies of this area were focused on salt marsh edge erosion and loss through barrier island migration. This study demonstrates that the site's salt marshes are low biomass, creating even greater likelihood of loss in the watershed. This watershed demonstrates the ability of this method to monitor salt marsh under a variety of change regimes.

4.3 Disturbance

The BFAST algorithm detected many disturbances. However, a large number of these disturbances were brief which is to be expected in salt marsh environments i.e. high inundation event or algal deposition on mudflats. Positive disturbances were common. However, these did not correspond with long-term increases (Figure 9). Both

the long-term trend analysis and disturbance analysis identified areas of loss (Figure 11). The disturbance pixels had less correlation with 2018 aboveground biomass than 2012 biomass in non-disturbed pixels. This correlation suggests that disturbed areas were less stable areas of the salt marsh. These disturbances illustrate the highly dynamic nature of these systems and the importance of monitoring salt marshes with time series data. Disturbances with an increase in aboveground green biomass could correspond with increased vegetation, changes to vegetation composition, algal deposition on mudflats, or algal blooms in pools. Temporary decreases could correspond with droughts, which have been observed as a driver of temporary salt marsh die-off in the southern United States (Alber *et al*. 2008).

5. Conclusion

This study puts forth an approach for understanding salt marsh change with a combination of medium resolution imagery and time series analysis. Declines in aboveground green biomass across the study area were identified with a mean of -17 g m^{-2} (Table 1). In the mid-Atlantic coastal watersheds, 52% of all area analyzed declined from 1999 to 2018. Areas of losses were evident across all watersheds likely driven by salt marsh stressors such as SLR, sediment starvation, and barrier island migration. Clusters of extensive loss corresponded with barrier island processes and interior drowning. This methodology was applied across the mid-Atlantic coastal zone including several barrier island watersheds and a sub-watershed of the larger Chesapeake Bay watershed. The BFAST algorithm successfully found large magnitude disturbances. However, there was little relationship found between all disturbances and long-term trends. The algorithm should be applied in salt marsh areas

following a major disturbance or other widespread change. It was evident that tidal range in areas with a < 0.8 m tidal range was influencing rates of loss in ditched salt marshes. The tidally filtered time series were necessary to determine the change experienced by the study sites. Landsat aboveground green biomass estimates had a positive relationship to changes in vegetation extent of VHR imagery. *In situ* biomass verification compared favorably with previous accuracy assessments and the time series analysis likely improves the accuracy of salt marsh change estimates.

GEE created a single processing environment facilitating the filtering of Landsat images, calculation of vegetation indices, the conversion of Landsat 7 surface reflectance into Landsat 8 surface reflectance, and processing of the raw time series. The limiting factor for the process was exporting data from GEE to be further analyzed. The Landsat archive is the only option for decadal time series of salt marsh environments with medium spatial resolution and an extensive archive. This approach demonstrates a promising method for both historic assessment and continued monitoring. However, higher spatial resolution imagery is necessary to increase the sensitivity of this methodology to fine-scale change. Next steps include applying the method to compare a broader range of sites and mapping areas identified as clusters of change with high spatial resolution imagery. Biomass is an important indicator of salt marsh sustainability, tied to ecogeomorphic feedbacks that contribute to salt marsh resilience. The current analysis demonstrates the use of aboveground biomass estimates as an indicator of salt marsh change at the watershed scale.

Table 1. The percentage of change, total area, and mean trend of estuarine emergent irregularly flooded, estuarine emergent regularly flooded, estuarine emergent irregularly flooded ditched, and estuarine emergent regularly flooded ditched classes from 1999 to 2018.

HUC 8 Code	Name	Decrease (%)	Increase (%)	Area (hectares)	Mean trend (g m^{-2})
02080110	Tangier	35	65	35650	15
02030202	Southern Long Island	76	24	7226	-48
02040301	Mullica-Toms	48	52	18891	1
02040302	Great Egg Harbor	49	51	21172	3
02040303	Chincoteague	62	38	14538	-63
02040304	Eastern Lower Delmarva	75	25	25880	-67
03010205	Albemarle	40	60	16223	5
	Mid-Atlantic coast	52	48	139580	-17

Table 2. The results of the Moran's I test of spatial autocorrelation for each of the watersheds. The neighbor distance was 200 m across all watersheds.

Watershed	Moran's Index	*P* value	z-score
Tangier	0.39	< 0.001	1572
Southern Long Island	0.41	< 0.001	1319
Mullica-Toms	0.53	< 0.001	1509
Great Egg Harbor	0.34	< 0.001	1050
Chincoteague	0.57	<0.001	1252
Eastern Lower Delmarva	0.45	<0.001	1513
Albemarle	0.41	<0.001	1319

Table 3. The results of the Kruskal-Wallis and Dunn's post hoc test for each of the 7 watersheds. The tests compared the four most common estuarine emergent vegetation subclasses including irregularly flooded (E2EM1N), regularly flooded (E2EM1P), ditched irregularly flooded (E2EM1Nd), ditched regularly flooded (E2EM1Pd).

Watershed	**Kruskal -Wallis**	**Dunn's post hoc test**					
		regularly flooded vs. ditched regularly flooded	regularly flooded vs. irregularly flooded	ditched regularly flooded vs. irregularly flooded	regularly flooded vs. ditched irregularly flooded	ditched regularly flooded vs. ditched irregularly flooded	irregularly flooded vs. ditched irregularly flooded
Tangier	H(3)=1239 , $p <$ 0.001	Z = 11.9 $p < 0.001$	Z = -27.3 $p < 0.001$	Z = -15.4 $p < 0.001$	Z = -16.5 $p <$ 0.001	Z = -16.5 $p < 0.001$	Z = -13.9 $p <$ 0.001
Southern Long Island	H(3)=248, $p <$ 0.001	Z = 9.0 $p < 0.001$	Z = 8.5 $p < 0.001$	Z = -3.9 $p = 0.001$	Z = 14.4 $p <$ 0.001	Z = -0.4 p =1.00	Z = 8.2 $p <$ 0.001
Mullica-Toms	H(3)=3099 , $p <$ 0.001	Z = 14.5 $p < 0.001$	Z = 2.5 $p = 0.4$	Z = -14.0 $p < 0.001$	Z = 36.9 $p <$ 0.001	Z = 5.7 $p < 0.001$	Z = 47.2 $p <$ 0.001
Great Egg Harbor	H(3)=4166, $p <$ 0.001	Z = 13.8 $p < 0.001$	Z = 4.1 p <0.001	Z = -12.8 $p < 0.001$	Z = 36.1 $p <$ 0.001	Z = 6.1 $p < 0.001$	Z = 57.9 $p <$ 0.001
Chincoteag	H(3)=12	Z = -5.3	Z = 2.1	Z = 6.8	Z =	Z = 28.2	Z =

ue	80, $p <$ 0.001	$p < 0.001$	$p = 0.11$	$p < 0.001$	28.2 $p <$ 0.001	$p < 0.001$	23.4 $p <$ 0.001
Eastern Lower Delmarva	H(2)=2262, $p <$ 0.001	NA	$Z = -47.5$ $p < 0.001$	NA	$Z = 2.3$ $p =0.04$	NA	$Z = 4.5$ $p <$ 0.001
Albemarle	H(3)=2142, $p <$ 0.001	$Z = -31.6$ $p < 0.001$	$Z = 14.7$ $p < 0.001$	$Z = 39.3$ $p < 0.001$	$Z =$ 19.9 $p <$ 0.001	$Z = 43.9$ $p < 0.001$	$Z = 1.6$ $p =$ 0.36

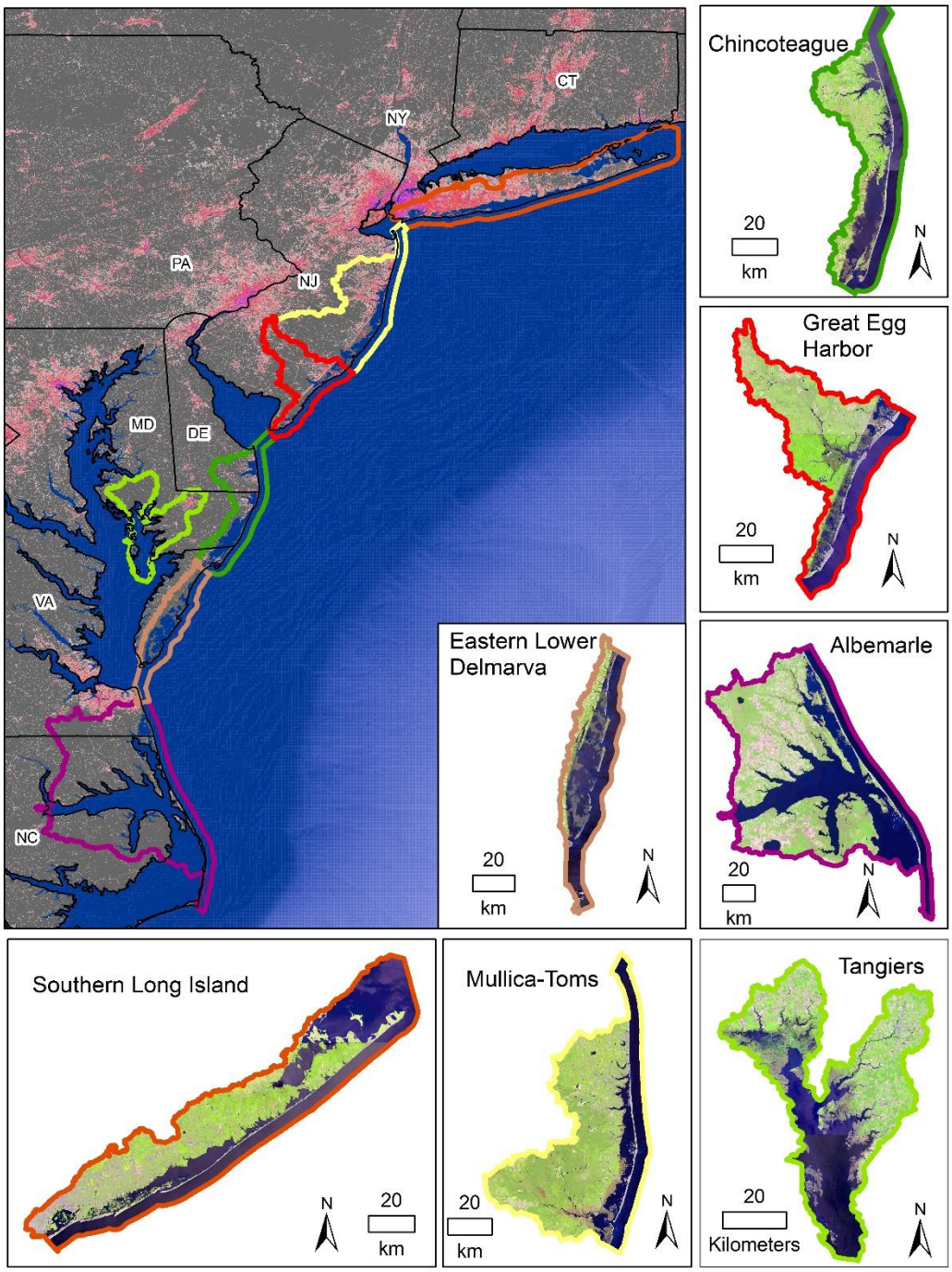

Figure 1: The seven study watersheds located across the mid-Atlantic coast. Background data in display are 100 m impervious surface and 30 arc-second GEBCO bathymetry data. Watershed subsets are true color Landsat 8 imagery.

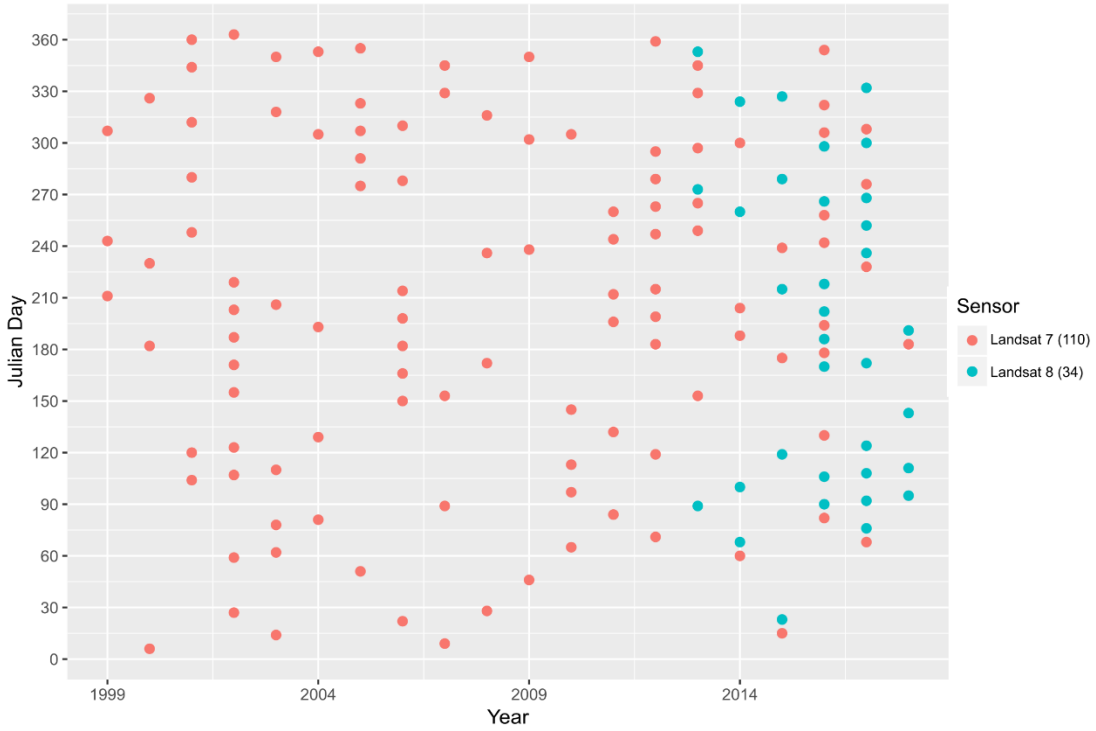

Figure 2: The year, Julian date, and Landsat sensor of each image after filtering by pixel cloud cover and TMII for a single Southern Long Island watershed time series.

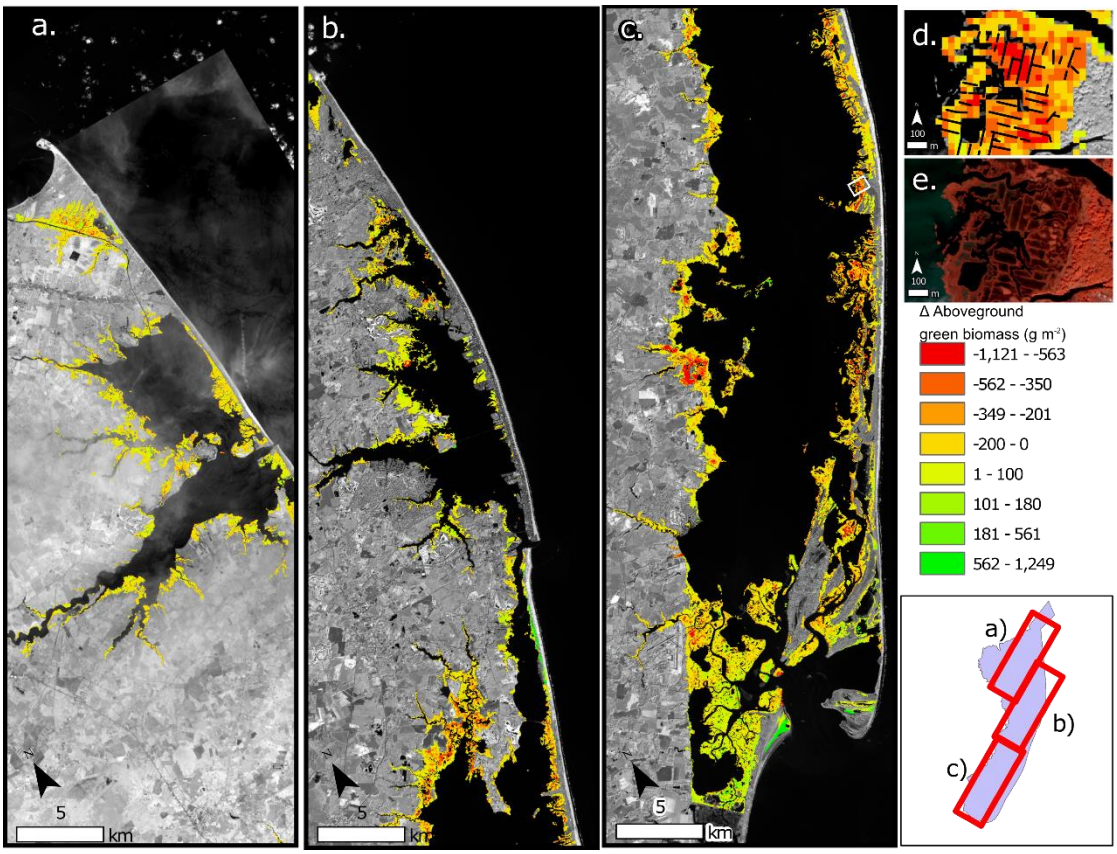

Figure 3: a-c. Change in aboveground green biomass from 1999-2018 for the Chincoteague watershed, encompassing the eastern shore of Maryland and a sections of Virginia and Delaware. d. Inset (white box in c.) of salt marsh change and mosquito ditches. e. Worldview-2 pseudo-color image of the same extent as d.

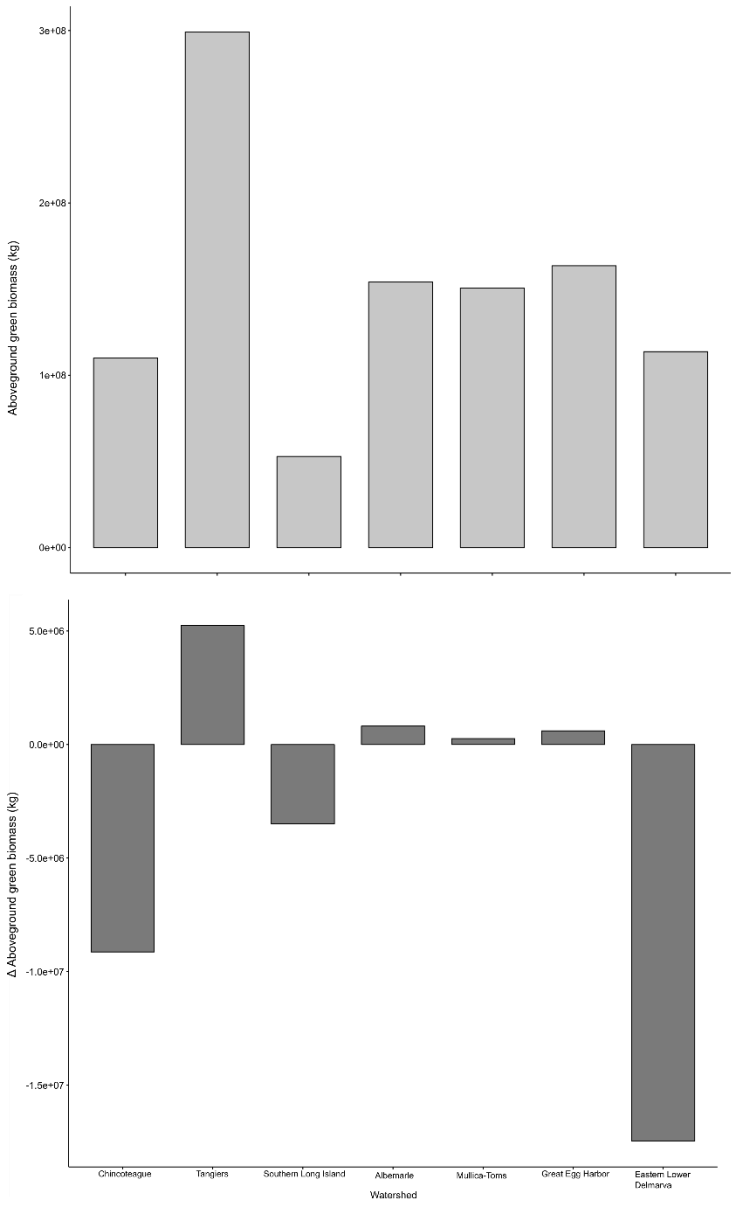

Figure 4: a) The sum of the average aboveground green biomass (1999-2018) for each watershed. b) The net change (1999-2018) in aboveground green biomass for each watershed.

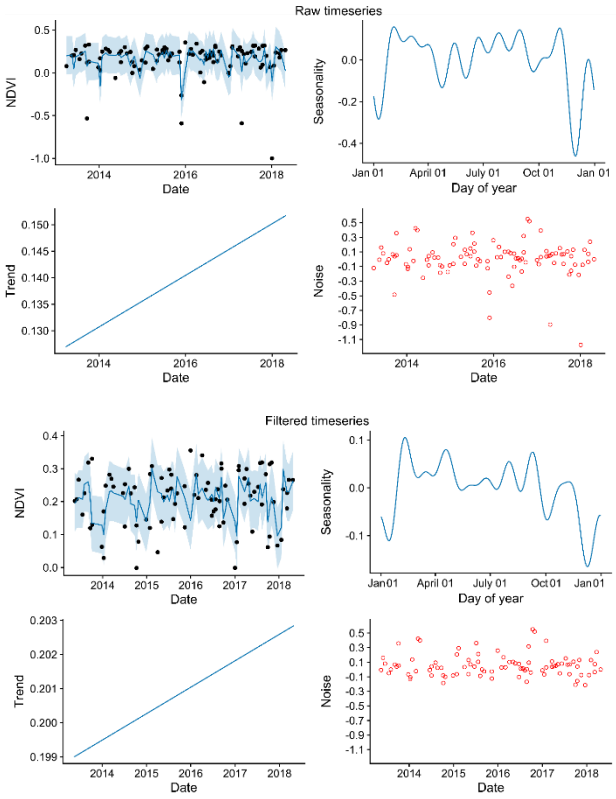

Figure 5: Evaluation of TMII with time series analysis using Landsat 7 and 8. Raw time series includes inundated dates. Filtered time series was excluded dates with TMII > 0.2.

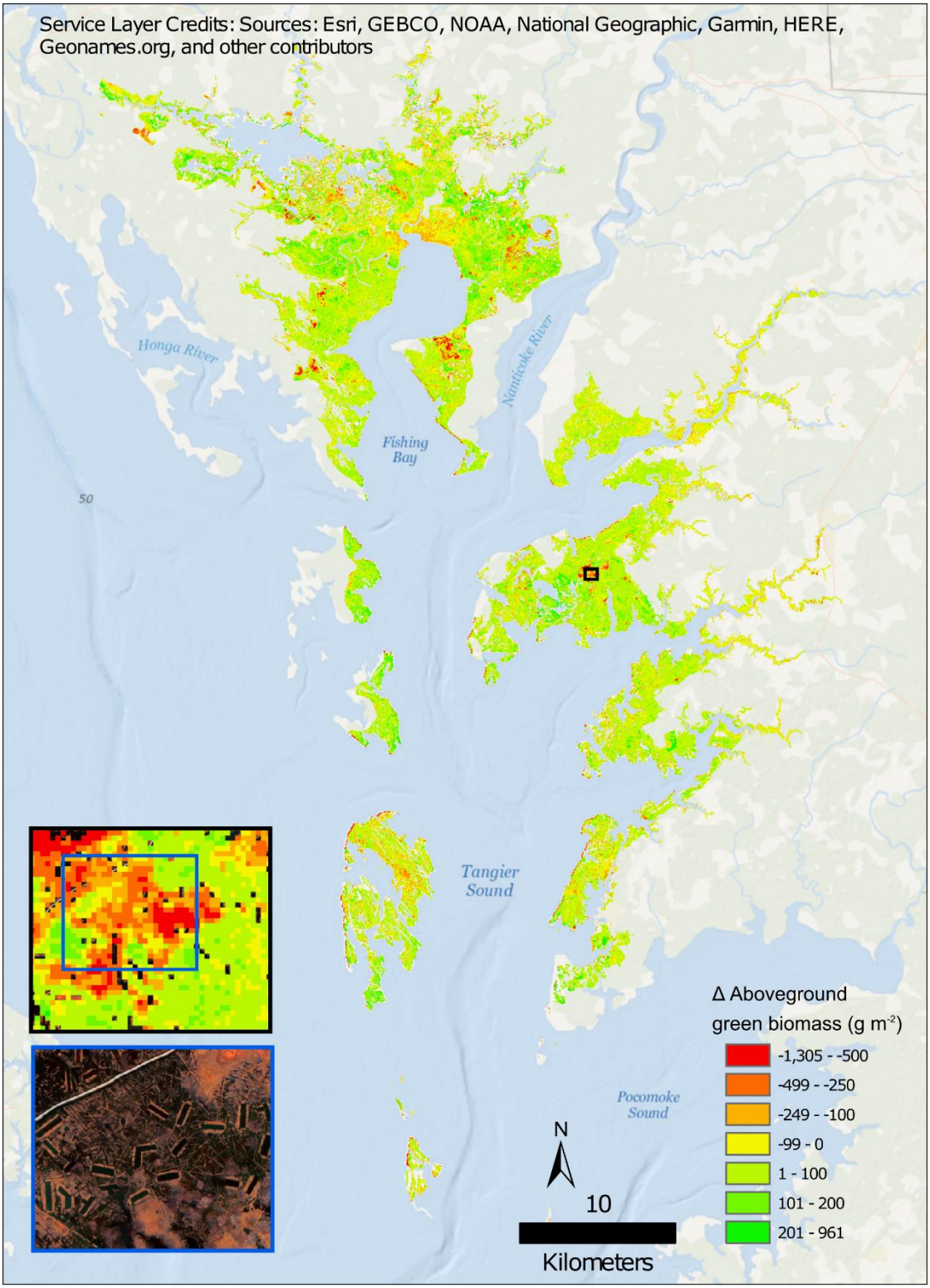

Figure 6: Change in aboveground green biomass from 1999 to 2018 in the Tangier watershed. a. Shows an inset area of concentrated change in the aboveground green biomass trend. b. shows a subset of the heavily ditched area with pseudo color NAIP imagery from 6/1/2017.

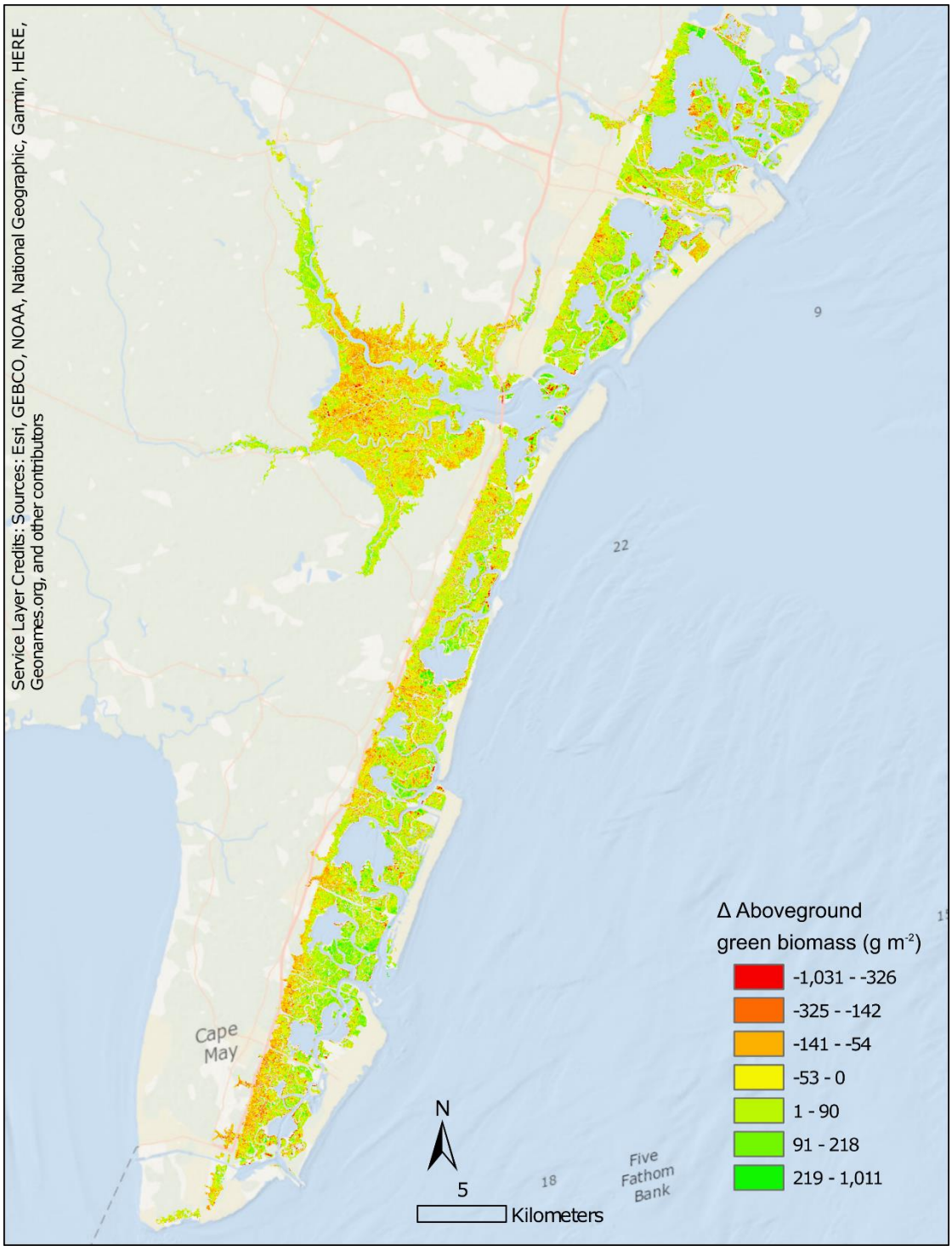

Figure 7: Great Egg Harbor watershed, stretching from Cape May, NJ to just south of Great Bay, NJ. The change of aboveground green biomass from 1999 to 2018.

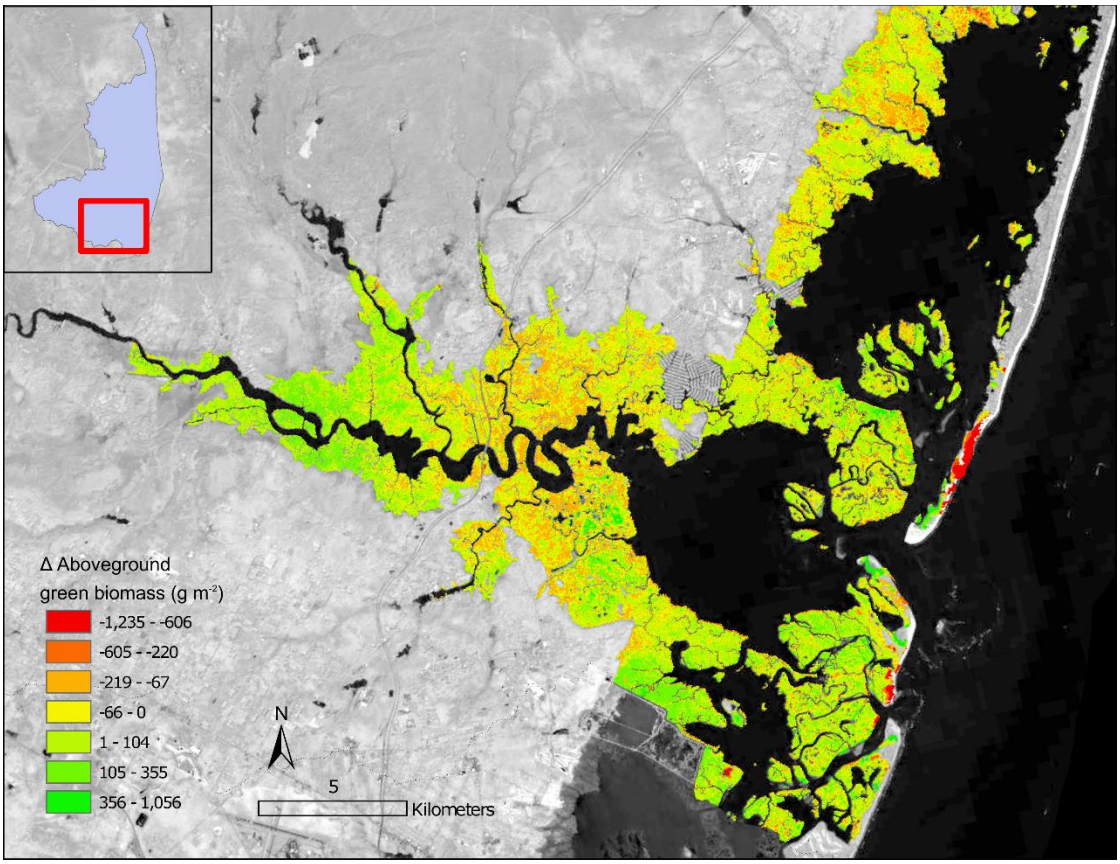

Figure 8: Change in aboveground green biomass from 1999-2018 for an area surrounding Great Bay, NJ, a section of the Mullica-Toms watershed.

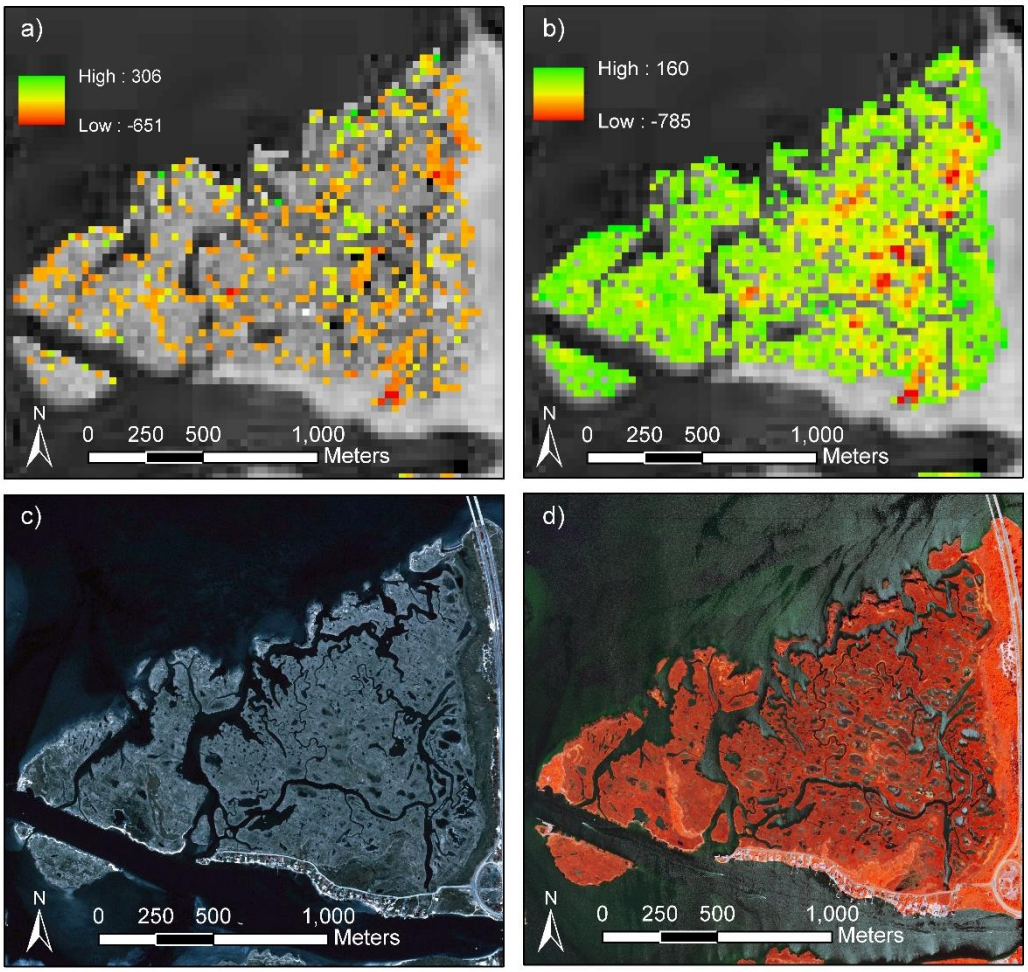

Figure 9: a) Aboveground green biomass disturbance magnitude (g m^{-2}). b) Aboveground green biomass trend 1999-2018 (g m^{-2}). c) 1996 digital orthophoto. d) NAIP image from 2017.

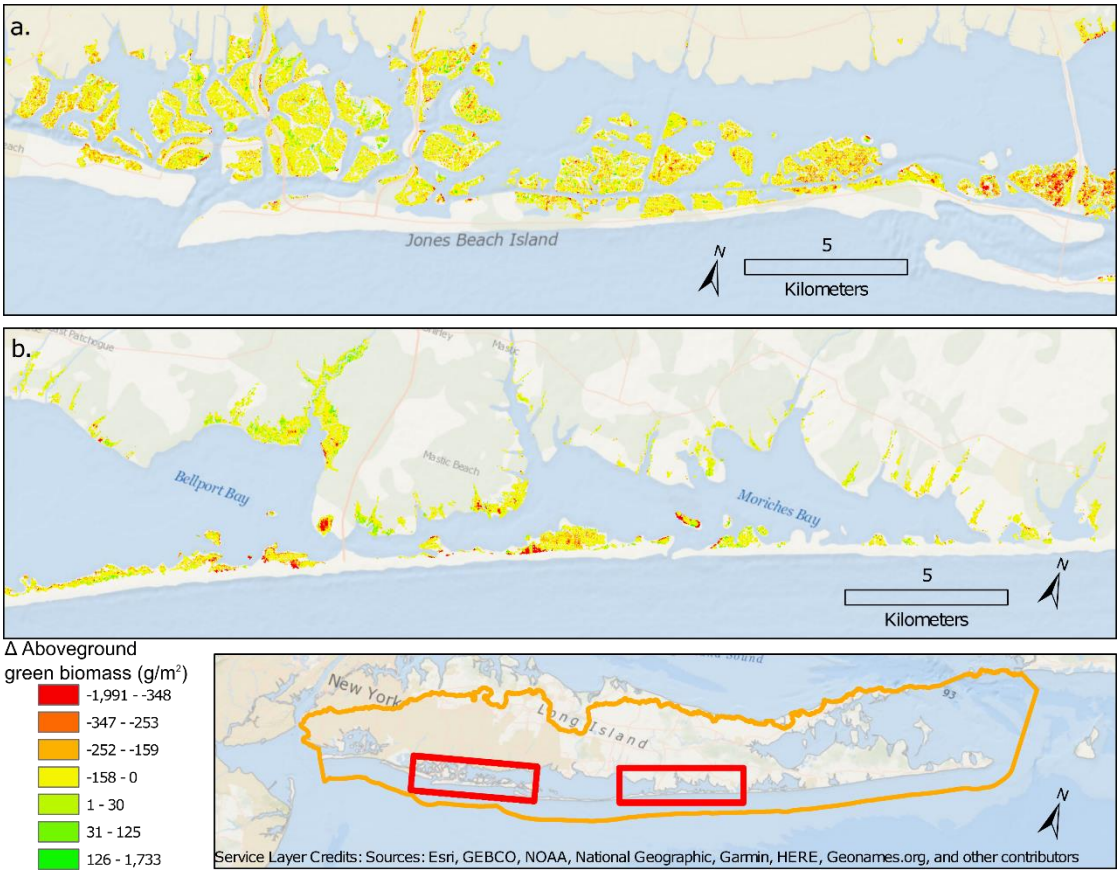

Figure 10: Two subsets of the Southern Long Island watershed. Change in aboveground green biomass from 1999-2018: a) the back bay salt marshes of Jones Beach Island; b) the north-eastern section of Fire Island and Moriches Bay.

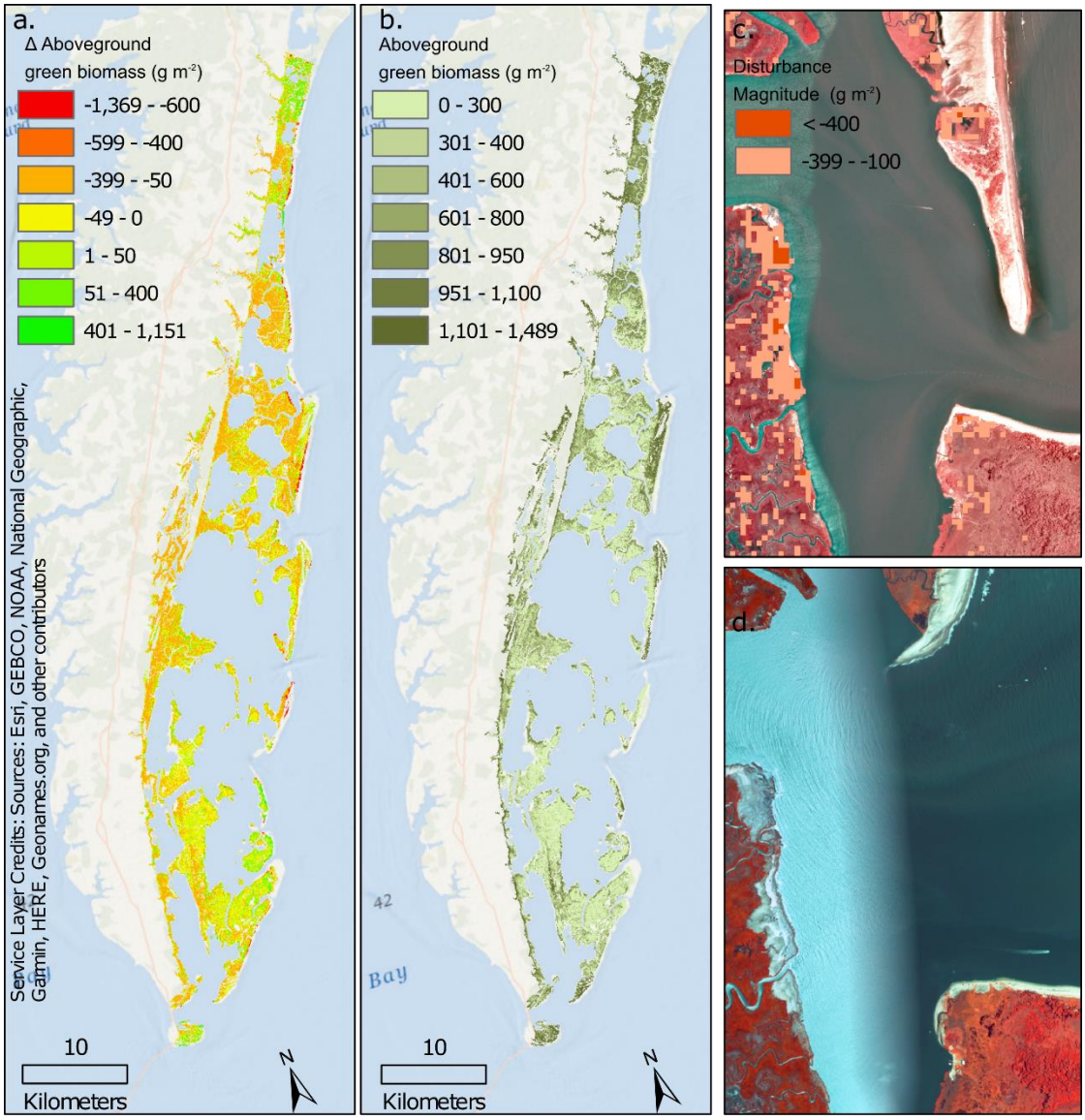

Figure 11: a) Eastern Lower Delmarva watershed change in aboveground green biomass from 1999 to 2018. b) Eastern Lower Delmarva watershed with the average aboveground green biomass in July, August, September of 2017.

Acknowledgments

This study was an extended investigation following a project funded by the Northeast Coastal and Barrier Network of the National Park Service on salt marsh mapping and change analysis using VHR Worldview-2 and Quickbird-2 data for the Jamaica Bay Unit of Gateway National Recreation Area (New York), Fire Island National Seashore, and Assateague National Seashore. The time series analysis and GEE engine work was funded by NASA RI Space Grant Summer fellowship. We thank the Virginia Coast Reserve Long-Term Ecological Reserve for sharing *in situ* biomass estimates with the support of NSF Grants BSR-8702333-06, DEB-9211772, DEB-9411974, DEB-0080381, DEB-0621014 and DEB-1237733.

References

Alber, M., Swenson, E.M., Adamowicz, S.C., & Mendelssohn, I.A. 2008. Salt marsh dieback: an overview of recent events in the US. *Estuarine, Coastal and Shelf Science*, 80, 1-11.

Anisfeld, S.C., Cooper, K.R. and Kemp, A.C., 2017. Upslope development of a tidal marsh as a function of upland land use. *Global change biology*, *23*(2), pp.755-766.

Armitage, A.R., Highfield, W.E., Brody, S.D., & Louchouarn, P. 2015. The contribution of mangrove expansion to salt marsh loss on the Texas Gulf Coast. *PloS one, 10*, e0125404.

Basu, S., & Meckesheimer, M. 2007. Automatic outlier detection for time series: an application to sensor data. *Knowledge and Information Systems, 11*, 137-154.

Byrd, K.B., O'Connell, J.L., Di Tommaso, S., & Kelly, M. (2014). Evaluation of sensor types and environmental controls on mapping biomass of coastal marsh emergent vegetation. *Remote Sensing of Environment, 149*, 166-180

Byrd, K.B., Ballanti, L., Thomas, N., Nguyen, D., Holmquist, J.R., Simard, M. and Windham-Myers, L., 2018. A remote sensing-based model of tidal marsh aboveground carbon stocks for the conterminous United States. *ISPRS Journal of Photogrammetry and Remote Sensing*, *139*, pp.255-271.

Boon, J.D., 2012. Evidence of sea level acceleration at US and Canadian tide stations, Atlantic Coast, North America. Journal of Coastal Research 28 (6), 1437-1445.

Cahoon, D.R., Lynch, J.C., Roman, C.T., Schmit, J.P., Skidds, D.E., 2018. Evaluating the Relationship Among Wetland Vertical Development, Elevation Capital, Sea-Level Rise, and Tidal Marsh Sustainability. Estuaries and Coasts 1-15.

Cameron Engineering and Associates. 2015. Long Island tidal wetlands trends analysis. *New England Interstate Water Pollution Control Commission*, 1:207.

Campbell, A., Wang, Y., Christiano, M., & Stevens, S. 2017. Salt Marsh Monitoring in Jamaica Bay, New York from 2003 to 2013: A Decade of Change from Restoration to Hurricane Sandy. *Remote Sensing, 9*, 131.

Campbell, A. Wang, Y. 2018. Examining the Influence of Tidal Stage on Salt Marsh Mapping using High Spatial Resolution Satellite Remote Sensing and Topobathymetric LiDAR. In Press. *IEEE Transactions on Geoscience and Remote Sensing.*

Christian, R. and L. Blum. 2014. End of Year Biomass in Marshes of the Virginia Coast Reserve 1999-2014. Virginia Coast Reserve Long-Term Ecological Research Project Data Publication knb-lter-vcr.167.22

(doi:doi:10.6073/pasta/44051c788e3bb5339b20a0ce9307d992)

Corman, S.S., Roman, C.T., King, J.W., Appleby, P.G., 2012. Salt marsh mosquito-control ditches: sedimentation, landscape change, and restoration implications. Journal of Coastal Research 28 (4), 874-880.

Cowardin, L.M., Carter, V., Golet, F.C., & LaRoe, E.T. 1979. Classification of wetlands and deepwater habitats of the United States. *Classification of wetlands and deepwater habitats of the United States*, 131.

Crosby, S.C., Angermeyer, A., Adler, J.M., Bertness, M.D., Deegan, L.A., Sibinga, N. and Leslie, H.M., 2017. Spartina alterniflora biomass allocation and temperature: implications for salt marsh persistence with sea-level rise. Estuaries and coasts, 40(1), pp.213-223.

Crosby, S.C., Sax, D.F., Palmer, M.E., Booth, H.S., Deegan, L.A., Bertness, M.D., et al. 2016. Salt marsh persistence is threatened by predicted sea-level rise. *Estuarine, Coastal and Shelf Science, 181*, 93-99.

Dahl, T.E. and Stedman, S.M., 2013. *Status and trends of wetlands in the coastal watersheds of the Conterminous United States 2004 to 2009*. US Department of the Interior, US Fish and Wildlife Service and National Oceanic and Atmospheric Administration, National Marine Fisheries Service.

Davranche, A., Lefebvre, G., & Poulin, B. 2010. Wetland monitoring using classification trees and SPOT-5 seasonal time series. *Remote Sensing of Environment, 114*, 552-562.

Deaton, C.D., Hein, C.J., & Kirwan, M.L. 2017. Barrier island migration dominates ecogeomorphic feedbacks and drives salt marsh loss along the Virginia Atlantic Coast, USA. *Geology, 45*, 123-126.

Deegan, L.A., Johnson, D.S., Warren, R.S., Peterson, B.J., Fleeger, J.W., Fagherazzi, S., et al. 2012. Coastal eutrophication as a driver of salt marsh loss. *Nature, 490*, 388.

DeVries, B., Verbesselt, J., Kooistra, L., & Herold, M. 2015. Robust monitoring of small-scale forest disturbances in a tropical montane forest using Landsat time series. *Remote Sensing of Environment, 161*, 107-121.

Dutrieux L., DeVries, B., Verbesselt, J. 2014. BfastSpatial: Set of utilities and wrappers to perform change detection on satellite image time-series. https://github.com/loicdtx/bfastSpatial. 0.6.2. DOI: 10.5281/zenodo.49693.

Elsey-Quirk, T., D.M. Seliskar, C.K. Sommerfield, and J.L. Gallagher, 2011. Salt marsh carbon pool distribution in a mid-Atlantic lagoon, USA: sea level rise implications, *Wetlands* , 31(1): 87- 99.

Estel, S., Kuemmerle, T., Alcántara, C., Levers, C., Prishchepov, A., & Hostert, P. 2015. Mapping farmland abandonment and recultivation across Europe using MODIS NDVI time series. *Remote Sensing of Environment, 163*, 312-325.

FitzGerald, D.M., Fenster, M.S., Argow, B.A., & Buynevich, I.V. 2008. Coastal impacts due to sea-level rise. *Annu.Rev.Earth Planet.Sci., 36*, 601-647.

Fu, B., Wang, Y., Campbell, A., Li, Y., Zhang, B., Yin, S., Xing, Z. and Jin, X., 2017. Comparison of object-based and pixel-based Random Forest algorithm for wetland vegetation mapping using high spatial resolution GF-1 and SAR data. *Ecological Indicators*, *73*, pp.105-117.

Fu, P., & Weng, Q. 2016. A time series analysis of urbanization induced land use and land cover change and its impact on land surface temperature with Landsat imagery. *Remote Sensing of Environment, 175*, 205-214.

Hird, J.N., DeLancey, E.R., McDermid, G.J., & Kariyeva, J. 2017. Google Earth Engine, Open-Access Satellite Data, and Machine Learning in Support of Large-Area Probabilistic Wetland Mapping. *Remote Sensing, 9*, 1315.

Holdredge, C., Bertness, M.D., & Altieri, A.H. 2009. Role of crab herbivory in die-off of New England salt marshes. *Conservation Biology, 23*, 672-679.

Jensen, J.R., Cowen, D.J., Althausen, J.D., Narumalani, S., & Weatherbee, O. 1993. An evaluation of the CoastWatch change detection protocol in South Carolina. *Photogrammetric Engineering and Remote Sensing, 59*, 1039-1044.

Kayastha, N., Thomas, V., Galbraith, J. and Banskota, A., 2012. Monitoring wetland change using inter-annual landsat time-series data. *Wetlands*, 32(6), pp.1149-1162.

Kearney, M.S., Rogers, A.S., Townshend, J.R., Rizzo, E., Stutzer, D., Stevenson, J.C. and Sundborg, K., 2002. Landsat imagery shows decline of coastal marshes in Chesapeake and Delaware Bays. *Eos, Transactions American Geophysical Union*, 83(16), pp.173-178.

Kearney, M.S. and Stevenson, J.C., 1991. Island land loss and marsh vertical accretion rate evidence for historical sea-level changes in Chesapeake Bay. *Journal of Coastal Research*, pp.403-415.

Kirwan, M.L., Guntenspergen, G.R., d'Alpaos, A., Morris, J.T., Mudd, S.M., Temmerman, S., 2010. Limits on the adaptability of coastal marshes to rising sea level. Geophysical Research Letters 37 (23).

Klemas, V. 2011. Remote sensing of wetlands: case studies comparing practical techniques. *Journal of Coastal Research, 27*, 418-427.

Mariotti, G., and S. Fagherazzi, 2013. Critical width of tidal flats triggers marsh collapse in the absence of sea-level rise, *Proceedings of the national Academy of Sciences* : 201219600.

Mckee, K.L., Patrick, W.H., 1988. The relationship of smooth cordgrass (Spartina alterniflora) to tidal datums: a review. Estuaries 11 (3), 143-151.

Morris, J.T., Sundareshwar, P.V., Nietch, C.T., Kjerfve, B., Cahoon, D.R., 2002. Responses of coastal wetlands to rising sea level. Ecology 83 (10), 2869-2877.

Mudd, S.M., Fagherazzi, S., Morris, J.T. and Furbish, D.J., 2004. Flow, sedimentation, and biomass production on a vegetated salt marsh in South Carolina: toward a predictive model of marsh morphologic and ecologic evolution. *The Ecogeomorphology of Tidal Marshes.* Coastal Estuarine Studies, *59*, pp.165-187.

Najjar, R.G., Walker, H.A., Anderson, P.J., Barron, E.J., Bord, R.J., Gibson, J.R., Kennedy, V.S., Knight, C.G., Megonigal, J.P., O¹Connor, R.E. and Polsky, C.D., 2000. The potential impacts of climate change on the mid-Atlantic coastal region. *Climate Research*, *14*(3), pp.219-233.

O'Connell, J.L., Mishra, D.R., Cotten, D.L., Wang, L., & Alber, M. 2017. The Tidal Marsh Inundation Index (TMII): An inundation filter to flag flooded pixels and improve MODIS tidal marsh vegetation time-series analysis. *Remote Sensing of Environment, 201*, 34-46.

O'Donnell, J.P., Schalles, J.F., 2016. Examination of abiotic drivers and their influence on spartina alterniflora biomass over a twenty-eight year period using Landsat 5 TM satellite imagery of the Central Georgia Coast. Remote Sensing 8 (6), 477.

Pasquarella, V.J., Holden, C.E., Kaufman, L., & Woodcock, C.E. 2016. From imagery to ecology: leveraging time series of all available Landsat observations to map and monitor ecosystem state and dynamics. *Remote Sensing in Ecology and Conservation, 2*, 152-170.

Raposa, K.B., Weber, R.L., Ekberg, M.C., Ferguson, W., 2017. Vegetation dynamics in Rhode Island salt marshes during a period of accelerating sea level rise and extreme sea level events. Estuaries and Coasts 40 (3), 640-650.

R Core Team. 2013. R: A language and environment for statistical computing. *, 3.5.0.*

Roman, C.T. 2017. Salt marsh sustainability: challenges during an uncertain future. *Estuaries and coasts, 40*, 711-716.

Roy, D.P., Kovalskyy, V., Zhang, H.K., Vermote, E.F., Yan, L., Kumar, S.S. and Egorov, A.,

2016. Characterization of Landsat-7 to Landsat-8 reflective wavelength and normalized difference vegetation index continuity. *Remote Sensing of Environment*, *185*, pp.57-70.

Saintilan, N., Wilson, N.C., Rogers, K., Rajkaran, A. and Krauss, K.W., 2014. Mangrove expansion and salt marsh decline at mangrove poleward limits. *Global change biology*, *20*(1), pp.147-157.

Schepers, L., Kirwan, M., Guntenspergen, G., Temmerman, S., 2017. Spatio-temporal development of vegetation die-off in a submerging coastal marsh. Limnol.Oceanogr. 62, 137-150.

Silliman, B.R., & Zieman, J.C. 2001. Top-down control of *Spartina alterniflora* production by periwinkle grazing in a Virginia salt marsh. *Ecology, 82*, 2830-2845.

Snedden, G.A., Cretini, K., & Patton, B. 2015. Inundation and salinity impacts to above-and belowground productivity in *Spartina patens* and *Spartina alterniflora* in the Mississippi River deltaic plain: Implications for using river diversions as restoration tools. *Ecological Engineering, 81*, 133-139.

Smith, S.M. 2015. Vegetation change in salt marshes of Cape Cod National Seashore (Massachusetts, USA) between 1984 and 2013. *Wetlands, 35*, 127-136.

Sweet W. V. Kopp R.E., Weaver, C.P., Obeysekera, J., Horton, R.M., Thieler, E.R., Zervas, C. 2017. "Global and regional sea level rise scenarios for the United States," NOAA, Silver Spring, MD, USA, Tech. Rep. NOS CO-OPS 083.

Taylor, S.J., & Letham, B. 2018. Forecasting at scale. *The American Statistician,* 72(1), 37-45.

Verbesselt, J., Hyndman, R., Newnham, G., & Culvenor, D. 2010. Detecting trend and seasonal changes in satellite image time series. *Remote Sensing of Environment, 114*, 106-115.

Vogelmann, J.E., Gallant, A.L., Shi, H., & Zhu, Z. 2016. Perspectives on monitoring gradual change across the continuity of Landsat sensors using time-series data. *Remote Sensing of Environment, 185*, 258-270.

Watson, E.B., Wigand, C., Davey, E.W., Andrews, H.M., Bishop, J., & Raposa, K.B. 2017. Wetland Loss Patterns and Inundation-Productivity Relationships Prognosticate Widespread Salt Marsh Loss for Southern New England. *Estuaries and Coasts, 40*, 662-681.

Wang, Y.Q., and A. Campbell. 2018. Monitoring salt marshes using high spatial resolution satellite imagery for mapping and change detection: Protocol development for northeast coastal parks. Natural Resource Report NPS/NCBN/NRR—2018/1717.

National Park Service, Fort Collins, Colorado.

Weston, N.B., 2014. Declining sediments and rising seas: an unfortunate convergence for tidal wetlands. *Estuaries and Coasts*, *37*(1), pp.1-23.

Zhao, B., Yan, Y., Guo, H., He, M., Gu, Y., & Li, B. 2009. Monitoring rapid vegetation succession in estuarine wetland using time series MODIS-based indicators: an application in the Yangtze River Delta area. *Ecological Indicators, 9*, 346-356.

Zhu, Z., Fu, Y., Woodcock, C.E., Olofsson, P., Vogelmann, J.E., Holden, C., et al., 2016. Including land cover change in analysis of greenness trends using all available Landsat 5, 7, and 8 images: A case study from Guangzhou, China (2000–2014). Remote Sensing of Environment 185 243-257.